

UNIVERSITY OF OKLAHOMA

GRADUATE COLLEGE

THE KINETIC AND CHEMICAL MECHANISM OF
SERINE ACETYLTRANSFERASE FROM *HAEMOPHILUS INFLUENZAE*

A Dissertation

SUBMITTED TO THE GRADUATE FACULTY

In partial fulfillment of the requirements for the

Degree of

Doctor of Philosophy

By Corey Marc Johnson
Norman, Oklahoma
2004

UMI Number: 3122286

INFORMATION TO USERS

The quality of this reproduction is dependent upon the quality of the copy submitted. Broken or indistinct print, colored or poor quality illustrations and photographs, print bleed-through, substandard margins, and improper alignment can adversely affect reproduction.

In the unlikely event that the author did not send a complete manuscript and there are missing pages, these will be noted. Also, if unauthorized copyright material had to be removed, a note will indicate the deletion.

UMI[®]

UMI Microform 3122286

Copyright 2004 by ProQuest Information and Learning Company.

All rights reserved. This microform edition is protected against unauthorized copying under Title 17, United States Code.

ProQuest Information and Learning Company
300 North Zeeb Road
P.O. Box 1346
Ann Arbor, MI 48106-1346

© Copyright by Corey Marc Johnson 2004
All Rights Reserved.

THE KINETIC AND CHEMICAL MECHANISM OF
SERINE ACETYLTRANSFERASE FROM HAEMOPHILUS INFLUENZAE

A Dissertation APPROVED FOR THE
DEPARTMENT OF CHEMISTRY AND BIOCHEMISTRY

BY



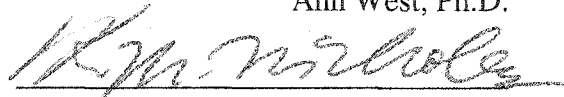
Paul Cook, Ph.D.



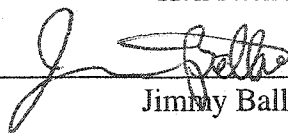
Phillip Klebba, Ph.D.



Ann West, Ph.D.



Ken Nicholas, Ph.D.



Jimmy Ballard, Ph.D.

Chapter 1

A Review of Acyltransferase Reactions

Acyl transfer is very common in nature. These reactions are used to activate a molecule for further chemistry, add additional functionality, and increase solubility among other things. A recent report even indicates a role for the reaction in regulation. Acyl transfer occurs to a number of nucleophiles including acids such as carboxylate and phosphate, amines, thiols and alcohols. This review will focus on enzymes that catalyze acyl transfer from acylpantothenyl donors to alcohols, and in particular how these enzymes compare in structure and mechanism. There are many ways to classify these enzymes. Although their structures vary, there are two general proposed mechanisms that predominate in enzymatic acyl transfer to alcohols. One mechanism makes use of direct nucleophilic attack to give products and the other makes use of a nucleophilic/covalent mechanism with an acylenzyme intermediate. The order of this review will be based upon these two general mechanisms, and will be used to help frame mechanistic questions to be asked of serine acetyltransferase, the focus of this dissertation.

ENZYMES CATALYZING DIRECT ATTACK

HEXAPEPTIDE ACYLTRANSFERASES

The hexapeptide enzymes fall under the first general category of mechanism mentioned, utilizing direct attack. This family of proteins is composed of imperfect tandem repeated copies of a hexapeptide sequence described as [LIV]-[GAED]-X₂-[STAV]-X (1, 2). Frequently, the sequence begins with an aliphatic residue (Leu, Ile, or Val) at position *i*, with a Gly at position *i*+1, and a small residue (Ser, Thr, Ala, or Val) at position *i*+4.

These acyltransferases participate in a variety of enzymatic processes, including cell wall biosynthesis, amino acid metabolism, and detoxification (3-7). They are found predominantly in higher plants and microorganisms. The hexapeptide acyltransferases bind the phosphopantotheryl moiety of acetyl Coenzyme A (4), or the acylated acyl carrier protein (3, 7), to which the acyl group to be transferred is in thioester linkage. Acyl transfer reactions studied to date include transfer of acetate (4), succinate (5), or R-3-hydroxy fatty acids (3, 7).

The crystal structures of this family of enzymes show that the hexapeptide repeat sequence directs folding of an unusual structural domain known as the left-handed parallel β -helix, which is unique to hexapeptide proteins (8). The L β H domain is a large coil as if wound in a left-handed spiral around the surface of an equilateral prism. The faces of the helical prism are formed by three, extremely flat parallel β -sheets. Each of the β -sheets is composed of three to five β -strands. The number of coils per β -helix varies with the particular enzyme. The active sites are located in the long narrow grooves at the interface between two left-handed parallel β -helix structural domains of the trimer. Some of these enzymes have an external loop that forms a short tunnel in the active site to which two

ligands can bind at opposite ends. Structural and limited kinetic data suggest a sequential kinetic mechanism for these enzymes where both substrates are bound previous to catalysis.

The crystal structures for several hexapeptide proteins have been solved including those of , *Escherichia coli* UDP-*N*-acetyl *O*-acyltransferase(8), carbonic anhydrase from *Methanosarcina thermophila*(10), a bacterial tetrahydrodipicolinate *N*-succinyltransferase (11), a xenobiotic acetyltransferase from *Pseudomonas aeruginosa* (12), Vat(D) acetyltransferase from *Enterococcus faecium*, and (13) serine acetyltransferase from *Haemophilus influenzae*(9). Three of these are shown in figure 1. A close up of the active sites of the enzymes shown in Fig. 1 are shown in figure 2. These will be discussed below.

All of these enzymes contain the six-residue periodicity and the left-handed β -helix structural domains. The hexapeptide acyltransferases also share a common active site location, separate binding sites for substrates, a conformational change to generate a tunnel that forms upon reactant binding that shields the substrates from bulk solvent and properly orients the substrates for catalysis, and a histidine residue important to catalysis which is possibly part of a catalytic dyad. Although these proteins share these common features, their reactions and substrates differ. The hexapeptide enzymes along with some of the nonhexapeptide enzymes share the same general form of acid base catalysis. Each will be considered in turn below. The physical parameters for all of the enzymes discussed are in table 1.

UDP-N-acetylglucosamine 3-O-acyltransferase

The product of the *LpxA* gene, UDP-*N*-acetylglucosamine 3-*O*-acyltransferase catalyzes the transfer of (R)-3-hydroxymyristic acid from its acyl carrier protein thioester to UDP-*N*-acetylglucosamine (8) (Scheme 1). This is the first step in the biosynthesis of Lipid A, the hydrophobic anchor of lipopolysaccharide in Gram-negative bacteria (20). *LpxA* is the first example of a protein with a left-handed β -helix as the predominating feature of its secondary structure to be crystallized (8). The 10 coils of the β -helix of *E. coli* *LpxA* are specified by 24 complete and six incomplete hexapeptide repeats (8). Three repeats make up one turn of the β -helix (21).

Scheme 1.

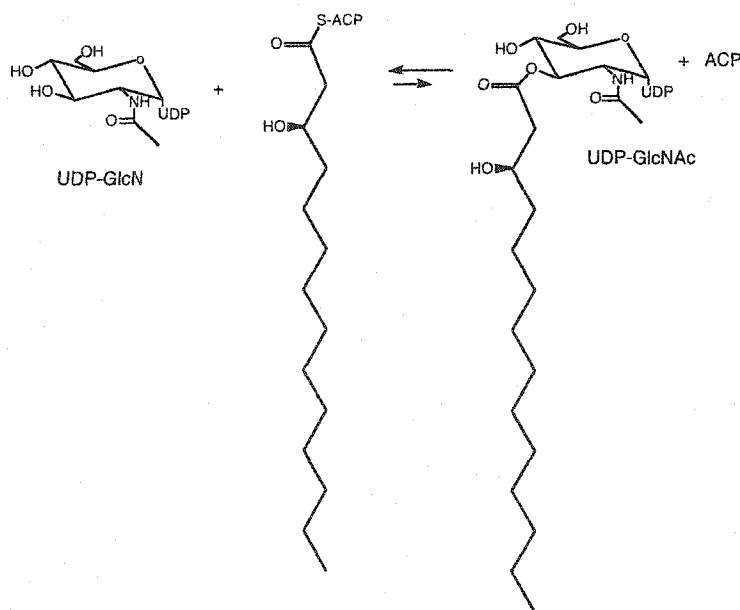


Table 1. Hexapeptide Proteins

Acyl Acceptor	Acyl Donor	E.C. Number	Species	Pathway/ Function	Subunit Composition	Subunit MW (kDa)	Ref.
Serine	AcetylCoA	2.3.1.301	<i>Haemophilus influenzae</i>	Cysteine biosynthesis	Hexamer	29.316	3
UDP-GlcNAc	R-3-hydroxyacyl-acyl carrier prot.	2.3.1.292	<i>Escherichia coli</i>	biosynthesis of Lipid A	Trimer	28.08	17
THDP	SuccinylCoA	2.3.1.173	<i>Mycobacterium bovis</i> BCG	DAP/lysine biosynthesis	Trimer	29.892	10
chloramphenicol	AcetylCoA	2.3.1.284	<i>Pseudomonas aeruginosa</i>	antibiotic	Trimer	23.53	9
Virginiamycin M1	AcetylCoA	unknown	<i>Enterococcus faecium</i>	antibiotic	Trimer	23.65	11
glucosamine chitin oligosacch. de-N acetylated-chitin derivatives	AcetylCoA	2.3.1.45	<i>Rhizobium leguminosarum</i>	LCO synthesis	Trimer	20.11	21
GlcN-1-Phosphate	AcetylCoA	2.3.1.576	<i>Escherichia coli</i>	UDP-GlcNAc biosynthesis	Trimer	49.2	13
galactosides, glucosides, lactosides	AcetylCoA	2.3.1.187	<i>Escherichia coli</i>	cellular detoxification	Trimer	19.96	12
Maltose, glucose	AcetylCoA	2.3.1.798	<i>Escherichia coli</i>	maltose transport system	Trimer	19.96	38
none	none	4.2.1.19	<i>Methanosarcina thermophila</i>	ion transport pH homeostasis	Trimer	22.88	28

Enzyme

1. Serine acetyltransferase 2. UDP-N-acetylglucosamine 3-O acyltransferase 3. THDP-N-Succinyltransferase 4. Xenobiotic acetyltransferase
5. Nod L protein 6. Gln U protein 7. Galactoside acetyltransferase 8. Maltose acetyltransferase 9. Carbonic anhydrase

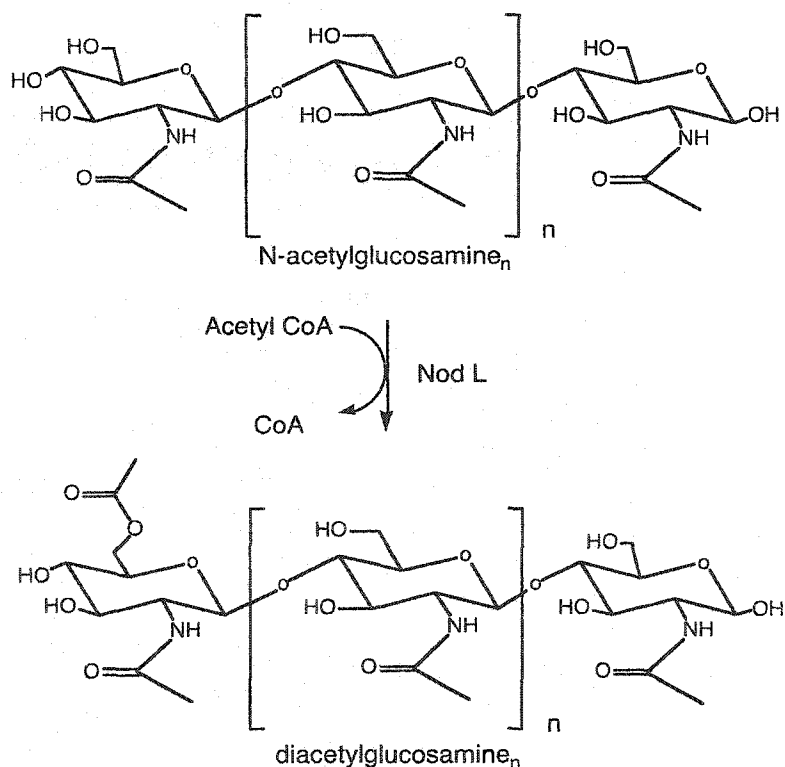
The active site cleft contains multiple histidines and other basic residues that complement the acidic substrate (21). Chemical modification and site-directed mutagenesis studies have shown the importance of the conserved histidine, lysine, and arginine residues in the cleft. Alanine mutants have been made for all conserved histidine, lysine, and arginine residues of the enzyme. Many of these mutant LpxA enzymes show a decrease in activity corresponding to an increased $K_{\text{UDP-GlcNAc}}$. The His 125 mutant had no activity under any assay conditions yet maintained its wild type $K_{\text{UDP-GlcNAc}}$ value. His 125 is therefore, thought to be directly involved in catalysis. The other residues are thought to participate in substrate binding. Initial kinetic work shows LpxA does not remove the acyl chain from UDP-3-O-(R-3-hydroxymyristoyl)-GlcNAc in the absence of a thiol-containing acyl acceptor. Therefore, a ping pong kinetic mechanism is unlikely. A more probable mechanism for LpxA would be a sequential mechanism in which H125 acts as a general base and abstracts the hydrogen from the 3-OH of UDP-GlcNAc and prepares the substrate for nucleophilic attack on the acyl chain carbonyl group of the acyl-ACP (21).

NodL product of *Rhizobium leguminosarum*

The product of the NodL gene from *Rhizobium leguminosarum* is homologous to two of the enzymes discussed in this review, the LacA gene product, thiogalactoside acetyltransferase, and the CysE gene product, serine acetyltransferase, according to the predicted protein sequence. For *Rhizobium leguminosarum* bv. *viciae*, it has been shown

that the presence of an *O*-acetyl group on the 6-OH group of the nonreducing terminal residue of lipo-chitin oligosaccharides (LCOs) is required for preinfection thread formation and nodule meristem formation (22, 23). This is a prerequisite for the formation of the nitrogen-fixing root nodules formed by leguminous plants (24). Mutagenesis studies revealed that the *nodL* gene product is required for the presence of this *O*-acetyl group (22). The *nodL* protein acetylates LCOs, chitin oligosaccharides, and N-acetylglucosamine *in vitro*, using acetyl CoA as the acetyl donor. NodL transfers this acetyl moiety only to the 6-OH group of the nonreducing terminal residue (25) (Scheme 2).

Scheme 2.



It is also of interest for this cytosolic protein that the pH optimum is 9, and the enzyme

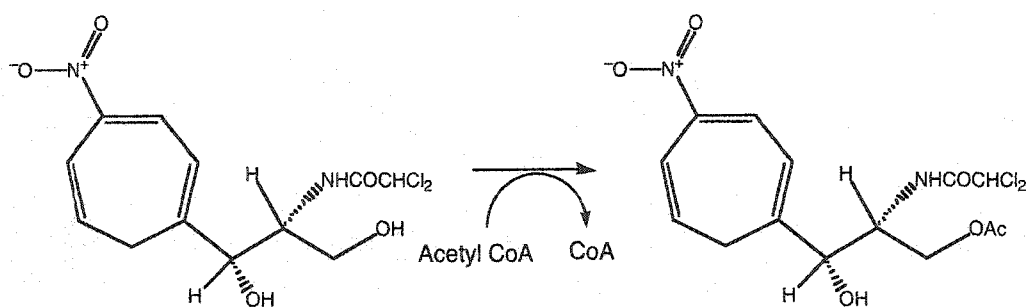
is stable at temperatures up to 48°C and has a temperature optimum around 35°C (25). Kinetic and hydrodynamic studies of NodL *O*-acetyltransferase are consistent with a steady-state random ternary complex mechanism in which the off rate of the *O*-acetyl chitosan (substrate analogue) oligomer appears to be partially rate-determining (18). The enzyme has also been shown to be trimeric with little tendency to self-associate.

PaXAT Acetyltransferase

One class of enzymes has been reported to catalyze acetyl transfer from CoA to chloramphenicol (Cm1) but appears to be unrelated structurally to the classic chloramphenicol acetyltransferases (CATs). This new class of enzymes is referred to as XATs (xenobiotic acetyltransferases) (6). These enzymes utilize acetyl CoA to *O*-acetylate a variety of natural products and may use a structurally diverse range of hydroxyl-containing compounds as acyl acceptors. The XATs can be further subdivided into two groups on the basis of shared amino acid sequence similarity and acceptor substrate specificity (6). The first group of enzymes include acetyltransferases from *Agrobacterium tumefaciens* C58 (26), the *E. coli* multiresistance transposon Tn2424 (27), and *Pseudomonas aeruginosa* PA103 (28). These enzymes are all able to catalyze the CAT_{III} reaction, the acetylation of chloramphenicol using acetyl CoA as an acyl donor (29-31) (Scheme 3). The second group of hexapeptide xenobiotic acetyltransferases has been associated with resistance to the virginiamycin class of antibiotics. These enzymes do not generally carry out the CAT_{III} reaction (12).

Kinetic work has been done on the XAT from *Agrobacterium tumefaciens* (*AtXAT*), an enzyme homologous to and from the same subdivision of XATs as the *Pseudomonas aeruginosa* enzyme. The *AtXAT* has the ability to acetylate Cm1, but with low efficiency compared to the CAT_{III} enzyme. The K_m for the XAT for Cm1 is 159 μ M, whereas the K_m for CAT_{III} is 12 μ M. It is possible that the main physiological role of the XAT may not be antibiotic resistance (6).

Scheme 3.



The crystal structure for the xenobiotic acetyltransferase from *Pseudomonas aeruginosa* PA103 (*PaXAT*) has been determined (12) (Fig. 1). *PaXAT* is an example of a hexapeptide protein that carries out the same reaction as a non-hexapeptide acetyltransferase (CAT). The crystal structure of the *PaXAT*:Cm complex for *PaXAT* cannot be superimposed on that of Cm bound to CAT_{III}, differing by 120° torsion angle rotations about the C1-C2 and C2-C3 bonds (12). However, His 78 may be analogous to the His 195 residue of CAT, Fig. 2, which has been identified as a general base in the catalytic mechanism (6). A histidyl residue is conserved in the sequence alignments of all XATs. The His 78 residue was further proved to be critical by using site-directed

mutagenesis to change the residue to alanine. The H78A XAT was found to be devoid of acyltransferase activity (6), suggesting His 78 is an important catalytic residue.

Another conserved residue in the *PaXAT* is the Trp 118 residue, Fig. 2. The indole ring of Trp 118A stacks against His 79B (B indicates the residue is provided by the adjacent subunit) in the structure of *PaXAT* (12). This tryptophan residue is conserved among all xenobiotic acetyltransferases and also in *E. coli* galactoside acetyltransferase and *Rhizobium leguminosarum* lipooligosaccharide acetyltransferase; two hexapeptide acetyltransferases that are not members of the xenobiotic class. The fluorescence response to acetyl CoA binding by the galactoside acetyltransferase has been shown to be entirely due to its homologous tryptophan residue (32). This suggests that some nonxenobiotic hexapeptide acetyltransferases may share active-site structural features in common with *PaXAT* and other members of the hexapeptide xenobiotic acetyltransferase class of enzymes (12).

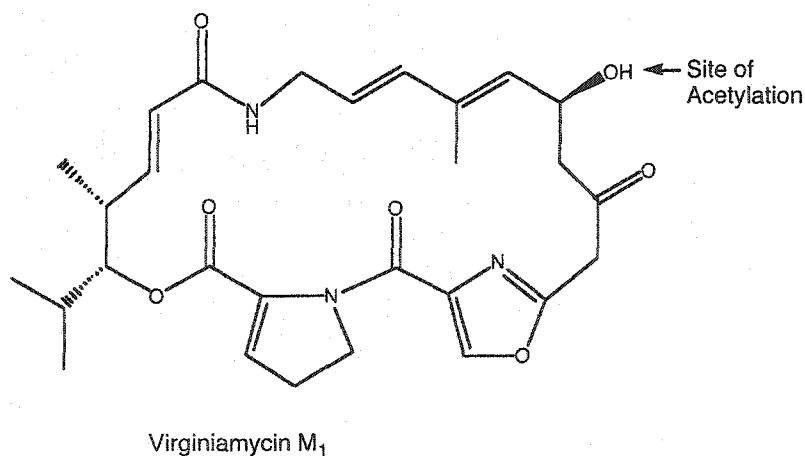
A comparison of the active sites of *PaXAT* and CAT_{III} (30, 31) might reveal the function of *PaXAT*. The overall polypeptide chain folds of these enzymes are completely unrelated. Both enzymes are trimers and bind similar substrates to opposite ends of an active-site tunnel located at the boundary of adjacent subunits. The His 79B residue from *PaXAT* (Fig. 2) projects into the active-site tunnel from an extended loop domain and appears to form interactions with its side chain that are identical to those made by CAT_{III} His 195 (12). Both residues appear to donate hydrogen bond from their imidazole N^{δ1} to a main-chain oxygen atom and to receive a hydrogen bond from the C-3 hydroxyl of Cm

with their imidazole N^{ε2} atoms. If the environmental similarities of these histidine residues indicate similar roles for the His 79B of *Pa*XAT and the His 195 of CAT_{III}, then the hydrogen bond donated by the imidazole N^{δ1} of *Pa*XAT His 79B to the peptide oxygen of Thr 86B would stabilize the proper tautomeric form of the imidazole lacking a proton on N^{ε2} and could promote the role of this residue as a general base catalyst capable of deprotonating the C-3 hydroxyl group of the Cm acceptor (12).

Vat (D) Acetyltransferase

Vat (D), also termed SatA, is a streptogramin acetyltransferase that inactivates virginiamycin M₁, a group A component of streptogramin, as well as the group A (dalfopristin) component of Synercid (Scheme 4).

Scheme 4.



A crystal structure has been determined for Vat (D) from the human urinary isolate

Enterococcus faecium BM4145 (13), which reveals the molecular basis for a reaction by which Gram-positive cocci acquire resistance to a last resort antibiotic (streptogramin).

The acyl donors for Vat enzymes are acetyl or succinyl CoA thioesters of the acyl carrier protein. The enzyme recognizes a diverse range of acceptors bearing free hydroxyl or amino groups, including antibiotics and intermediates involved in cell wall biosynthesis and amino acid metabolism (13).

Vat (D) is a homotrimer. Its subunit is folded into three domains: a large coiled L β H structural domain, an extended loop domain that projects from the L β H domain, and a C-terminal domain (Fig. 1). The largest structural domain is the L β H domain. His 82B of Vat (D) donates a hydrogen bond from its N $^{\delta 1}$ group to the main chain carbonyl oxygen of Thr 88B and participates in a ring stacking interaction with Trp 121A (Fig. 2). These interactions should increase its basicity and facilitate the histidine's proposed role as a general base. The histidine is positioned at the acetyltransferase active site in a binary complex of the enzyme with CoA. The imidazole ring stacks against the aromatic ring of a tyrosine, while its N $^{\delta 1}$ group interacts with the sidechain of a glutamate. This general pattern of interactions is observed in Vat (D), *PaXAT*, and *GlmU* from *E. coli* (13).

Vat (D) and *PaXAT* are very similar in their overall polypeptide chain fold and the key active site residues of Vat (D) are conserved in *PaXAT*. Despite these similarities, the substrate specificities of these two enzymes do not overlap. *PaXAT* is not known to use any substrate other than chloramphenicol. On the other hand, Vat (D) will utilize virginiamycin M₁ but has no activity when chloramphenicol is used as a substrate. The

differences in the active sites of these enzymes prohibit the utilization of the other substrate due to steric conflicts (13).

Lac A enzyme family: Thiogalactoside Acetyltransferase, Galactoside Acetyltransferase and Maltose Acetyltransferase

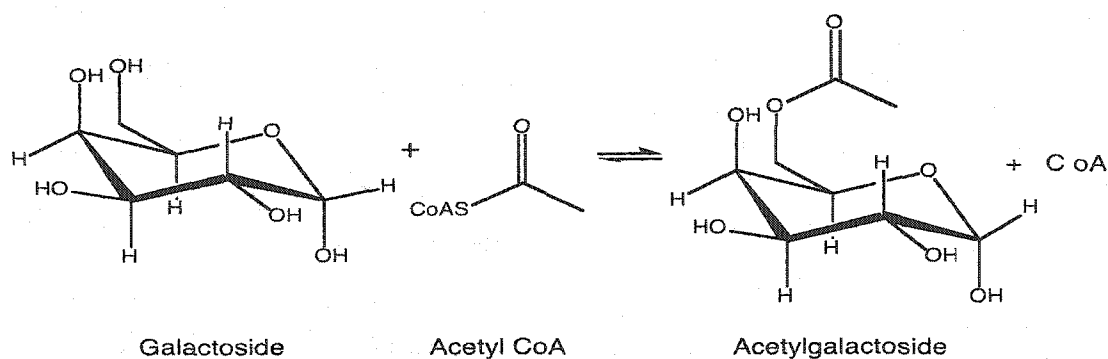
LacA, which encodes thiogalactoside acetyltransferase, transfers the acetyl group of acetyl-coenzyme A to the 6-OH of thiogalactosides(33). Galactoside acetyltransferase (GAT) catalyzes the CoA-dependent transfer of an acetyl group to the 6-*O*-methyl position of a range of galactosides, glucosides, and lactosides (34, 35) (Scheme 5).

Kinetic studies using IPTG as substrate demonstrate that GAT follows an ordered bi-bi ternary complex mechanism with acetyl CoA as the leading substrate and CoA as the final product (32, 36, 37). Histidine 115 has also been identified as catalytically important (32) (Fig 2). GAT contains the L β H structural domain, which contains 5.3 coils (Fig. 1). The third turn of each coil contains variation in the number of amino acids inserted (38). These turns have been shown to donate residues to the active sites of THDP-*N*-succinyltransferase(11), a xenobiotic acetyltransferase(*Pa*XAT) (10), and the bifunctional uridyltransferase/ pyrophosphorylase (GlmU) (39-41). The loops are responsible for the structural and functional diversity of this enzyme family (38).

Due to the binding proximity of the C6-hydroxyl group of the IPTG substrate and the carbonyl carbon atom of the acetyl CoA thioester, the crystal structures of GAT suggest a bi-bi ternary complex mechanism in which His 115B appears to be well

positioned to abstract a proton from the C6-hydroxyl and act as a general base catalyst (Fig. 2) (36, 38). The crystal structures of GAT also suggest that substrate specificity is accomplished by recruitment of residues from the NH₂-terminal domain as well as by the extended T3 loop and coiled portions of the LβH domains (38).

Scheme 5.



GAT is a 65,300 Da trimer and has been reported to have extensive homology throughout its amino acid sequence to the *nodL* gene product of *Rhizobium leguminosarum* (4). More limited homology has been found in the C-terminal regions of GAT, serine acetyltransferases, and xenobiotic acetyltransferases (4, 27). This homology could represent a structural feature required for binding of coenzyme A (32).

GAT has a broad substrate specificity, acetylating galactosides, glucosides, and lactosides. Kinetic studies show that acetyl CoA binds to free enzyme and the association rate constant for acetyl CoA and the dissociation rate constant for CoA are much greater than k_{cat} . The rate-determining step is likely either the loss of acetylated acceptor from the

binary complex or the interconversion of the substrate and the product ternary complexes

(32, 42).

Figure 1. Crystal structures of (A) galactoside acetyltransferase (pdb codes 1KRR, 1KRU), (B) Virginiamycin acetyltransferase (pdb code 1KK4), and (C) xenobiotic acetyltransferase. (pdb code 1XAT) The program pymol was used to visualize the structure from the pdb file. Galactose and CoA are bound to galactose acetyltransferase. Desulfo CoA is bound to the Virginiamycin acetyltransferase. The substrates chloramphenicol and desulfo CoA are bound to the enzyme active site of the xenobiotic acetyltransferase.

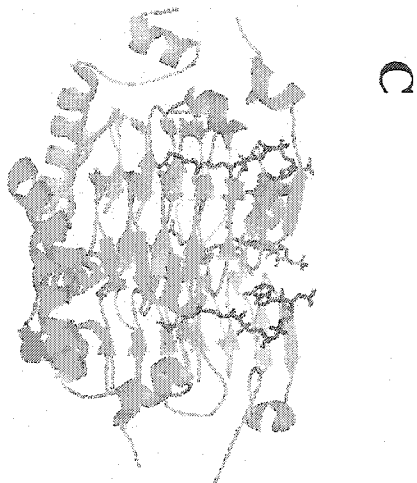
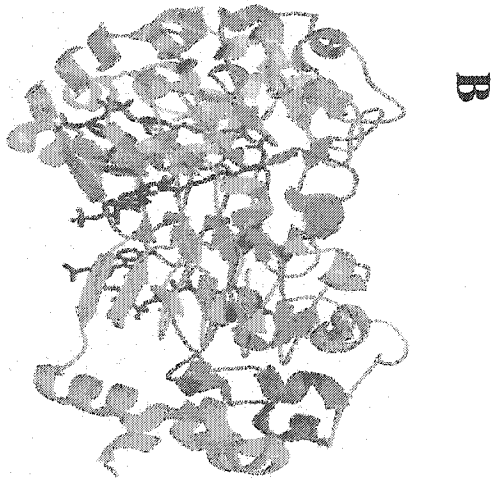
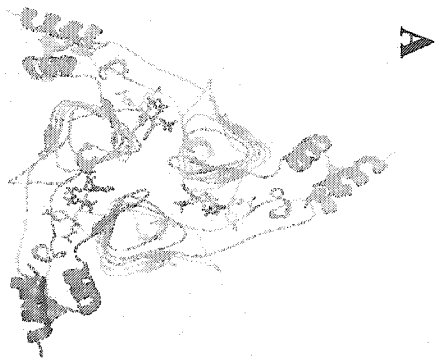
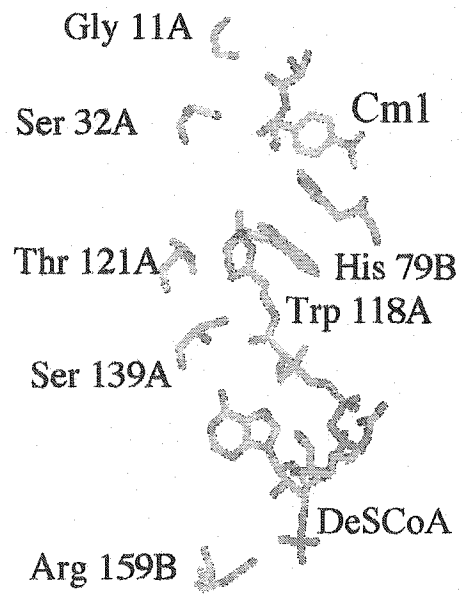
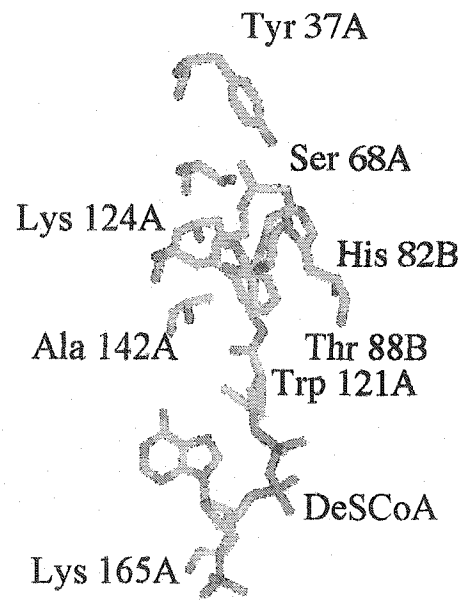
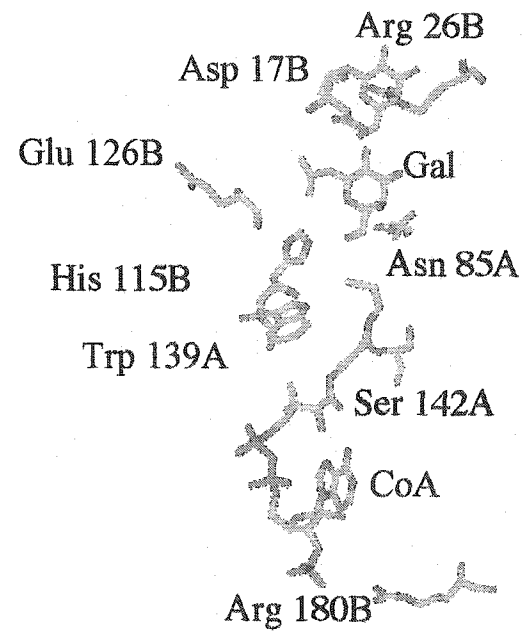
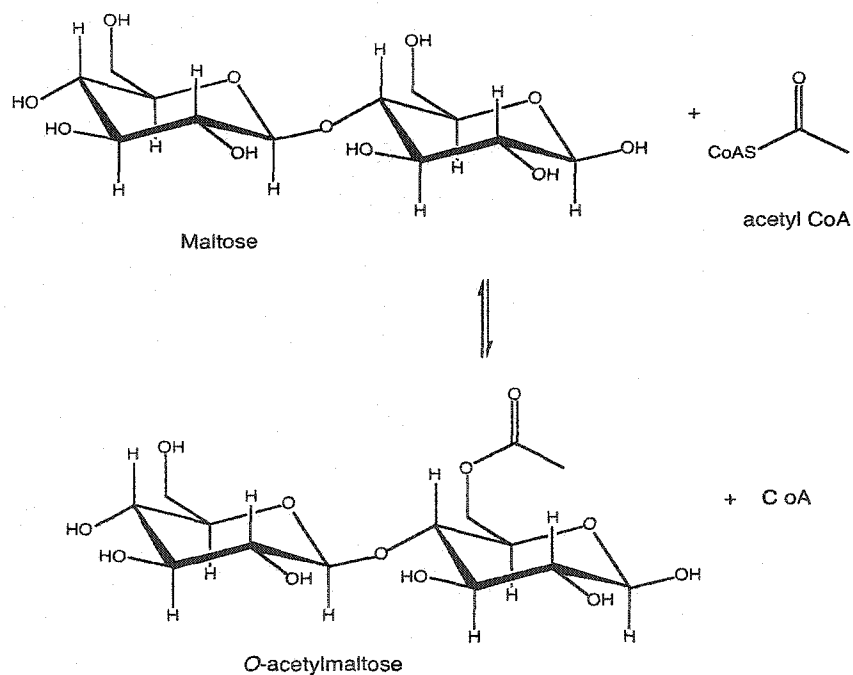


Figure 2. A close up of the active sites for (A) xenobiotic acetyltransferase, (B) virginiamycin acetyltransferase, and (C) galactose acetyltransferase. Substrates are labeled and some residues thought to be involved in substrate binding are shown. The histidine residues 79B, 82B, and 115B have been identified as important for catalysis. The tryptophan residues below each histidine are also conserved. Each catalytic histidine in the figure is part of a catalytic dyad with either a threonine or a glutamate residue.

A**B****C**

The crystal structure of maltose acetyltransferase (MAT) has also been determined (42). MAT has a high (41%) sequence identity to GAT. This is reflected by very high structural similarity also in the non-LβH regions. MAT contains 5.3 coil LβH domains. The acceptor sites of the two enzymes are clearly different, however. MAT is regiospecific, catalyzing transfer to the C6 position only of glucose and the same position on maltose (Scheme 6). This regiospecificity mimics that of the product of the *NodL* gene (25). MAT even exhibits a marked preference for the β-anomeric form of glucose. Reaction rates of MAT with oligomaltosides were also tested. The length of the oligomaltoside was shown to be inversely proportional to the reaction rate (42). This is in contrast with the *NodL* gene product (24).

Scheme 6.

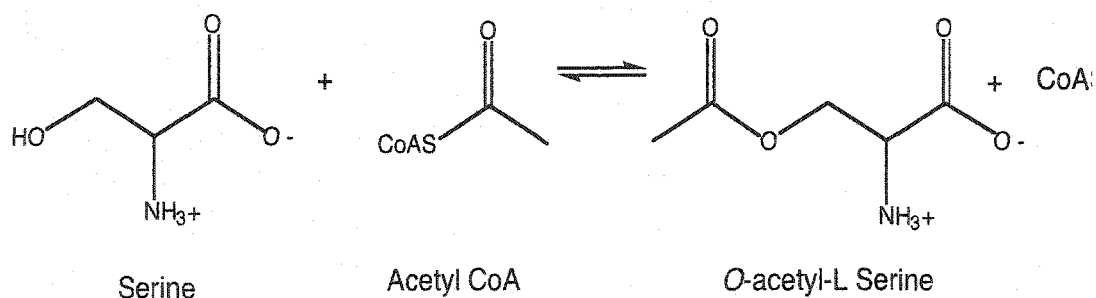


The proposed kinetic mechanism for MAT is a sequential bi-bi, similar to GAT. His 113B is situated in a long loop protruding from the L β H domain at the interface between two monomers and is in an equivalent position to the previously identified catalytically important histidine residues of other L β H enzymes (42). The specific cellular functions of MAT and GAT are not clear. Roles in detoxification have been proposed for both (34, 43).

Serine Acetyltransferase

The biosynthesis of L-cysteine in bacteria and plants proceeds via a two-step pathway. L-Serine is the amino acid precursor of L-cysteine, which is first acetylated at its β -hydroxyl by acetyl CoA to give *O*-acetyl-L-serine (OAS). This reaction is catalyzed by the enzyme serine acetyltransferase (SAT) (14). *O*-Acetyl-L-serine is the immediate precursor of the carbon moiety of cysteine. The final step in cysteine synthesis, replacement of the acetoxy side chain by a thiol, is catalyzed by *O*-acetylserine sulfhydrylase (OASS), and inorganic sulfide acts as the source of sulfur (15). The SAT reaction is shown in scheme 7.

Scheme 7.



This is the enzyme to which the research in this dissertation is directed. The structural and mechanistic work accomplished for *HiSAT* will be discussed throughout the rest of the dissertation. The physical parameters for the enzyme are included in table 1.

N-Acyltransferase Hexapeptides

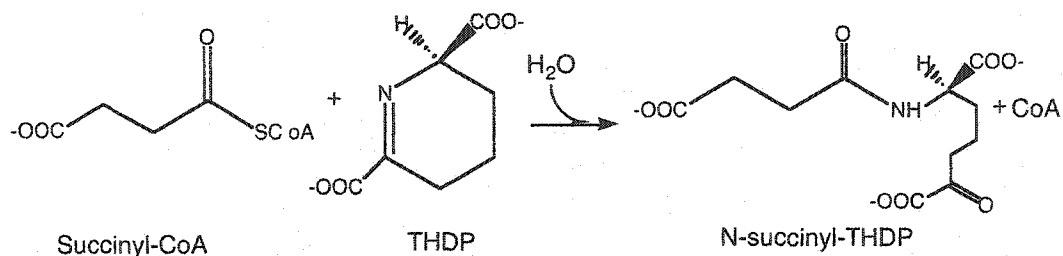
Not all of the hexapeptiderepeat enzymes transfer an acyl group to an alcohol. Some of the well-studied enzymes in this family transfer an acyl group to an amine (*N*-acyltransferases), and one enzyme identified as a hexapeptide enzyme does not catalyze acyl transfer at all. These enzymes are discussed briefly in terms of structural and mechanistic similarity to the L β H *O*-acyltransferases.

Tetrahydrodipicolinate (THDP) N-succinyltransferase

Tetrahydrodipicolinate-N-succinyltransferase catalyzes the conversion of tetrahydrodipicolinate (THDP) and succinyl-CoA to L-2-(succinylamino)-6-oxopimelate and CoA (11) Scheme 8. This is the committed step of the succinylase branch of the DAP/lysine biosynthetic pathway used by Gram-negative bacteria and higher plants to synthesize L-lysine from aspartate and pyruvate (5). Crystal structures of the enzyme in complex with the substrate/cofactor pairs L-2-aminopimelate/coenzymeA and L-2-amino-6-oxopimelate/coenzymeA showed the active site and provided knowledge of a conformational change during the reaction (12). In the active site, the side chain of the amino acid and the pantetheine arm of the cofactor (succinyl CoA) are in rough colinear

alignment and oriented parallel to the 3-fold axis of the enzyme.

Scheme 8

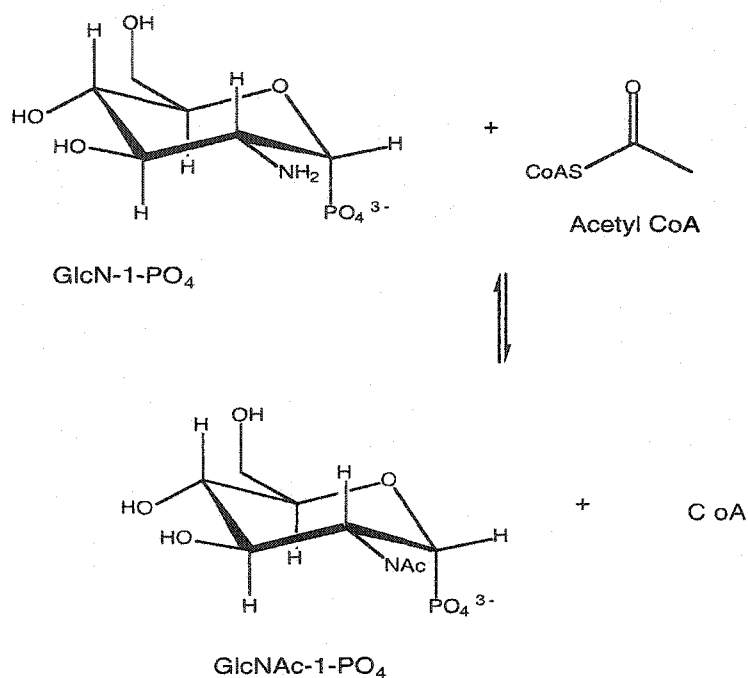


Upon binding of substrates, significant conformational changes are apparent in the following three distinct polypeptide segments: a portion of the NH₂-terminal domain containing the first three α -helices, a polypeptide loop excluded from the L β H domain, and the C-terminal 18 residues. The NH₂-terminal domain and the flexible loop excluded from the L β H domain are in contact and move in the same direction to cover the active site. The C-terminal 18 residues form a short α -helix and combine with the residues from the flexible loop excluded from the L β H structural domain to form one wall of the extended active site tunnel. The tunnel formed by these conformational changes serves to shield the ligands from bulk solvent and to orient the nucleophilic amino group of the amino acid acceptor toward the mercaptoethylamine group of the cofactor. The conformational change observed in the two crystals confirms the hypothesized sequential kinetic mechanism obtained from initial velocity studies, where both substrates must be bound before catalysis (12). This is a mechanism that is similar to that proposed for UDP-N-acetylglucosamine acyltransferase (21).

N-Acetylglucosamine-1-PO₄ uridylyltransferase (GlmU)

GlmU is similar to Vat (D) and PaXAT, both in structure and mechanism. The enzyme is trimeric and bifunctional, catalyzing the last two sequential reactions in the *de novo* biosynthetic pathway for UDP-GlcNAc (39-41) (Scheme 9).

Scheme 9.



The C-terminal domain catalyzes the CoA dependent acetylation of GlcN-1-PO₄ to GlcNAc-1-PO₄. This domain displays the longest left-handed parallel β -helix that has been observed, containing 11 complete or partial coils (40). The N-terminal domain catalyzes uridylyl transfer from UTP to GlcNAc-1-PO₄ to form the final products UDP-GlcNAc and pyrophosphate. This domain with the pyrophosphorylase activity does not contain the

LβH structure (40). The two active sites are segregated into domains that are thought to act independently (44, 45). The two domains are connected by a long 21-residue helix oriented nearly perpendicular to the 3-fold axis of the enzyme. The result is a trimeric molecule with a mushroom-like appearance consisting of a left-handed β-helical stalk connected to a globular pyrophosphorylase domain cap (40).

Carbonic Anhydrase

Carbonic anhydrases are Zn²⁺-containing enzymes that catalyze the reversible hydration of CO₂ (Scheme 10). The carbonic anhydrase from *Methanosarcina thermophila* that contains the hexapeptide repeat exhibits no significant sequence similarities to other known carbonic anhydrases (46). It is also unique as a hexapeptide protein in that it does not catalyze the transfer of a phosphopantotheryl moiety.

Scheme 10.



Other Enzymes

A few other enzymes have been identified as hexapeptide proteins and isolated. Little is known, however, about their kinetic and chemical mechanisms. Dap D, which codes for succinyldiaminopimelate aminotransferase, transfers an amino moiety from glutamate to N-succinyl-ε-keto-α-aminopimelate (47). This is a unique hexapeptide enzyme

in that it is an aminotransferase, containing the pyridoxal phosphate cofactor. The Ssc protein of *Salmonella typhimurium* is a hexapeptide protein determined to be essential for growth and for the integrity of the outer membrane of *E. coli* and *Salmonella typhimurium* (48). The tms protein of *Salmonella* is another example. Tms has an analogue in *Bacillus subtilis* known as gcaD. The gcaD gene encodes N-acetylglucosamine 1-phosphate uridyltransferase

NONHEXAPEPTIDE ACYLTRANSFERASES

Not all acetyltransferases/ acyltransferases are hexapeptide proteins containing the L β H structural motif. In fact, many acyltransferases have been shown not to contain the hexapeptide repeat. These enzymes are involved in acetylating antibiotics (49), fatty-acid β -oxidation (50), and methionine biosynthesis (51). Many of the identified acyltransferases are involved in lipid metabolism. Only two of the nonhexapeptide acyltransferases have been crystallized. Those two enzymes are chloramphenicol acetyltransferase (30) and human peroxisomal carnitine acetyltransferase (52). The properties of the enzymes in this class are summarized in table 2.

Table 2. Non Hexapeptide Acyltransferases

Acyl Acceptor	Acyl Donor	E.C.number	Species	Pathway	Subunit Composition	MW (kDa)	Ref.
chloramphenicol	AcetylCoA	2.3.1.28 ¹	<i>Escherichia coli</i>	antibiotic	trimer	25	57
homoserine	SuccinylCoA	2.3.1.46 ²	<i>Escherichia coli</i>	methionine/ SAM biosynth.	dimer	35.79	71
homoserine	AcetylCoA	2.3.1.31 ³	<i>Haemophilus influenzae</i>	methionine biosynthesis	dimer	40	72
carnitine	PalmitoylCoA	2.3.1.21 ⁴	<i>Homo sapiens</i>	fatty-acid beta oxidation	monomer	66.4	63
carnitine	AcetylCoA	2.3.1.7 ⁵	<i>Homo sapiens</i>	energy metabolism	monomer	70.78	58
choline	AcetylCoA	2.3.1.6 ⁶	<i>Homo sapiens</i>	cholinergic synapses	monomer	70.48	68
CoA	acetyl phosphate	2.3.1.8 ⁷	<i>Methanosarcina thermophila</i>	energy-yeilding pathway	monomer	35.22	137
cholesterol		2.3.1.43 ⁸	<i>Homo sapiens</i>	cholesteryl ester synth.	monomer	49.59	119
N-acetylneruaminic acid	AcetylCoA	2.3.1.44 ⁹	<i>Homo sapiens</i>	glycoprotein biosynthesis		40.31	138

Non Hexapeptide Acyltransferases

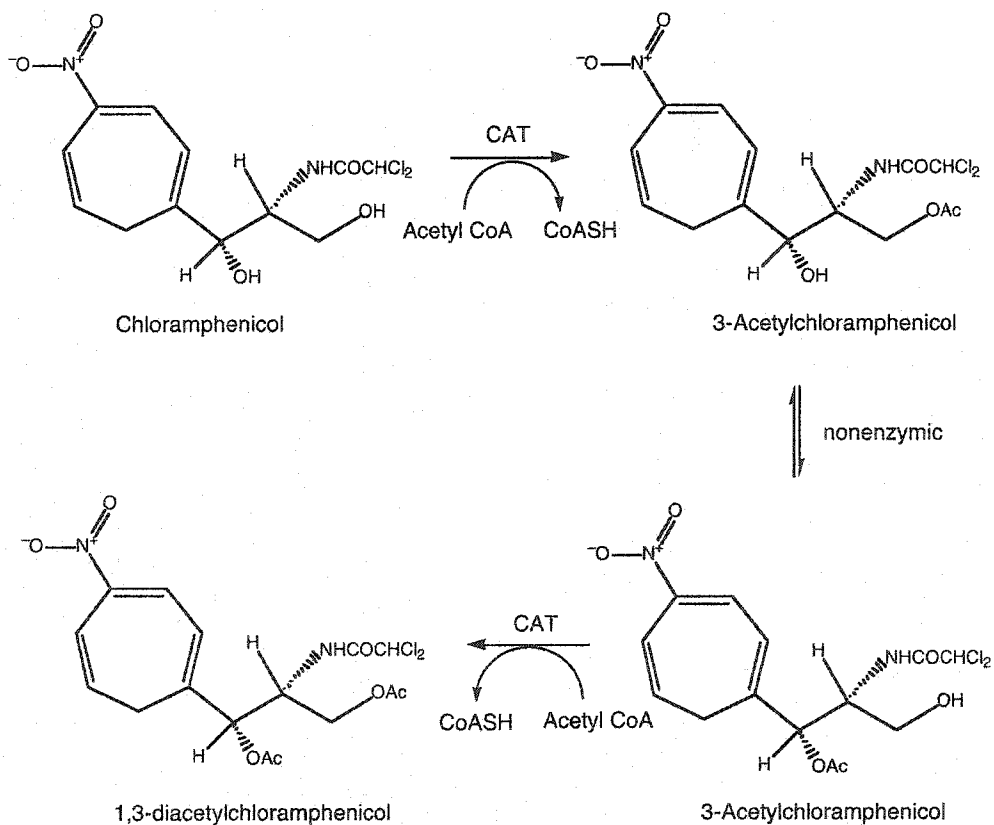
Acyl Acceptor	Acyl Donor	E.C.number	Species	Pathway	MW (kDa)	Reference
glycero-3-phosphate	fatty acyl or acyl carrier prot.	2.3.1.15 ¹⁰	<i>Escherichia coli</i>	lipid metab.	91.39	139
lysophosphatidic acid	fatty acyl or acyl carrier prot.	2.3.1.51 ¹¹	<i>Salmonella typhimurium</i>	lipid metab.	27.34	106
monoacylglycerol	fatty acyl or acyl carrier prot.	2.3.1.51	<i>Homo sapiens</i>	lipid metab.	38.2	231
glycerone phoph.	fatty acyl	2.3.1.42 ¹²	<i>Saccharomyces cerevisiae</i>	lipid metab.	84.7	230
2-acylglycerophosphatidylethanol amine	fatty acyl or acyl carrier prot.	2.3.1.42	<i>Escherichia coli</i>	lipid metab.	80.78	139
lysophosphatidyl choline	fatty acyl or acyl carrier prot.	2.3.1.23 ¹³	<i>Homosapiens</i>	lipid metab.	46.67	84
Lysophosphatidyl inositol	fatty acyl or acyl carrier prot.	2.3.1.23	<i>Homo sapiens</i>	lipid metab.	52.08	106

- 1.Chloramphenicol acetyltransferase 2.Homoserine transsuccinylase 3.Homoserine acetyltransferase 4.Carnitine palmitoyltransferase 5.Carnitine acetyltransferase 6.Choline acetyltransferase 7.Phosphotransacetylase 8.lécithin:cholesterol acyltransferase 9.N-acetylneuraminatase acetyltransferase 10.glycerophosphate acyltransferase 11.lysophosphatidic acid acyltransferase (monoacylglycerol acyltransferase) 12.Lysophosphatidicinositol acyltransferase (Lysophosphatidylethanolamine acyltransferase) 13.lysophosphatidylcholine acyltransferase (Dihydroxyacetone phosphate acyltransferase)

Chloramphenicol acetyltransferase

The prototypical and most widely studied example of a non-hexapeptide acetyltransferase is chloramphenicol acetyltransferase. Chloramphenicol acetyltransferase (CAT) catalyzes the 3-*O*-acetylation of chloramphenicol using acetyl-CoA as an acyl donor (Scheme 11). The acetylated antibiotic (chloramphenicol) does not inhibit protein synthesis as it fails to bind to the peptidyltransferase center of prokaryotic ribosomes (49, 53, 54). Of all the variants of CAT described, the type III enzyme (CAT_{III}) has been studied in the greatest detail.

Scheme 11.



The structures of the binary complexes of CAT_{III} with chloramphenicol and CoA have been determined (30, 31) (Fig. 8). CAT_{III} is a trimer of identical subunits of M_r 25,000 with three active sites per trimer located at each of the subunit interfaces. Chloramphenicol and CoA approach each active site from opposite faces of the protein via a tunnel that is formed upon the binding site of the two substrates (55). This structural separation of substrate binding sites explains the steady-state kinetic studies, which demonstrated that CAT_{III} follows a rapid-equilibrium random kinetic mechanism (56, 57). Although there is no similarity in the overall polypeptide chain folds for CAT_{III} and the hexapeptide enzymes discussed previously, its trimeric structure, substrate bound tunnel, and sequential mechanism are similar to that reported for the LβH enzymes.

The chloramphenicol and CoA binding sites in the subunit interface are largely composed of residues from a single subunit. However, His 195, which is supplied by the opposing subunit, has been identified as an essential catalytic residue. Using 3-(bromoacetyl)chloramphenicol as an active-site directed inhibitor of CAT, Kleantous did chemical modification studies to identify His195. The inhibitor inactivates the enzyme by specific and stoichiometric alkylation at N^{ε2} of His195 (29). A mechanism for CAT was then proposed in which N^{ε2} of His195 acts as a general base to deprotonate the 3-hydroxyl group of chloramphenicol, thereby promoting nucleophilic attack at the carbonyl of the thioester of acetyl CoA (29). Further studies of the His195 residue, including site-directed mutagenesis of His 195 to alanine and glutamine, have shown that it is the residue primarily responsible for catalytic activity (55). The role of a histidine as a general base is another

similarity to the L β H enzymes.

Although the kinetic mechanism for CAT had been determined previously (56), further kinetic studies using both steady-state and transient methods have shown that the formation of the ternary complex of CAT with both substrates is rapid in both the forward and reverse directions. Also, the rate of product release from the CAT:product binary complexes is slow. It has been suggested that a minor modification of the proposed mechanism allows catalysis to occur rapidly, unimpeded by slow product release steps, such that interconversion of the central ternary complexes determines the overall rate of the reaction (58).

Carnitine and Choline Acetyltransferase

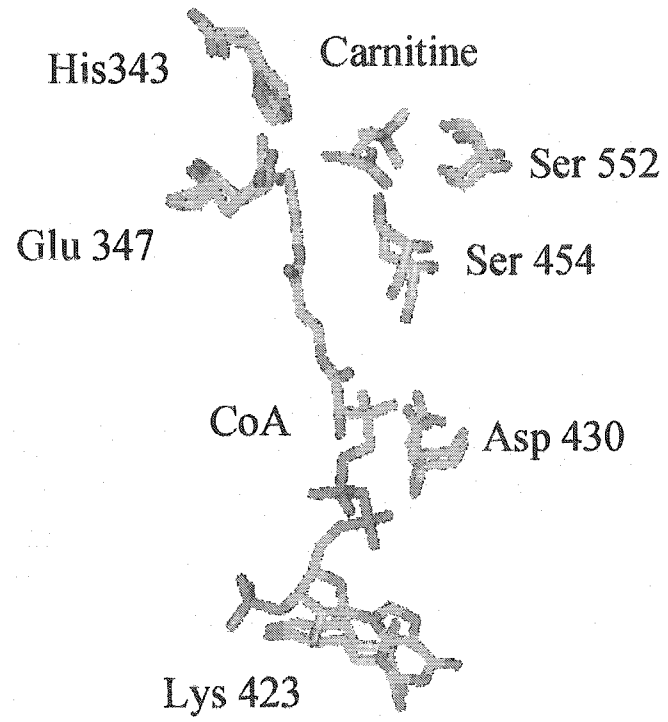
Carnitine acyltransferases catalyze the reversible transfer of acyl groups between CoA and carnitine (50) (Scheme 12). Carnitine acetyltransferase has a substrate preference for short chain acyl CoAs and is found in the mitochondrial matrix, the endoplasmic reticulum, and the peroxisome (59). Recently, the structure of human peroxisomal carnitine acetyltransferase (hpCAT) was published providing a molecular basis for fatty acyl transfer (52) (Fig. 3).

Figure 3. (A) Crystal structure of carnitine acetyltransferase (pdb code 1NM8 (human); 1NDI and 1NDF (mouse)). The program pymol was used to visualize the structure from the pdb file. (B) A close up of the active site is provided with bound substrate labeled. Some of the residues important for binding are shown. Histidine 343 has been shown to be important for catalysis.

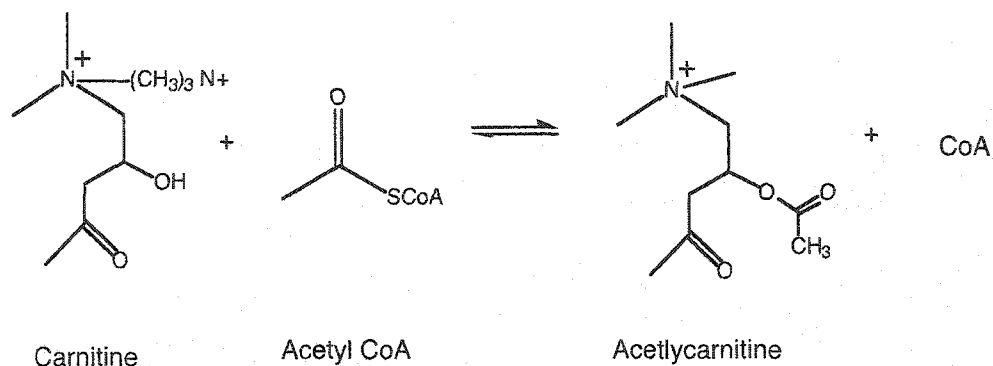
A



B



Scheme 12



HpCAT has two equally sized α/β domains that form a central tunnel. The tunnel traverses the molecule and defines a solvent-accessible surface in the center of the protein, which constitutes the putative active site of the enzyme (52). This is again a similar structural feature as that discussed for chloramphenicol acetyltransferase and the L β H enzymes. A histidine residue, His 322, Fig. 3, is completely conserved among CATs, and is positioned in the center of the active site tunnel. This allows access to this essential residue from either side, suggesting that the binding sites for CoA and carnitine lie on opposite sides of this tunnel. Each substrate approaching the active site tunnel from opposite sides independently is consistent with the rapid equilibrium ordered kinetic mechanism proposed for this enzyme (60). His 322 adopts an unusual conformation which most probably allows positioning of the imidazole N3 to align with carnitine, enabling the abstraction of a proton from its primary alcohol (52). A similar active site histidine has been observed for chloramphenicol acetyltransferase (see above) (30, 61). The histidine residue is essential for catalysis in all members of the carnitine/choline acyltransferase

family (52).

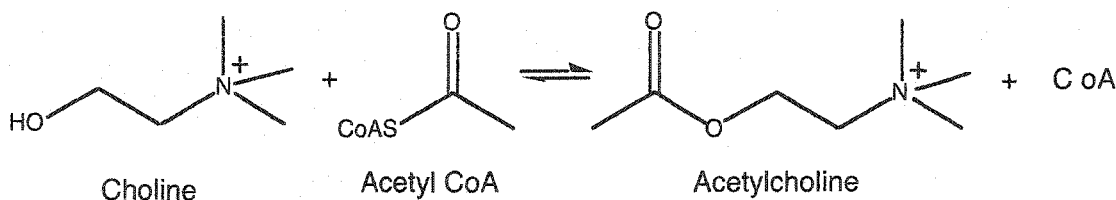
Based on the structure of hpCAT, a catalytic mechanism utilizing a His-Glu/Asp dyad has been proposed (52). This is similar to serine acetyltransferase, which has a proposed catalytic dyad made up of His 154A and Asp 139B (9). His 322 acts as a general base to deprotonate the primary alcohol of carnitine as it attacks the acetyl CoA, resulting in a positively charged histidine. Glu 326 serves to polarize the histidine to increase catalytic activity while also stabilizing the positive charge that develops on the imidazole ring. The deprotonation of carnitine facilitates the nucleophilic attack of the carbonyl carbon of the thioester bond of acetyl coenzyme A, resulting in the formation of a tetrahedral intermediate. Ser 533 in the active site is in the proper orientation to stabilize the negatively charged oxyanion intermediate. The intermediate then collapses to generate acetylcarnitine and coenzyme A. This catalytic mechanism is likely conserved across the carnitine/choline acyltransferase family (52). CAT shares about 30-35% amino acid sequence identity to the other carnitine acyltransferases(62).

Carnitine palmitoyltransferase (CPT1) is an integral mitochondrial membrane protein that catalyzes the transfer of the long-chain acyl group of the acyl CoA ester to carnitine (62). This is the first component of the carnitine palmitoyltransferase system, which imports long-chain fatty acids into the mitochondrial matrix (63, 64). CPT1 is regulated by malonyl-CoA, its physiological inhibitor (65, 66) and is anchored in the mitochondrial outer membrane (67). CPT1A protein contains a highly folded, trypsin-resistant core within its C-terminal catalytic domain and a catalytic histidine residue.

According to mutagenesis studies and structural modeling studies, the enzyme contains conserved residues in the catalytic site consisting of two structurally important glycines and an alanine (62). The glycine residues are structurally part of the hydrophobic core of the catalytic site and create additional space for binding the long acyl chains. The alanine residue is crucial to the stability of CPT1. Mutants of this residue caused conformational changes affecting the active site (62).

Choline acetyltransferase (ChAT) catalyzes the reversible formation of acetylcholine, transferring the acetyl group of acetyl CoA to choline (Scheme 13). ChAT is a single-strand globular protein and is used to monitor the functional state of cholinergic neurons in the central and peripheral nervous systems (68). A Theorell-Chance mechanism has been proposed for the enzyme by means of isotope exchange at equilibrium (69). The mechanism is random with a low steady state level of ternary complexes. The kinetically predominant pathway is one in which acetyl CoA binds prior to choline and acetylcholine is released prior to CoA.

Scheme 13.



ChAT is a member of the carnitine/choline acyltransferase family and is thought to

have a chemical mechanism similar to carnitine acetyltransferase (52). Kinetic and chemical modification studies of rat ChAT have identified an active site arginine (R452) as an important residue for binding CoA (70).

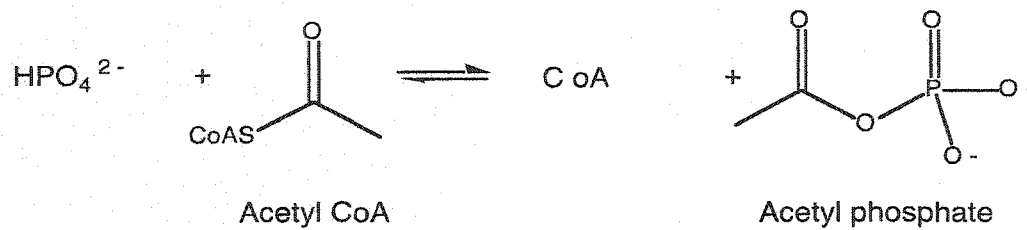
Phosphotransacetylase

Phosphotransacetylase catalyzes the transfer of an acetyl group from acetyl phosphate to coenzyme A (CoA) (Scheme 14). The enzyme is an important component of the energy-yielding pathway in most anaerobic microbes. The phosphotransacetylase from *Methanosarcina thermophila* has been studied as a model for all phosphotransacetylases (71).

This enzyme shares a 51% to 79% deduced sequence similarity to phosphotransacetylases from at least 34 different organisms. Several residues important to the phosphotransacetylase reaction have been identified via chemical modification and site-directed mutagenesis studies (72-74). A cysteine has been identified as an essential active-site residue for the enzyme from *Clostridium kluyveri* (72). However, mutagenesis studies for the *M. thermophila* enzyme have shown that its active site cysteine is nonessential for catalysis (74). A second cysteine (Cys 159) has been identified as being important for structural stability (74). Residues Arg 87 and Arg 133 are completely conserved and shown to be important for binding CoA, having increased K_{CoA} values for all variants relative to wild type. Arg 87 forms a salt bridge with the 3'-phosphate of CoA while Arg 133 is thought to either form a salt bridge with one of the two 5'-phosphate

groups of CoA or participate in a hydrogen bond with another part of the CoA molecule (71).

Scheme 14.



Inhibition studies have shown that phosphotransacetylase binds desulfo-CoA 200 times more tightly than CoA. This suggests that the enzyme selectively destabilizes the substrate CoA, utilizing the binding energy to increase the rate of the reaction rather than to cause tight binding (75). Kinetic studies with Arg 87 and Arg 133 mutants suggest that these residues are important but not essential for catalysis. They may be important to optimally position the substrate for nucleophilic attack of the thiolate anion of CoA on the carbonyl carbon of acetyl phosphate (71).

Arg 310 is also conserved among all phosphotransacetylases. Its function is unknown but it is hypothesized to interact with acetyl phosphate to orient the substrate or to polarize the carbonyl group, facilitating a nucleophilic attack by CoA (76). Inhibition studies indicate this residue may be important for catalysis (71).

NUCLEOPHILIC/COVALENT ENZYMES

The acyltransferases discussed throughout the remainder of this review are members of the protease/lipase/hydrolase family. These enzymes differ in mechanism from those discussed previously, falling under the second general category mentioned in the introduction, the covalent/nucleophilic mechanism.

Homoserine Acetyltransferase/Succinyltransferase

L-Homoserine is a common precursor in the synthesis of methionine, threonine, and isoleucine. The first unique step in methionine biosynthesis is the acetylation of homoserine to *O*-acetylhomoserine (OAH)/ or *O*-succinylhomoserine (OSH). This step activates the C4 carbon of homoserine for the subsequent nucleophilic attack by cysteine.

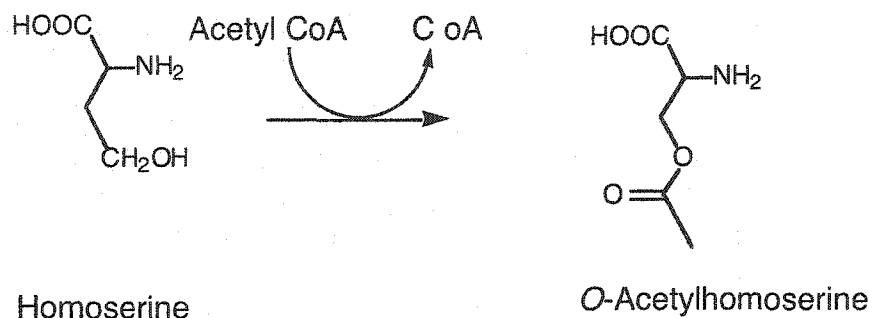
The homoserine acetyltransferase (HAT) from *Haemophilus influenzae* catalyzes the transfer of acetate from acetyl-CoA to homoserine (77) while homoserine succinyltransferase (HST) transfers a succinyl group from a succinyl CoA donor (Scheme 15). Unlike homoserine succinyltransferase, HATs are not feedback inhibited by L-methionine or SAM (51, 78). They are, however, reversibly inhibited by zinc (79).

The crystal structure for HAT or HST has not yet been solved. Kinetic data indicate that HAT and HST utilize a ping-pong kinetic mechanism where the acyl group is transferred to an active-site nucleophile during the first half-reaction, followed by transfer to homoserine during the second half-reaction (77, 80), a mechanism similar to that proposed for serine acetyltransferase from *Salmonella typhimurium* (16, 81). For HAT,

there is no dependence of the maximal velocity on pH from pH 5.5-9. The dependence of $V/K_{\text{acetyl-CoA}}$ on pH shows a single group exhibiting a pK value of 8.6 that must be protonated. The $V/K_{\text{homoserine}}$ profile also appears to be pH independent over the range tested (77).

Along with the kinetic and pH data, isotope effects and rapid quench labeling studies allow a chemical mechanism to be proposed in which an HAT nucleophile attacks the thioester bond of acetyl CoA to form an initial tetrahedral intermediate. The intermediate must then break down to form the acetylated enzyme and CoA. Homoserine binds to the acetyl-enzyme intermediate in the second half-reaction. An active-site base is required to remove the proton from the γ -hydroxyl group before it can attack the acetyl-enzyme to form a tetrahedral intermediate. This base is not observed in the $V/K_{\text{homoserine}}$ pH profile over the range tested. Finally, the tetrahedral intermediate breaks down to form the final product, *O*-acetylhomoserine, and regenerate active enzyme (77).

Scheme 15.



The identity of the catalytic nucleophile is unknown. The catalytic nucleophile for the similar homoserine succinyltransferase has been identified as a cysteine residue (80). However, there are no conserved cysteine residues in HAT nor is there any physicochemical evidence for the involvement of a cysteine residue in HAT. The conserved residues in the active site include three serines, two histidines, and six aspartic acid residues. The conserved S143 is found in a G-G-S-X-G-G sequence. This motif, G-X-S/C-X-G has been identified as a signature sequence for the lipase superfamily (77). The enzymes in this superfamily contain a catalytic "triad" of serine, aspartic acid, and histidine (82, 83). The histidine has been assigned the role of general base to activate serine for nucleophilic attack. The aspartic acid in some cases has been shown not to be essential (77).

Acyltransferases from phospholipid biosynthesis and fatty acid remodeling

Some acyltransferases are involved in the acylation of lysophospholipids and the biosynthesis of phospholipids and fatty acid remodeling (84-89). These acyltransferases maintain membrane lipid composition and the asymmetrical distribution of unsaturated fatty acids within phospholipids, and control free arachadonic acid levels. It has been suggested that the distinct molecular compositions of phospholipids is intimately linked to cellular functions (90).

Some of the enzymes participating in fatty acid remodeling are shown in table 2. Little is known structurally or mechanistically about these enzymes and they will therefore

not be discussed.

Lecithin:cholesterol Acyltransferase (LCAT)

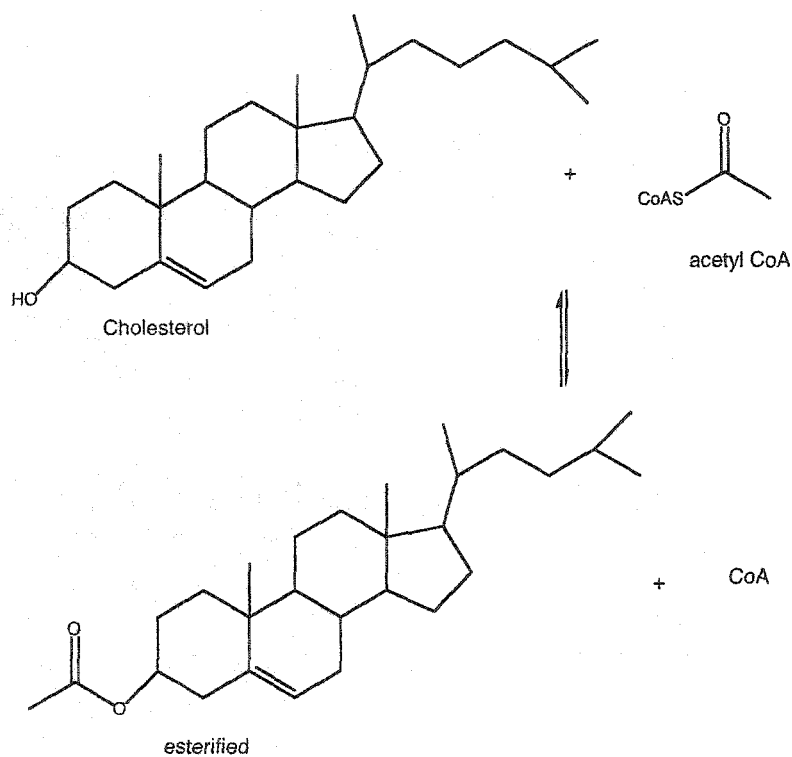
High-density lipoproteins (HDL) have a protective effect against atherosclerosis (91). The unesterified cholesterol of HDL is the primary substrate for LCAT, which plays a role in the reverse cholesterol transport pathway. This pathway consists of cholesterol efflux from the tissue surface, esterification of free cholesterol by LCAT (this step generates the majority of plasma cholesteryl esters (CE)), and delivery of HDL back to the liver to be degraded (92, 93). The LCAT activity that catalyzes this esterification requires the presence of ApoA-I as a cofactor (94) (Scheme 16).

The X-ray structure of the human apoA-I has been solved (95). The crystal structure is a twisted circular four-helix bundle, consisting of four molecules of ApoA-I, where four copies of LCAT are located. The tetramer forms a ring structure with the LCAT activating domains located outside the ring structure and aromatic-rich strong lipid-binding domains located inside. Each monomer contains two tryptophans (Trp50 and Trp72), which are oriented toward the center of the ring in order to initiate lipid binding. Conformational rotations are induced by lipid binding.

The activity of LCAT that utilizes HDL is termed α -LCAT, while activity of LCAT that utilizes low-density lipoproteins (LDL) and does not require ApoA-I as a cofactor is termed β -LCAT (94). LCAT is an interfacial enzyme that catalyzes the transesterification of cholesterol at the lipid-water interface of the lipoprotein particle. The

enzyme must bind to the lipoprotein surface, and then accept its substrate by diffusion into its substrate-binding pocket (96). LCAT contains a 24 amino acid lid domain in a disulfide-bonded surface loop (97). The lid may be involved in regulating substrate access to the active site (98) and interfacial activation of lipases (99, 100). The lids removal abolishes LCAT activity using lipoprotein substrates (101).

Scheme 16.



Computer modeling of LCAT identified it as a member of the α/β hydrolase fold family, containing a central seven-stranded β -sheet domain flanked by two sets of α -helices (102). The N-terminal region of LCAT is highly conserved with the first ten residues

highly hydrophobic. It is hypothesized that these residues interact with residues near the substrate-binding pocket to help anchor the lid domain into the proper orientation for enzyme function (96). Modeling also suggests that three critical arginine residues in ApoA-I (Arg 149, Arg 153, Arg 160) would be directly involved in interactions with LCAT to facilitate activation (103, 104). Mutagenesis studies suggest that N-terminal deletion of the enzyme results in a loss of activity but does not affect substrate binding (96)

CONCLUSION

In the review of hexapeptide acyltransferases, many similarities can be seen. Structurally, all of the hexapeptide enzymes contain the amino acid hexapeptide repeat, which encodes the left-handed β -helix domain. The L β H domains vary in length, but all contribute to the active sites of the enzymes. The long narrow clefts between these domains compliment the various lengths of acyl chains from the acylpantothenyl donors. Separate binding sites for substrates are also afforded by the active site structures. This is another similarity shown by crystal structures of enzyme substrate complexes. Once the substrates are bound to the enzyme, a short tunnel is formed by an external loop. These conformational changes takes place to block substrate from bulk solvent and properly orient the substrates for catalysis. The separate binding sites also allow for the common sequential kinetic mechanism of the enzymes.

The mode of catalysis of the enzymes also appears to be similar. All of the L β H enzymes follow the same general mechanism utilizing acid-base catalysis. A conserved histidine residue acts as a general base to deprotonate the alcohol of the nucleophilic substrate, promoting its nucleophilic attack on the carbonyl of the acyl group to be transferred. Another seemingly common feature of the acid base catalysis is that the histidine is part of a catalytic dyad. The other residue participating in the dyad serves to polarize the histidine and increase catalytic activity while also stabilizing the positive charge that develops on the imidazolering. The crystal structure of serine acetyltransferase identifies a residue for this role. Although these mechanistic features are similar for the majority of hexapeptide enzymes, some exceptions such as hexapeptide enzymes that transfer acyl groups to amines and a hexapeptide enzyme that does not transfer an acyl group at all were noted.

More structural and mechanistic variety can be observed in the nonhexapeptide acyltransferases. The chloramphenicol, carnitine, choline, and phospho-acyltransferases, although not hexapeptide proteins, follow the same general base mechanism. These enzymes are not structurally similar to the hexapeptide enzymes but do maintain many of the same catalytic features. The enzymes have separate binding sites for the substrates allowing for approach from opposite sides of the proteins. A tunnel forms upon binding of the two substrates and, subsequently, all of the enzymes have a proposed sequential kinetic mechanism. The above nonhexapeptide enzymes also appear to have a histidine residue as the catalytic general base. The histidine is again part of a catalytic dyad.

Carnitine acetyltransferase for example, contains a glutamine residue, which polarizes the histidine and stabilizes the positive charge that develops on the imidazole ring. The histidine residue again acts as a general base to deprotonate the alcohol of the nucleophilic substrate, promoting its nucleophilic attack on the carbonyl of the acyl group to be transferred.

The remaining nonhexapeptide proteins discussed differ in mechanism from the chloramphenicol, carnitine, choline, and phospho-acyltransferases. These enzymes utilize a covalent/nucleophilic form of catalysis and are members of the hydrolase, lipase, and protease families according to their solved structures and/or amino acid sequence homologies. Unfortunately, little kinetic or mechanistic work has been done with these enzymes. Different kinetic mechanisms have been proposed for these acyltransferases. Homoserine acetyltransferase has a proposed ping pong kinetic mechanism. The covalent/nucleophilic mode of catalysis involves a catalytic triad rather than the dyad utilized by the general base catalyzed enzymes. Homoserine acetyltransferase is an example of an enzyme with this proposed catalytic triad, in which histidine is assigned the role of general base. However, the similar homoserine succinyltransferase has a cysteine residue as its general base and the enzymes involved in fatty acid remodeling have a proposed aspartate residue general base.

In this brief review of acyl transfer to alcohols, it is evident that a variety of enzyme structures and mechanisms are involved. Not all enzymes catalyzing acyl transfer are hexapeptide proteins. Not even all hexapeptide proteins are involved in acyl transfer

(carbonic anhydrase). Some kinetic and chemical mechanisms of the hexapeptide enzymes are proposed to be the same while others differ. Even a nonhexapeptide acyltransferase can catalyze the same reaction as a hexapeptide acyltransferase; as in the case of chloramphenicol acetyltransferase and xenobiotic acetyltransferase. However, the existing knowledge of these acyltransferases can be utilized to direct further research and aid in the elucidation of the kinetic and chemical mechanism of serine acetyltransferase from *Haemophilus Influenzae* (HiSAT).

This review provides the questions that will be asked to determine the kinetic and chemical mechanism of HiSAT. The HiSAT is a hexapeptide protein containing the L β H structural domains and it catalyzes the transfer of an acetyl group to an alcohol. Therefore, the following questions can be asked concerning the mechanism of the reaction: Does the HiSAT proceed by a sequential mechanism? Is it a random or ordered mechanism? What are the rate limiting steps of the reaction? What type of catalysis does HiSAT utilize? Is it a general base mechanism or a covalent/nucleophilic mechanism? What residues are important for catalysis and binding? If it is a general base mechanism, what is the general base? The answers to these questions and others will be provided by the experiments in the following chapters and will hopefully lead to a better understanding of the HiSAT reaction and the mechanism of acyl transfer to alcohols in general.

Chapter 2

Cysteine Biosynthesis

Sulfur exists in a wide range of oxidation states in nature. Various organisms are able to interconvert sulfur between its oxidized and reduced forms and living organisms assimilate inorganic sulfur into organic acids in different ways. Cysteine and methionine, the two common sulfur-containing amino acids, are related with respect to routes for their synthesis. Cysteine can be synthesized by transulfuration of homocysteine, which is a product of methionine degradation. It can also be synthesized by the incorporation of the sulfur from inorganic sulfate into cysteine (105). This dissertation deals exclusively with this latter pathway.

Inorganic sulfate is the sulfur source for the *de novo* synthesis of L-cysteine. Sulfate is taken up by the cell and subsequently reduced to sulfide. Sulfide, which is a substrate for the final enzyme-catalyzed reaction in this pathway, is unstable in an aerobic environment. This instability necessitates the uptake of the most highly oxidized form of sulfur, sulfate. The uptake of sulfate is carried out via the sulfate reduction pathway (106).

All sulfate-assimilating organisms carry out this process by an essentially identical sequence of reactions (107). A detailed description of the genes participating in all steps of the pathway (the *cys* regulon) has been provided for both *Escherichia coli* and *Salmonella enterica*(106).

Sulfate Reduction in Enteric Bacteria

Sulfate metabolism begins with its entrance into the cell. This is done by sulfate permease, which also can transport thiosulfate into the cell. The uptake of sulfate into the periplasmic space takes place via a membrane channel, which is activated by a membrane-associated nucleotide binding protein (108). There are two separate binding proteins for sulfate (109) (*sbp*), and thiosulfate (*cysP* gene product) (110) in the periplasm. Each protein has a leader sequence to aid transport across the inner membrane into the cytoplasm.

The uptake of sulfate must be followed by activation and reduction reactions before it can be utilized metabolically, Fig. 4. There are two forms of activated sulfate, adenosine 5'-phosphosulfate (APS) and 3'-phosphoadenyl 5'-phosphosulfate (PAPS). Sulfate first forms a mixed anhydride with AMP catalyzed by the enzyme ATP-sulfurylase (111), a heterooctamer of four catalytic and four regulatory subunits (112). ATP-sulfurylase catalyzes the conversion of MgATP and sulfate to adenosine 5'-phosphosulfate (APS) and PP_i , which has a solution equilibrium constant of approximately 10^{-8} (111). To compensate for the low K_{eq} , inorganic pyrophosphate is hydrolyzed to help drive the reaction toward APS production. The hydrolysis of GTP by the Ras-like regulatory subunit is coupled to the formation of an AMP- (ATP sulfurylase) complex, from which APS is formed upon attack by sulfate (113-116).

Fig. 4. Pathway for L-cysteine biosynthesis and function of the cysteine regulon. The genes making up the cysteine regulon and the enzymes for which they code are labeled. Sulfate is brought into the cell and subsequently reduced to sulfide. Sulfide is the oxidation state of sulfur utilized for the *O*-acetylserine sulfhydrylase reaction to produce the final product cysteine. All enzymes and reactions are discussed in chapter 2.

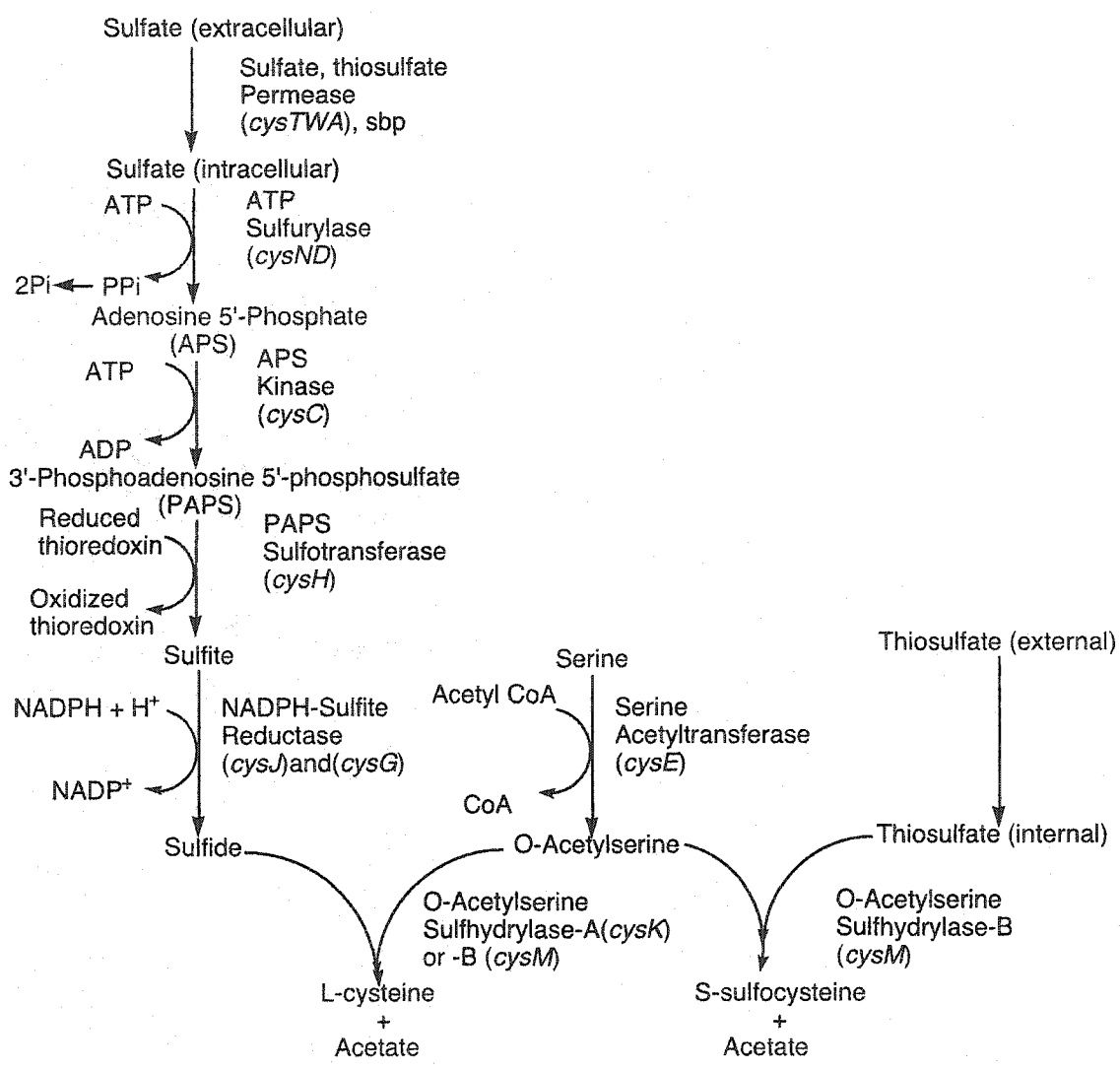


Figure 4.

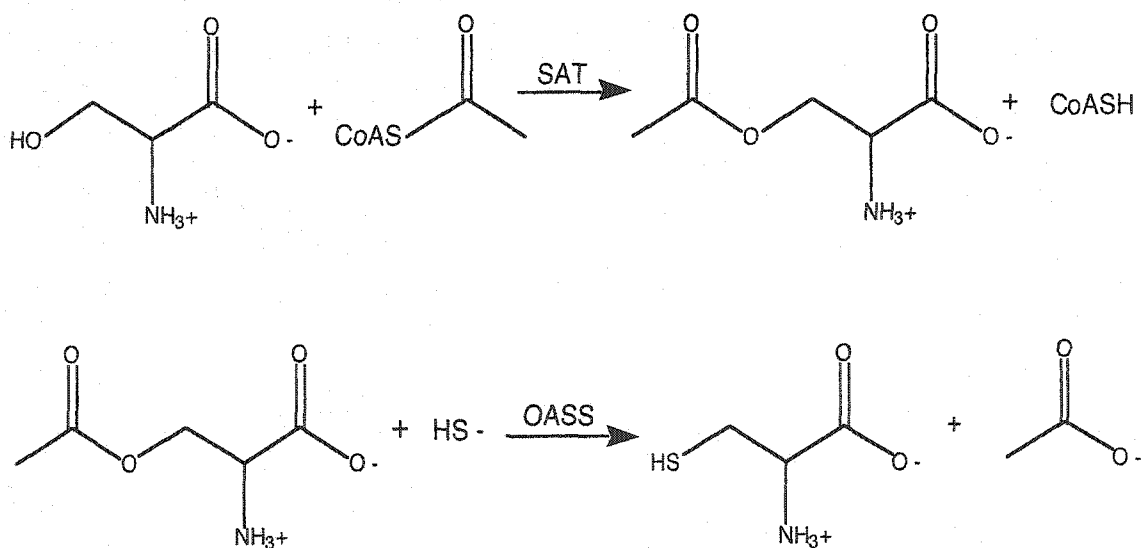
The APS is then converted to 3'-phosphoadenosine 5'-phosphosulfate(PAPS) via a second MgATP-dependent phosphorylation, catalyzed by the dimeric APS kinase. The reaction is thought to proceed via a phosphoenzyme intermediate(117, 118). ATP-sulfurylase and APS kinase are specified by the *cysD* and *cysC* genes, which in *Salmonella typhimurium* are closely linked and probably contiguous (119).

The homodimeric PAPS sulfotransferase then generates sulfite (120). The enzyme catalyzes the transfer of the sulfonyl moiety of PAPS to one of the thiols of a redox active disulfide of thioredoxin to form acceptor-S-SO₃⁻, which generates oxidized thioredoxin and sulfite (121, 122). The PAPS sulfotransferase is specified by *cysH*. The final step of the pathway is the six-electron reduction of sulfite to sulfide catalyzed by sulfite reductase. The sulfite reductase is a complex enzyme, composed of two different polypeptides, α , a flavoprotein with either FMN or FAD bound, and β , a hemoprotein with a Fe₄S₄ cluster and siroheme components (123). The α and β proteins are specified by *cysJ* and *cysI*; the two genes are contiguous. The overall stoichiometry of the complex is $\alpha_8\beta_4$, with four FAD and four FMN bound to the eight α -subunits. The pathway for the electron transfer is from the physiologic electron donor NADPH→FAD→FMN→Fe₄S₄→siroheme→sulfite (124, 125). Another protein required for the reduction of sulfite is the *cysG* gene product, an S-adenosyl-methionine dependent uroporphyrinogen III methylase, responsible for synthesis of siroheme (126). The sulfide subsequently produced is the precursor for the synthesis of cysteine in enteric bacteria.

Cysteine Biosynthesis in Enteric Bacteria

The biosynthesis of L-cysteine in bacteria and plants proceeds via a two-step pathway (scheme 16). L-Serine is the amino acid precursor of L-cysteine, which is first acetylated at its β -hydroxyl by acetyl-CoA to give *O*-acetyl-L-serine (OAS). This reaction is catalyzed by the enzyme serine acetyltransferase (SAT) (14). *O*-Acetyl-L-serine is the immediate precursor of the carbon moiety of cysteine. The final step in cysteine synthesis, replacement of the acetate side chain by a thiol, is catalyzed by *O*-acetylserine sulfhydrylase (OASS), and inorganic sulfide acts as the thiol donor (15). In addition to the utilization of sulfate to form L-cysteine, thiosulfate, a more reduced form of sulfur, can be used in place of sulfide to give *S*-sulfo-cysteine (127), which is subsequently reduced to L-cysteine.

Scheme 17.



The regulation of cysteine biosynthesis in enteric bacteria, *E. coli* and *Salmonella*

typhimurium, has been well documented. Regulation is achieved by gene regulation, feedback inhibition by cysteine, and enzyme degradation (106). A regulon is formed by the genes in *S. typhimurium* that encode the enzymes involved in the cysteine biosynthetic pathway. The regulon is made up of the following genes, Fig. 4: *cysTWA* (sulfate permease), *sbp* (periplasmic sulfate-binding protein), *cysND* (ATP sulfurylase), *cysC* (APS kinase), *cysH* (PAPS sulfotransferase), *cysIJ* (sulfite reductase), *cysG* (siroheme synthesis), *cysK* (*O*-acetylserine sulfhydrylase-A), *cysM* (*O*-acetylserine sulfhydrylase-B), *cysE* (serine acetyltransferase), and *cysB* (regulatory protein). The genes are arranged in positively regulated operons, the negatively autoregulated *cysB* gene, and the nonregulated *cysE* and *cysG* genes.

Transcription initiation is facilitated by binding of a tetramer of the *cysB* protein upstream from the positively regulated promoters. *CysB* also regulates its own synthesis by binding to the promoter of the *cysB* gene and inhibiting transcription (106). Gene expression is regulated by both derepression and induction. The activities of the enzymes in the pathway decrease progressively with increased levels of sulfate, sulfide, cysteine, or cystine. Djenkolic acid and reduced glutathione have shown maximum derepression. *O*-Acetylserine, the product of the SAT reaction and the precursor of cysteine, will also intramolecularly rearrange to form *N*-acetyl-L-serine which enhances transcription by binding to the *CysB* protein (128). Sulfide opposes this action.

The major physiologically significant form of the kinetic regulation in the pathway of SAT either free or in complex with OASS is feedback inhibition of SAT by the end

product L-cysteine. Cysteine is a potent inhibitor, with a K_i of 1 μM at 0.1 mM acetyl-CoA for SAT (129). Cysteine therefore regulates its own biosynthesis.

Cysteine Synthetase Mult-enzyme complex

SAT and OASS are physically associated to form a multienzyme complex, cysteine synthetase. The complex accounts for 5% of the total cellular OASS activity, the remaining 95% existing out of complex (129). OAS at concentrations of $\geq 10^{-4}$ M causes the cysteine synthetase complex to dissociate to free SAT and OASS-A. The complex is reconstituted by mixing resolved SAT and OASS-A in the absence of OAS (130). The stoichiometry of complex dissociation indicates that it is composed of a single $\sim 160,000$ Da hexamer (9) of SAT and two 69,000 Da dimers of OASS-A.

Multienzyme complexes like tryptophan synthase utilize the complex to channel the intermediate product between the active sites of the two component enzymes. This is not the case for cysteine synthetase. OAS is actually released into solution and must reassociate with OASS to be converted to L-cysteine (131). Multienzyme complexes usually play a specific role in the regulation of metabolic pathways (132). This kind of role has not been shown for cysteine synthetase as of yet. Therefore, cysteine synthetase is unique in its physical association. The role of the cysteine synthetase complex in L-cysteine biosynthesis is under investigation but is still not fully known.

Recent work on the *E.coli* SAT has provided more insight into the function of the complex. A M256I mutant shown to be less susceptible to cysteine inhibition has been

studied along with a truncated SAT missing the last twenty amino acid residues from the C-terminus (133). The truncated SAT will not form a complex with OASS-A, but is active and shows sensitivity to cysteine inhibition similar to the M256I mutant enzyme. The mutant enzyme forms a complex with OASS-A, and is active either in complex with OASS-A or as the uncomplexed enzyme. No proven relationship between complex formation and sensitivity to inhibition by L-cysteine has been shown. The twenty amino acids of the truncated SAT appear to be at least partially responsible for the interaction with OASS-A to form the complex (134). Terminal regions of SAT from bacteria and higher plants are well conserved (135). Two residues in particular, an aspartic acid and a glutamic acid, located less than 10 residues from the C-terminus, are thought to be key amino acids for interaction between SAT and OASS (136). Studies of the *E. coli* SAT with a different number of residues eliminated at the C-terminus have shown that while the last ten residues of the protein are involved in hienzyme formation, they are not involved in regulation. Studies of residues 11-20, however, have been shown to be partially responsible for the sensitivity to L-cysteine inhibition (136). Studies of SATs from other sources are in agreement. Several amino acids around Met 256 are thought to be involved in the conformational changes necessary for the sensitivity (137, 138).

The C terminal region of SAT is thought to interact with the OASS-A active site (17). OASS-A, as stated earlier, is 50% active in complex (106). However, OASS is present in a large excess to SAT in higher plants (139-141) and bacteria (129). The large excess of OASS-A ensures the formation of the cysteine synthetase multi-enzyme complex

(136)

Although work with mutant and truncated forms of SAT have provided useful information regarding the purpose of the complex, the points of interaction between the enzymes, and even important residues involved in complex formation and regulation, the only significant advantages of the complex to be proven has been stabilization of SAT. The complex protects SAT from cold inactivation and proteolysis (142). Addition of excess OASS-A accelerates the recovery of SAT activity after cold inactivation by acting as a chaperone in the reactivation. By forming the complex, it is possible that OASS depresses the aggregation of the subunit trimers. Protection against proteolysis depends on the kind of protease used. Only proteases acting away from the interaction region of the complex were unhindered by complex formation. The physiological significance of the increased stability against cold inactivation and proteolysis due to complex formation is not yet known (142).

O-Acetylserine Sulphydrylase

O-Acetylserine sulphydrylase-A (OASS-A) is the enzyme in complex with SAT that forms cysteine synthetase. OASS-A catalyzes the last enzymatic step in the pathway; the formation of L-cysteine from sulfide and O-acetyl-L-serine (143). There are two isozymes of OASS, A and B, in enteric bacteria (15). The enzymes from *Salmonella typhimurium* are best studied. The A and B isozymes are thought to be expressed under aerobic and anaerobic conditions, respectively. The large excess of the A isozyme over the

B isozyme during aerobic growth indicates that the former accounts for the majority of L-cysteine synthesis from *O*-acetyl-L-serine and sulfide (144, 145). Both enzymes catalyze the same reaction, but the B isozyme is capable of using thiosulfate as an alternative reactant in *Salmonella typhimurium* (144, 145). Thiosulfate uptake provides an alternative means for cysteine biosynthesis, which eliminates the need for sulfate reduction (146). OASS-A is a homodimer of 68,900 Da (147) and is a PLP dependent enzyme containing one mole of pyridoxal 5'-phosphate (PLP) per subunit (14).

The crystal structure of OASS-A has been solved (148). Both domains of the monomer are type α/β and contain a central β sheet surrounded by several α -helices. One stretch of the N-terminal domain "crosses over" into the C-terminal domain, forming the first two strands of its central β -sheet. The overall structure of OASS-A is similar to that of β -tryptophan synthase (β TRPS) with some exceptions (149). The PLP cofactor is located at the interface between the N- and C-terminal domains and is buried deeply within the protein. It is covalently bound through a Schiff base linkage (internal aldimine) (150) to the ϵ -amino group of Lys41 (151). The 5'-phosphate of PLP is tightly hydrogen-bonded to a glycine/threonine rich loop, with each of the phosphate oxygens accepting two hydrogen bonds from the protein. This finding agrees with the ^{31}P NMR studies of OASS-A (152-154).

The kinetic mechanism of OASS is bi bi ping pong where OAS (the amino acid substrate) binds first to the internal aldimine form of the enzyme (E) and acetate (the nucleophilic product) is released as the first product. Sulfide (the nucleophilic substrate)

is then utilized as the second substrate, adding to the α -aminoacrylate form of the enzyme (F), and L-cysteine (the amino acid product) is released as the final product (152-154).

The first half reaction is rate-limiting overall, while the second half reaction is very rapid (128). A chemical mechanism has been proposed based on the pH dependence of kinetic parameters (155, 156), spectral properties (155, 156), site-directed mutagenesis (151), and deuterium isotope effects (157). The internal Schiffbase is protonated to begin the reaction (152) and OAS binds as the monoanion. The α -amine of the amino acid substrate approaches C4' of the imine for nucleophilic attack at the *re* face. The OAS external Schiff base is formed presumably via *gem*-diamine intermediates. The ϵ -amine of K41 (151), the internal aldimine lysine, is unprotonated (152, 155) and acts as a general base to accept the α -proton of OAS to generate the α -aminoacrylate intermediate. It is not possible to determine whether a quinonoid intermediate forms upon deprotonation of the external aldimine. However, no evidence has been obtained for this intermediate (158). Once the aminoacrylate is formed, the first half of the reaction is complete. Sulfide then binds as SH⁻ (155) and generates the L-cysteine external Schiff base with K41 acting as a general acid to protonate the α -carbon. Again, it is unlikely that a quinonoid intermediate exists in this reaction. Transamination via K41 then occurs to release L-cysteine, and regenerate free enzyme (158).

Conformational changes along the OASS reaction pathway have been predicted by UV-visible (153), fluorescence (159-161), and phosphorescence (162) spectroscopy, site-directed mutagenesis (151), and X-ray structural determination (148, 163). The internal

aldimine exists in an open conformation, while the external aldimine exists in a closed conformation. The α -aminoacrylate external aldimine also exists in a conformation that differs from those of the internal and external aldimines (153, 158, 160-162). The reaction therefore occurs with alternating open and closed conformations of the enzyme.

More recent crystal structures of OASS-A have been solved with chloride bound to an allosteric site on the enzyme and sulfate bound to both the allosteric site and active site (164). The bound anions result in a new partially inhibited conformation that is different from the conformations of the internal and external aldimines. The allosteric site is located at the OASS dimer interface (164). These crystal structures and the characterization of the allosteric site (158) confirm structural changes in the OASS reaction pathway and update the mechanism to show the partially inhibited pathway. Based on these findings, it can also be said that OASS represents a new class of PLP-dependent enzymes that are regulated by small anions. The regulation, in the case of OASS, aids in the regulation of L-cysteine biosynthesis.

Serine Acetyltransferase

A ping pong bi bi kinetic mechanism has been proposed for the SAT from *Salmonella typhimurium* (16). Initial velocity studies in both reaction directions suggested that the enzyme catalyzes the conversion of acetyl-CoA and L-serine to *O*-acetylserine (OAS) and coenzyme A (CoA) by binding acetyl-CoA first and releasing CoA to form an acetylenzyme intermediate. Irreversible inhibition studies with alkylating agents such as

diisopropylfluorophosphate (DFP) and phenylmethylsulfonylfluoride (PMSF) suggested acylation of an active site serine residue (81). Subsequently, L-serine is bound and OAS is released. Inhibition studies were also carried out by measuring initial velocity patterns in the presence of inhibitors. Product inhibition by OAS is competitive with respect to acetyl-CoA and noncompetitive against L-serine, while product inhibition by L-serine is competitive against CoA and noncompetitive against OAS. Glycine and S-methyl-cysteine (SMC) were used as dead-end analogs of L-serine and OAS, respectively. Glycine is competitive against L-serine and uncompetitive against acetyl-CoA. SMC is competitive against OAS and uncompetitive against CoA. All of the inhibition patterns are consistent with those predicted for a single site ping pong bi bi kinetic mechanism. The equilibrium constant was also measured by monitoring the change in CoA concentration obtained for reactions in which the ratio of acetyl-CoA/CoA was constant and the ratio of OAS/serine was varied. The K_{eq} is 15 in the direction of L-serine acetylation. The K_{eq} calculated by the Haldane relationship was in good agreement with the directly measured value (16).

Kinetic work has also been done on the SAT from *Escherichia coli*. A ping pong bi bi kinetic mechanism was proposed for wild type SAT both in and out of the cysteine synthetase complex at pH 7.5 (17). This kinetic work was done to investigate the cysteine synthetase complex, which was discussed previously in this chapter. The ping pong bi bi kinetic mechanism proposed here for the *E. coli* enzyme agrees with the mechanism proposed for the *Salmonella* enzyme by Leu and Cook (16).

The alternative acetyl acceptor threonine and the alternative acyl donor, propionyl

coenzyme A (PrCoA) were used to further investigate the reaction mechanism of SAT from *E. coli* (19). Acetyl transfer to threonine conformed to a steady-state ordered mechanism while the propionyl transfer reaction conformed to a rapid-equilibrium random-ordered mechanism. The propionyl reaction is thought to differ with a slower k_{cat} due to a slower rate of interconversion of the enzyme:substrate and enzyme:product ternary complexes. The specificity of the serine binding pocket was also probed utilizing the three substrate mimics, β -hydroxypropionic acid, glycine, and ethanolamine. These studies show that the amino and hydroxyl moieties of serine contribute to binding, while the carboxyl group provides the most essential binding contribution. The study of the serine binding pocket also provides insight into the mode of inhibition by cysteine. The methylene moiety of threonine appears to be accommodated by the hydroxymethyl contact region of the serine binding site, showing the site is unlikely to exclude cysteine due to short range contacts. The data obtained by means of substrate analogue and microcalorimetric studies satisfies the requirements of a random-order ternary complex mechanism for the SAT from *E. coli* at pH 7.5 (18, 19). The discrepancy in the findings of Leu and Hindson above make it a point of interest to further study and confirm the true kinetic mechanism of serine acetyltransferase.

Chapter 3

Kinetic Mechanism of the Serine Acetyltransferase from *Haemophilus influenzae*

Introduction

As discussed in chapter 2, a ping pong bi bi kinetic mechanism has been proposed for the SAT from *Salmonella typhimurium* (16). Initial velocity studies in both reaction directions suggested that the enzyme catalyzes the conversion of acetyl-CoA and L-serine to *O*-acetylserine (OAS) and coenzyme A (CoA) by binding acetyl-CoA first and releasing CoA to form an acetylenzyme intermediate. Subsequently, L-serine is bound and OAS is released. Inhibition studies were also carried out by measuring initial velocity patterns in the presence of inhibitors. All of the inhibition patterns are consistent with those predicted for a single site ping pong bi bi kinetic mechanism.

Kinetic work has also been done on the SAT from *Escherichia coli*. A ping pong bi bi kinetic mechanism was proposed for wild type SAT both in and out of the cysteine synthetase complex at pH 7.5 (17). The ping pong bi bi kinetic mechanism proposed for the *E. coli* enzyme agrees with the mechanism proposed for the *Salmonella* enzyme by Leu and Cook (16).

Analogs of both serine and acetyl CoA were used to further investigate the reaction mechanism of SAT from *E. coli* (19). Acetyl transfer to threonine conformed to a steady-

state ordered mechanism while the propionyl transfer reaction conformed to a rapid-equilibrium random mechanism. The specificity of the serine binding pocket was probed utilizing the three substrate mimics, β -hydroxypropionic acid, glycine, and ethanolamine. The data obtained by means of substrate analogue and microcalorimetric studies satisfies the requirements of a random-order ternary complex mechanism for the SAT from *E. coli* at pH 7.5 (18, 19).

The discrepancy in the findings of Leu and Hindson above make it a point of interest to further study and confirm the true kinetic mechanism of serine acetyltransferase. The following research was carried out to provide information on the kinetic mechanism of *HiSAT*. In this manuscript, we report an equilibrium ordered kinetic mechanism at pH 6.5 for *HiSAT*.

Materials and Methods

Chemicals. L-Serine, L-cysteine, O-acetyl-L-serine, glycine, DTNB, ammonium sulfate, streptomycin sulfate, acetyl CoA, coenzyme A, desulfocoenzyme A, and S-methyl-L-cysteine were from Sigma. The buffers Mes, Tris, and Hepes were from Research Organics, Inc. All other chemicals were obtained from commercial sources, were reagent grade, and used without purification.

Enzyme. Serine acetyltransferase from *Haemophilus influenzae* was purified according to (9) and stored frozen in 20 mM Tris pH 7.5, 50 mM NaCl, and 0.02% (by weight) sodium azide. When highly diluted for use in assays, SAT was unstable and lost

activity throughout the day. Studies were carried out to find suitable conditions to stabilize SAT in dilute solution. Storage buffer for a 1.3 $\mu\text{g/mL}$ SAT solution included 50 mM Tris, pH 7.5, 15% glycerol, and 100 $\mu\text{g/mL}$ BSA. Control experiments were carried out to insure no interference from BSA in the assays. The enzyme is stable for several days at 4°C under these conditions.

Enzyme Assays and Initial Velocity Studies. Two assays were used for SAT dependent on conditions. The appearance of CoA was coupled to the production of TNB via a disulfide exchange reaction with DTNB (131), and this coupled assay was used except when cysteine was used as an inhibitor. In addition the appearance or disappearance of the thioester bond of acetyl CoA was monitored at 232 nm, and this direct spectrophotometric assay was used in the direction of OAS formation, in the presence of cysteine, and in the reverse reaction direction. Initial rate data were obtained with both assays in the direction of OAS formation to be certain they gave the same parameters. Reactions using the DTNB coupled assay were carried out at 25°C in cuvettes of 1 cm pathlength in a final volume of 0.4 mL containing the following: 100 mM Tris-HCl, pH 7.5 or Mes, pH 6.5; DTNB, 0.45 mM; acetyl CoA, 0.1 mM; L-serine, 5 mM; and an appropriate amount of enzyme. The buffer concentration was at times raised depending on the nature of the substrate and the concentration of substrate required for saturating conditions. Rates were calculated using an extinction coefficient of 13,600 $\text{M}^{-1}\text{cm}^{-1}$ for TNB at 412 nm. For initial velocity measurements in both reaction directions and in the presence of L-cysteine, the absorbance of the thioester bond was monitored spectrophotometrically at 232 nm ($\Delta\epsilon_{232} = 4500 \text{ M}^{-1}$

cm⁻¹). Assays were carried out in 100 mM phosphate, pH 6.5, in the direction of serine acetylation using the conditions for the DTNB assay, but in the absence of DTNB. Phosphate buffer was used to eliminate the absorbance of Mes at 232 nm. Both assays were used in the forward reaction direction for accuracy comparison and to obtain average values for parameters. Parameters for both assays in the forward direction are shown in table 1. In the direction of CoA acetylation, assays were in 100 mM phosphate, pH 6.5, using a 0.2 cm pathlength cuvette. Phosphate at the concentration used does produce a small amount of inhibition as found for the *Salmonella typhimurium* SAT (16). Solutions of OAS were prepared fresh and adjusted to pH 6.5 prior to the experiments. A unit of SAT is defined as the amount of enzyme required to produce 1 μ mol of product in 1 min at pH 7.5 and 25°C.

For the initial velocity studies, reactions were initiated by the addition of enzyme and the time course was monitored continuously using a Beckman DU 640 spectrophotometer. A plot of steady-state velocity vs. SAT concentration is linear over the concentration range used and passes through the origin for both assays in both reaction directions. Initial velocity patterns were obtained by measuring the initial rate at several concentrations of one reactant and a fixed concentration of the other. The experiment was then repeated at several different concentrations of the fixed reactant. Reactant concentrations were varied from less than K_m to 5-fold greater than K_m whenever possible. Product and dead-end inhibition patterns were obtained by measuring the initial velocity at variable concentrations of one reactant with the second reactant fixed at its K_m value, and

at several concentrations of inhibitor including zero. The K_m for reactant in one direction was taken as an initial estimate of the inhibition constant of a product in the opposite direction. An estimate of the K_i for a dead-end inhibitor was obtained from a Dixon analysis as follows. The substrate that was an analog of the putative inhibitor was fixed at K_m , while the second was maintained saturating. The initial rate was then measured at several concentrations of inhibitor, and data were plotted as $1/v$ vs. I . Assuming competitive inhibition, the abscissa intercept is $\sim -2K_i$ when variable substrate is fixed at K_m . In all cases where the Dixon analysis was used, inhibitors were competitive.

Data Processing Reciprocal initial velocities were plotted as a function of reciprocal substrate concentrations and all plots and replots were linear. All of the initial rate data in the absence of added inhibitors were fitted to equations 1 and 2. Data at pH 6.5 were fitted to eq. 1, and either did not converge or gave a negative value for K_a when fitted to eq. 2. Data were fitted using the appropriate rate equations and the program EnzFitter. Data conforming to an equilibrium ordered mechanism were fit using eq 1. Data in both reaction directions conforming to a sequential kinetic mechanism were fitted using eq 2. Data for linear competitive, uncompetitive, and noncompetitive inhibition were fitted using eqs 3-5, respectively. In eqs 1-5, v and V represent initial and maximum velocities, respectively; K_a and K_b are K_m values for A and B, respectively; K_{is} and K_{ii} are slope and intercept inhibition constants, while A, B, and I represent reactant and inhibitor concentrations, respectively.

$$v = \frac{VAB}{K_{ia}K_b + K_bA + AB} \quad (1)$$

$$v = \frac{VAB}{K_{ia}K_b + K_aB + K_bA + AB} \quad (2)$$

$$v = \frac{VA}{K_a \left(1 + \frac{I}{K_{is}}\right) + A} \quad (3)$$

$$v = \frac{VA}{K_a + A \left(1 + \frac{I}{K_{ii}}\right)} \quad (4)$$

$$v = \frac{VA}{K_a \left(1 + \frac{I}{K_{is}}\right) + A \left(1 + \frac{I}{K_{ii}}\right)} \quad (5)$$

Results

Effect of Glycine. Enzyme was incubated with DTNB to test whether the enzyme was inactivated by DTNB. DTNB does not inactivate the enzyme. Time courses using either the DTNB or A_{232} assays exhibited slight downward curvature over the entire time course of the assay (data not shown). As shown previously (16), addition of 10 mM glycine to the reaction mixture results in a longer linear time course. Therefore, 10 mM glycine was added to all assays in both reaction directions in order to more accurately measure initial velocities. Glycine was used at low concentration compared to its K_i ($\leq 0.2 K_i$). The effects of the glycine are negligible and corrected parameters within error equal to values in the absence of glycine.

Initial Velocity Studies in the Absence of Products. Assays were carried out at pH 6.5 where the product of the reaction, OAS, is stable, since initial rate studies were planned in both reaction directions. All DTNB assays contained 0.45 mM DTNB, which was sufficient to eliminate any lag phase in the coupled assays monitoring the appearance of TNB at 412 nm. Initial velocities were calculated on the basis of the initial linear portion of the time courses at pH 6.5. A double reciprocal plot of the initial rate in the direction of L-serine acetylation at concentrations of L-serine varied around its K_m and a fixed concentration of acetyl CoA is linear. A repeat of this experiment at concentrations of acetyl CoA varied around its K_m gave a family of lines that intersect on the y-axis, Fig. 5. Data are consistent with an ordered addition of acetyl CoA prior to L-serine. An identical pattern was obtained monitoring the disappearance of absorbance at 232 nm. Kinetic parameters obtained from a fit of equation 1 to the data are shown in Table 3. A small but significant amount of substrate inhibition was obtained at high OAS concentration. The substrate inhibition was not further characterized. In the direction of CoA acetylation, the reaction is followed at 232 nm, monitoring the appearance of acetyl CoA. The initial velocity pattern exhibits a family of lines that intersect to the left of the ordinate (data not shown). Kinetic parameters are given in Table 3.

An initial velocity pattern was also obtained at pH 7.5 so that data could be compared to those obtained for the *Salmonella* enzyme (16). The initial velocity pattern with the concentration of L-serine varied at different levels of acetyl CoA exhibits near parallel lines (data not shown). Kinetic parameters are provided in Table 3.

Figure 5. Initial velocity pattern for SAT in the direction of serine acetylation. Concentrations of L-serine are as indicated in the plot, while acetyl CoA concentrations are 0.2, 0.29, 0.5, 2.0 mM. Points are experimental, while lines are theoretical based on a fit using eq. 1.

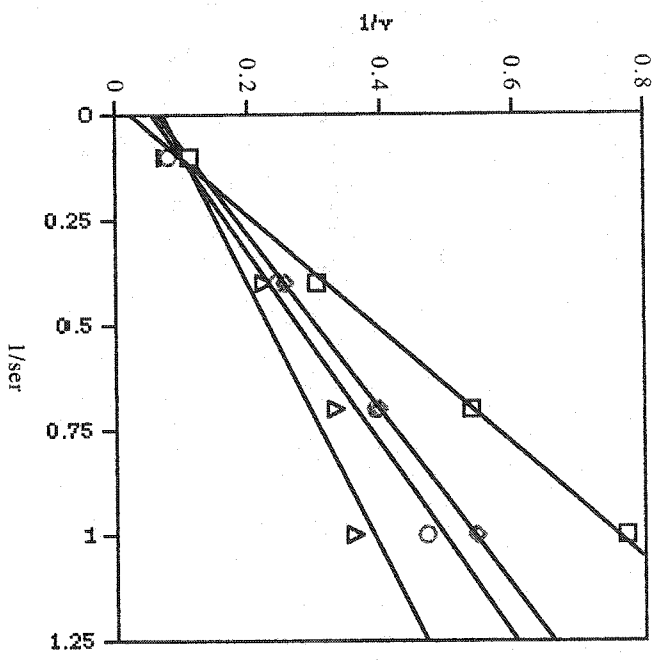


Table 3. Kinetic Parameters of Serine Acetyltransferase at pH 6.5

Parameter	Direction of Serine Acetylation	
	DTNB	A ₂₃₂
V _i /E _t (s ⁻¹)	1350 ± 250 ^a (2200 ± 80) ^b	1080 ± 170
V _i /K _{Ser} E _t (M ⁻¹ s ⁻¹)	(1.8 ± 0.7) × 10 ⁵ (4.7 ± .04) × 10 ⁵	(8.5 ± 2.3) × 10 ⁴
K _{i AcCoA} (mM) (K _{AcCoA} (mM))	0.9 ± 0.3 (0.7 ± 0.1)	0.4 ± 0.1
K _{Ser} (mM)	8 ± 3 (4.7 ± 0.4)	13 ± 3

Parameter	Direction of CoA Acetylation	
		A ₂₃₂
V _i /E _t (s ⁻¹)		300 ± 30
V _i /K _{CoA} E _t (M ⁻¹ s ⁻¹)		(1.2 ± 0.1) × 10 ⁴
V _i /K _{OAS} (M ⁻¹ s ⁻¹)		(2.8 ± 1.7) × 10 ⁵
K _{CoA} (mM)		1.02 ± 0.03
K _{OAS} (mM)		24 ± 14
K _{i CoA} (mM)		0.55 ± 0.05

^aSubstrates were at fixed concentrations of 3 mM Serine and 0.8 mM Acetyl CoA.

^bAt pH 7.5, the patterns obtained with glycine as a dead end inhibitor are qualitatively identical to those obtained at pH 6.5. The estimated K_{ii} and K_{is} values are 25 ± 5 mM and 10 ± mM, respectively.

Product Inhibition Studies. In the direction of L-serine acetylation, OAS was tested as a product inhibitor of both L-serine and acetyl CoA at pH 6.5. O-Acetyl-L-serine (OAS) is noncompetitive (NC) against acetyl CoA, while it is uncompetitive (UC) against L-serine. In the direction of CoA acetylation, L-serine is a NC inhibitor against both OAS and CoA. Kinetic parameters are given in Tables 4 and 5.

Dead-End Inhibition. In addition to its use in providing a longer linear time course, glycine was also utilized as a dead-end analog of L-serine. In the direction of L-serine acetylation at pH 6.5, glycine is uncompetitive against acetyl CoA and competitive (C) against L-serine. Desulfo-CoA was used as a dead-end analog of acetyl CoA, and is a competitive inhibitor against both acetyl CoA and L-serine. Kinetic parameters are summarized in Table 4.

S-Methyl-L-cysteine (SMC) is a dead-end analog of OAS in the direction of CoA acetylation. SMC is competitive as an inhibitor against OAS and uncompetitive against CoA. Desulfo-CoA was used again in the direction of CoA acetylation, this time as a dead-end analog of CoA. Desulfo-CoA is competitive as an inhibitor against CoA and is a noncompetitive inhibitor against OAS. Kinetic parameters are summarized in Table 5.

Cysteine has been shown to regulate the cysteine biosynthetic pathway by inhibiting SAT in a feedback manner (129). Utilizing the 232 nm assay, inhibition patterns using L-cysteine as a dead-end inhibitor were obtained in both reaction directions at pH 6.5. L-Cysteine is a competitive inhibitor against both substrates in both reaction directions.

Table 4. Kinetic Parameters from Inhibition Studies in the Direction of CoA Acetylation.

Product Inhibition

Varied Substrate	Fixed Substrate ^a	Inhibitor	Pattern	$K_{is} \pm \text{S.E.}$ mM	$K_{ii} \pm \text{S.E.}$ mM	Enzyme Form
Acetyl CoA	Serine	OAS	NC	100 ± 20	550 ± 100	E:CoA
Serine	Acetyl CoA	OAS	UC		60 ± 10	E:CoA

Dead End Inhibition

Varied Substrate	Fixed Substrate ^a	Inhibitor	Pattern	$K_{is} \pm \text{S.E.}$ mM	$K_{ii} \pm \text{S.E.}$ mM	Enzyme Form
Acetyl CoA	Serine	Glycine ^b	UC		50 ± 10	E:AcCoA
Serine	Acetyl CoA	Glycine	C	200 ± 30		E:AcCoA
Acetyl CoA	Serine	Desulfo CoA	C	1.4 ± 0.3		E
Serine	Acetyl CoA	Desulfo CoA	C	4.6 ± 0.3		E
Acetyl CoA	Serine	Cysteine	C	0.05 ± 0.01		E
Serine	Acetyl CoA	Cysteine	C	0.010 ± 0.005		E

Table 5. Kinetic Parameters from Inhibition Studies in the Direction of CoA Acetylation.

Product Inhibition

Varied Substrate	Fixed Substrate ^a	Inhibitor	Pattern	$K_{is} \pm \text{S.E.}$ mM	$K_{ii} \pm \text{S.E.}$ mM	Enzyme Form
OAS	CoA	Serine	NC	68 ± 66	18 ± 12	E:CoA
CoA	OAS	Serine	NC	24 ± 19	30 ± 14	E:CoA

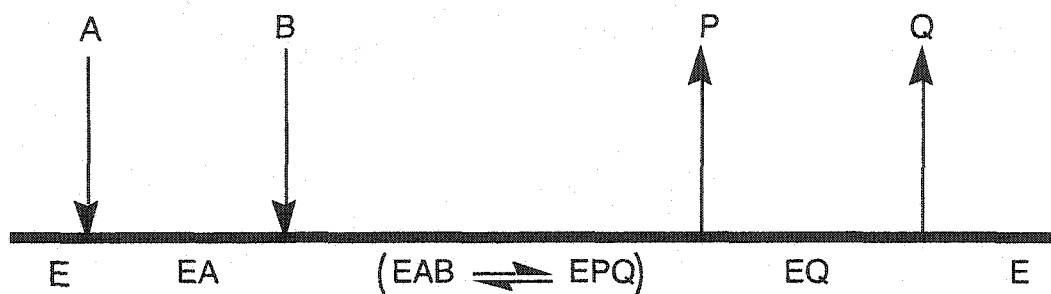
Dead End Inhibition

Varied Substrate	Fixed Substrate ^a	Inhibitor	Pattern	$K_{is} \pm \text{S.E.}$ mM	$K_{ii} \pm \text{S.E.}$ mM	Enzyme Form
OAS	CoA	SMC ^c	C	10 ± 2		E:CoA
CoA	OAS	SMC	UC		13 ± 5	E:CoA
OAS	CoA	Desulfo CoA	NC	2.9 ± 0.9	6 ± 4	E
CoA	OAS	Desulfo CoA	C	5.1 ± 0.9		E
OAS	CoA	Cysteine	C	0.046 ± 0.014		E
CoA	OAS	Cysteine	C	0.042 ± 0.009		E

^aSubstrate was fixed at concentrations of 60-80 mM OAS and 1.5 mM CoA.

DISCUSSION

Initial Velocity Patterns. Both the DTNB and A_{232} assays were used to collect initial velocity patterns in the forward reaction direction at pH 6.5. The initial velocity patterns obtained varying serine around its K_m at different fixed concentrations of acetyl CoA exhibits a series of lines that intersect on the ordinate, Fig. 12. This pattern is diagnostic for an equilibrium ordered addition of acetyl CoA and L-serine, Scheme 18. The mechanism requires that acetyl CoA and the last product released, CoA, are in equilibrium



Scheme 18. Schematic depiction of the kinetic mechanism of SAT. In scheme 2, A, B, P and Q represent acetyl CoA, L-serine, OAS, and CoA, respectively.

with free enzyme. At any concentration of acetyl CoA (theoretically $\geq E_t$) saturation with L-serine eliminates the dependence of the rate on the concentration of acetyl CoA as the equilibrium between E:CoA, E, and E:acetyl CoA is displaced toward the ternary complex(es). Thus, acetyl CoA has no K_m , and the $K_{i \text{ AcCoA}}$ has an average value of 0.6 mM. The average value of K_{Ser} taken from both the DTNB and A_{232} assays, 10 mM, is quite high at pH 6.5, and does not change significantly as the pH is increased to 7.5, Table 3.

In the reverse reaction direction, the initial velocity pattern intersects to the left of

the ordinate consistent with a sequential kinetic mechanism. The ratio of V_f/V_r is about 4, suggesting the enzyme is a good catalyst in both reaction directions. All of the reactant V/K values are in the range 10^4 - 10^5 $M^{-1}s^{-1}$ indicating the reaction is not diffusion limited in either reaction direction, and consistent with the equilibrium ordered kinetic mechanism in the direction of OAS formation. In addition, the values for K_{iAcCoA} (~0.6 mM) and K_{iCoA} (0.55 mM) are within error identical, indicating the acetyl moiety of acetyl CoA provides an insignificant contribution to its overall affinity for enzyme.

The Michaelis constant for L-serine (K_{ser}) of 7.6-12.6 mM is higher than the K_{ser} of 0.56-2.8 mM reported for the *Salmonella typhimurium* SAT (14, 16) and the K_{ser} of 1.17 mM reported for the *Escherichia coli* SAT (19).

Product Inhibition. Inhibition by the first product, OAS, released in a reversible ordered kinetic mechanism is expected to be noncompetitive vs. both reactants, as a result of combination with the E:CoA and reversal of the reaction. Inhibition by OAS is noncompetitive vs. acetyl CoA, but uncompetitive vs. serine. If OAS binds to enzyme in its normal capacity as a product it will combine with the E:CoA complex. For an equilibrium ordered mechanism, an equilibrium is established between E:CoA, E and E:AcCoA. The level of the E:CoA product complex will thus depend on the concentrations of the two substrates. With serine fixed at 3 mM ($0.3 K_{ser}$), the amount of E:CoA will be finite but low at low concentrations of acetyl CoA. As the concentration of acetyl CoA tends to infinity, the concentration of E:CoA tends to zero. Thus, the noncompetitive pattern observed for OAS vs. acetyl CoA is as expected with a lower K_{is} than K_{ii} . With

acetyl CoA fixed at K_{AcCoA} and serine tending to zero, the amount of E:CoA will be lower than the amount present at low serine and acetyl CoA, and the K_i for OAS would be expected to be greater than 100 mM, i.e. outside the range of OAS concentrations used in the experiment. As the concentration of serine increases the concentration of E:CoA should tend to zero, and one would expect no inhibition by OAS. Thus, the uncompetitive inhibition vs. serine indicates combination with an enzyme form that accumulates in the steady state after serine binds, but not the E:CoA complex. These are the only conditions that will generate a high, nearly 100%, E:AcCoA:serine complex, and it is likely this complex to which OAS binds to give the uncompetitive inhibition. These data are consistent with an equilibrium ordered kinetic mechanism with a dead-end E:AcCoA:serine:OAS complex. The nature of this complex will have to await future studies.

In the direction of CoA acetylation, the results are also consistent with an ordered mechanism in which L-serine is a noncompetitive inhibitor vs. both OAS and CoA. The noncompetitive inhibition results from combination of serine with E:acetyl CoA. The slope inhibition constant estimated from the NC pattern vs. OAS is not well defined. This pattern is difficult to perform because of the high K_m for OAS, but the inhibition pattern is clearly noncompetitive, and data do not fit the equation for uncompetitive inhibition as well. The results are consistent with the ordered kinetic mechanism.

Dead End Inhibition. In addition to its use in providing a longer linear time course, glycine is a dead-end analog of L-serine. In the direction of L-serine acetylation at pH 6.5,

glycine is competitive against L-serine and uncompetitive against acetyl CoA, consistent with the ordered addition. Combination of glycine in both cases is with the E:acetyl CoA complex, and thus correction of the K_i for the presence of the fixed substrate should give the same true K_i value from the measured respective K_{is} and K_{ii} values. The $K_{ia}K_b/V$ term in the denominator of eq. 1 represents free enzyme and is multiplied by $(1 + I/K_i)$ to account for the inhibition. Substitution of this term into eq. 1 and deriving the expressions for the apparent K_i for C and UC inhibition vs. serine and acetyl CoA, respectively, gives $K_i(1 + K_{ia}/A)$ for K_{is} and $K_i(1 + B/K_b)$ for K_{ii} . Values of K_i estimated using the fixed concentrations of acetyl CoA and serine are 85 ± 13 mM and 42 ± 8 mM, respectively.

Desulfo-CoA, as predicted by the equilibrium ordered mechanism is competitive vs. both substrates as a result of the ability of serine to force enzyme into the central complexes at infinite concentration. The apparent K_i measured with acetyl CoA varied is the true K_i since both bind to free enzyme. The apparent K_i measured with serine varied however, must be corrected for the fixed concentration of acetyl CoA by dividing the K_{is} value by $(1 + A/K_{ia})$. True K_i values are 1.4 ± 0.3 mM and 2.3 ± 0.2 mM, respectively, in very good agreement with one another.

In the direction of CoA acetylation, SMC is noncompetitive against OAS and uncompetitive against CoA, while desulfo CoA is competitive vs. CoA and noncompetitive vs. OAS. Data are qualitatively consistent with the ordered mechanism. Correction of the K_i values gives values of 5 ± 1 mM and 6.5 ± 2.5 mM, respectively, for the true K_i for SMC. A value of 5.1 ± 0.9 mM is obtained for the K_i of desulfo CoA vs. CoA. The NC

pattern of Desulfo CoA against OAS gives a K_{is} value of 2.9 ± 0.9 mM and a K_{ii} value of 6 ± 4 mM. On the basis of the two experimental values, corrected values of the K_i are 1 ± 0.3 mM and 4 ± 2.5 mM, respectively, in good agreement, within error with values calculated from data in the forward reaction direction. The quantitative analysis is also consistent with the ordered mechanism.

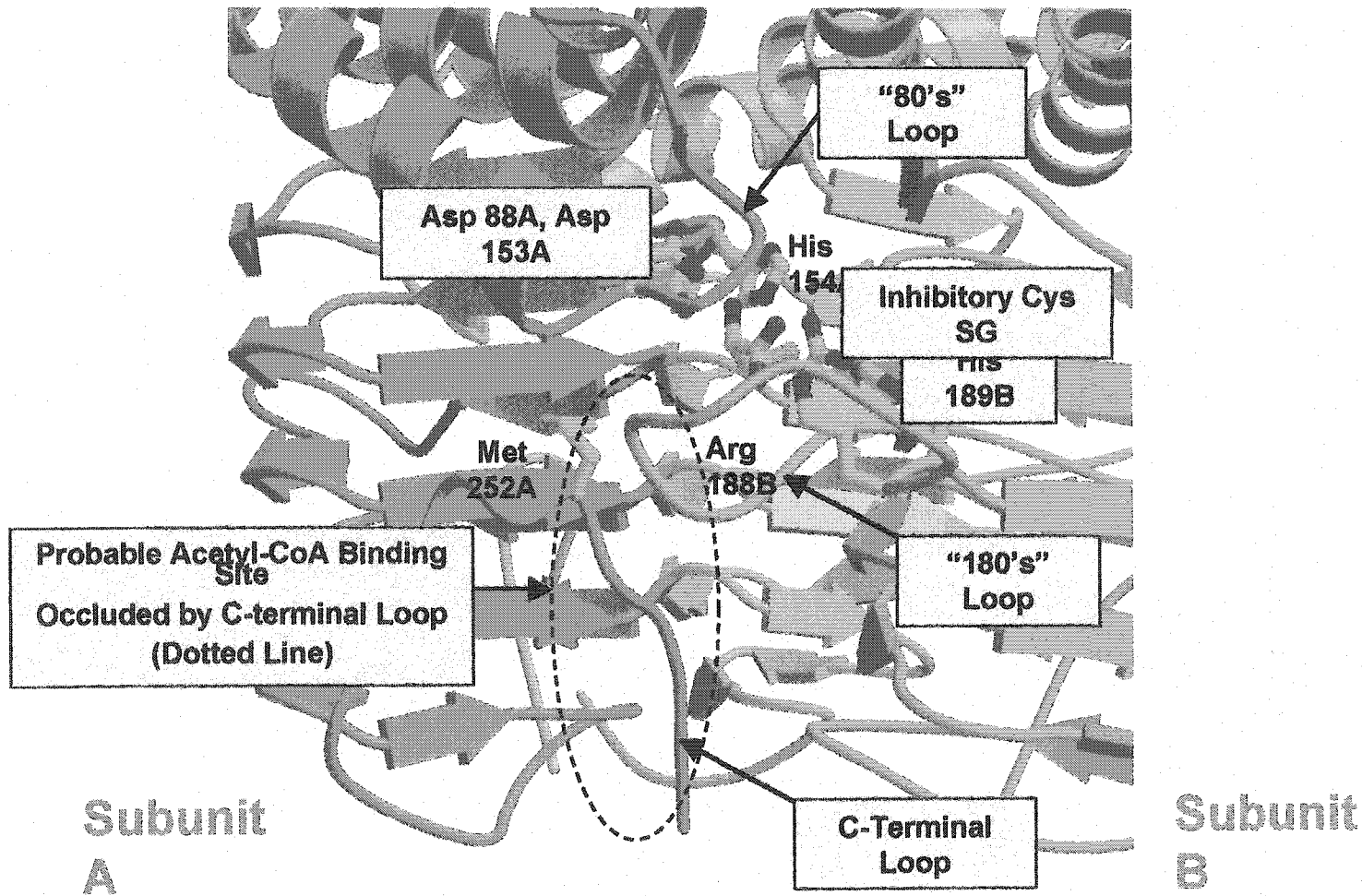
Haldane Relations. Another test of the internal consistency of the data is agreement of the Haldane relationship and the equilibrium constant obtained by direct measurement. An equilibrium constant of 15 was measured directly by Leu and Cook (16) monitoring the change in CoA concentration at varied OAS/serine ratios using the enzyme from *Salmonella typhimurium*. One of the kinetic Haldane equations for an equilibrium ordered mechanism is given in eq. 6.

$$K_{eq} = \frac{V_1 K_p K_{ia}}{V_2 K_b K_{iq}} \quad (6)$$

Substitution of kinetic parameters from Tables 3 and 5 gives a value of 9 ± 6 for K_{eq} , within error equal to the value of 15.

Cysteine Regulation. Cysteine participates in the regulation of its own biosynthetic pathway by inhibiting SAT in a feedback manner (129). It is a potent inhibitor with a K_i of 10-50 μ M and is competitive against both substrates in the direction of L-serine acetylation. A recent crystal structure, Fig 6., supports the kinetic results, showing L-

Figure 6. Close up of the active site of serine acetyltransferase from *Haemophilus influenzae* with cysteine bound to the serine binding site. The C-terminal loop, the L β H loop, and the “180s” loop undergo conformational changes upon binding of serine and prohibit binding of acetyl CoA. Cysteine is bound tightly by all of its functional groups. Asp 88 and Asp 153 bind the amino group of cysteine. Arg 188 forms 2 interactions with the carboxyl of cysteine, and the side chain thiol interacts with His 154 and 189. Active site residues are donated by both A and B subunits shown.



cysteine bound to free enzyme (9). L-Cysteine is an analogue of L-serine and the structural data suggest that cysteine binds to the active site and directly competes with serine. This is in agreement with data concerning cysteine-desensitized mutants. All mutants desensitized to cysteine inhibition have also displayed a loss of activity (136, 137, 142, 165). Upon binding of cysteine, a loop on the C-terminus undergoes a conformational change, which prevents the binding of acetyl CoA, Fig. 6 (9). Cysteine is therefore also shown to be a competitive inhibitor of acetyl CoA. Kinetic studies with serine analogues and micro-calorimetric data support these findings (19). The competitive inhibition patterns exhibited by cysteine are in agreement with the proposed mechanism of inhibition.

Comparison with Other Similar Enzymes. SAT is a member of the hexapeptide acyltransferase family of enzymes in which a six amino acid residue motif directs folding of a structural domain known as the left-handed β -helix ($L\beta H$). It has been stated that all known hexapeptide acyltransferases have a similar active site location and pattern of interactions (13). Although only limited mechanistic work is available for the enzymes of this family, those studied are reported to exhibit sequential kinetic mechanisms (12, 13, 40, 166). The one exception is the SAT from *Salmonella typhimurium*, proposed to have a ping pong kinetic mechanism (16). The authors, on the basis of parallel initial velocity data and an apparent burst of CoA formation upon mixing enzyme and acetyl CoA, proposed an acetyl-enzyme intermediate in the overall reaction. Indeed, the initial velocity pattern for the *Haemophilus influenzae* enzyme is nearly parallel at pH 7.5, the pH used for the *Salmonella* enzyme, and the inhibition patterns are also consistent with either mechanism.

We have tried, without success, to repeat the burst kinetic experiment. On the basis of data obtained at pH 6.5 in this study and the data obtained for the closely related enzyme from *E. coli* (19), it appears the kinetic mechanism proposed previously for the *Salmonella* enzyme is in error. The kinetic mechanism is sequential at pH 7.5 (with $K_{ia} < K_a$) as correctly pointed out by Hindson (19), who proposed a random mechanism for the *Escherichia coli* SAT at pH 7.5. The ordered mechanism reported in these studies differs from the random mechanism reported by Hindson, but the two could be the same at the higher pH. Changes in the kinetic mechanism of creatine kinase, for example, as a function of pH have been reported. An equilibrium ordered mechanism is reported at low pH with MgATP adding prior to creatine (167), and this mechanism changes to steady state random at neutral pH (168) and to rapid equilibrium random at high pH (169).

Chapter 4

Acid-Base Chemical Mechanism and Solvent Deuterium Isotope Effects of Serine Acetyltransferase from *Haemophilus Influenzae*

The kinetic mechanism of the SAT from *Haemophilus influenzae* (*HiSAT*) discussed in Chapter 3, and a manuscript describing these studies is now in press in *Archives of Biochemistry and Biophysics* (170). *HiSAT* catalyzes an ordered mechanism where acetyl CoA is the first substrate bound followed by L-serine, and products are released in order with CoA released last. At pH 6.5 the mechanism is equilibrium ordered, while it is steady state ordered at pH 7.5.

Little is presently known of the chemical mechanism for any of the hexapeptide enzymes or acyltransferases in general. Enzymes catalyzing this reaction fall under two commonly proposed chemical mechanism categories. Most hexapeptide enzymes, such as SAT, have a proposed direct attack catalyzed reaction based upon structural and limited kinetic data. All of these enzymes have a histidine residue important to catalysis. Other acyltransferases are proposed to have a covalent/nucleophilic catalyzed reaction. In this manuscript, we use the pH dependence of the kinetic parameters and solvent deuterium kinetic isotope effects to probe the chemical mechanism of the *HiSAT*, a member of the hexapeptide family. A general base chemical mechanism with rate-limiting chemistry is proposed for *HiSAT*.

Materials and Methods

Chemicals. L-Serine, O-acetyl-L-serine, glycine, 5,5' dithiobis(2-nitrobenzoic acid) (DTNB), acetyl coenzyme A, and coenzyme A were from Sigma. The buffers Mes, Tris, Hepes, Ches, Taps, and Bis-Tris were from Research Organics, Inc. Deuterium oxide was from Cambridge Isotope Laboratories, Inc. Monobasic and dibasic potassium phosphate were from EM Science. All other chemicals and reagents were obtained from commercial sources, were reagent grade, and used without purification.

Enzyme. Serine acetyltransferase from *Haemophilus influenzae* was purified according to (9) and maintained and stored frozen in 20 mM Tris pH 7.5, 50 mM NaCl, and 0.02% (w/v) sodium azide. Enzyme dilutions (1.3 $\mu\text{g}/\text{mL}$) were prepared fresh in 50 mM Tris, pH 7.5, 15% glycerol, and 100 $\mu\text{g}/\text{mL}$ BSA for use in assays. Control experiments were carried out to insure no interference from BSA in the assays. The diluted enzyme is stable for several days under these conditions.

Enzyme Assays. In the direction of OAS formation, two assays for SAT were used. Reactions were carried out in cuvettes of 1 cm pathlength in a final volume of 0.4 mL containing the following: buffer, 100 mM; DTNB, 0.45 mM; acetylCoA (varied); L-serine (varied); and an appropriate amount of enzyme. The buffer concentration was at times raised depending on the nature of the substrate and the concentration of substrate required for saturating conditions. The production of CoA was coupled to a disulfide exchange reaction with DTNB and the appearance of TNB was monitored spectrophotometrically (131). Rates were calculated using an extinction coefficient of $13,600 \text{ M}^{-1}\text{cm}^{-1}$ for TNB

at 412 nm. For initial velocity measurements in the direction of acetyl CoA formation the absorbance of the thioester bond was monitored spectrophotometrically at 232 nm ($\Delta\epsilon_{232} = 4500 \text{ M}^{-1}\text{cm}^{-1}$). Assays were in 100 mM phosphate using a 0.2 cm pathlength cuvette. Phosphate buffer was used to eliminate the absorbance of Mes or other buffers at 232 nm. Phosphate at the concentration used does produce a small amount of inhibition (16). Solutions of OAS were prepared fresh and adjusted to pH 6.5 where it is stable prior to the experiments. A unit of SAT is defined as the amount of enzyme required to produce 1 μmol of product in 1 min at pH 7.5 and 25°C.

pH Studies. The initial velocity was measured at pH 7.5 as a function of acetyl CoA concentration and a fixed concentration of serine, and this was repeated at several different fixed concentrations of serine to generate an initial velocity pattern. The initial velocity pattern was then repeated at pH 6.5, 8.5, and 9.5 to determine kinetic parameters at the extremes of pH and to obtain information on the pH dependence of the kinetic mechanism (170). Initial rate data were then obtained as a function of pH by fixing one reactant at a saturating concentration ($5 \times K_m$ for acetyl CoA) and varying the concentration of the other reactant. In this way the pH dependence of V_1 , V_1/K_{serine} , V_1/K_{AcCoA} , V_2 , V_2/K_{OAS} , and V_2/K_{CoA} were measured. So that the maximum rates in both reaction direction were normalized to the same enzyme concentration, data were obtained from the same enzyme stock varying substrate concentrations in a constant ratio and extrapolating to infinite substrate concentration. Profiles in the direction of CoA acetylation were obtained from pH 5.5-8 due to the instability of OAS at high pH. The pH was measured before and

after the reaction with changes limited to ≤ 0.1 pH unit. The pH was maintained using the following buffers at 100 mM concentration (or higher) in the direction of L-serine acetylation: Mes, 5.5-6.5; Bis-Tris, 6.0; Hepes 6.5-8.5; Tris, 7.5; Taps, 8.5; Ches, 9.0-10.0. In the direction of CoA acetylation, 100 mM phosphate was used from pH 5.5-8.

Data were also obtained for an inhibitor competitive with substrate in the direction of L-serine acetylation. The dissociation constants for glycine (competitive vs. L-serine) was obtained at pH 6 and 8. Acetyl CoA was fixed at $5K_{AcCoA}$ and serine was fixed at K_{serine} , and the initial rate was measured at different concentrations of glycine. Data were then analyzed as $1/v$ vs. glycine with the abscissa intercept equal to $-2K_i$ glycine.

Solvent Deuterium Kinetic Isotope Effects (SKIE). The pH-rate profiles were repeated in both reaction directions in D_2O . All stock solutions and buffers were prepared in D_2O with the same buffers listed above. The buffer pH was adjusted using KOH and HCl, while pD was adjusted using KOD and DCl. The maximum percentage of protons in solution on the basis of the concentration of exchangeable protons for the solution components is 4.5% and the isotope effects were thus calculated with 0.96 as the fraction of label. The pD value of each reaction mixture was obtained immediately after initial velocity data were collected by addition of 0.4 to the pH meter reading to correct for the isotope effect on the pH electrode (171). The pK values obtained from the pD profiles were shifted 0.4-0.6 units to higher pD as a result of equilibrium isotope effects on the dissociation constant for the acid dissociable group. The isotope effect is then estimated as the ratio of the pH(D) independent values.

Proton Inventory Experiments and Solvent Deuterium Isotope Effects. In the forward reaction direction, finite isotope effects were observed, and proton inventory experiments were carried out to more accurately measure the solvent deuterium kinetic isotope effect and estimate the number of protons in flight in the rate-determining transition state. Both the DTNB and 232 nm assays were utilized to measure V_1 and V_1/K_{serine} at pH(D) 7.5, 8.0, and 8.5 in 100% H_2O , 46% D_2O , and 96% D_2O .

SKIE Theory. The number of protons in flight in the rate-determining transition state may be determined using the Gross-Butler equation, eq. 4. Fitting data to the equation and solving for the isotope exchange equilibrium constant (or fractionation factor (ϕ)) provides a full account of the contributions of various classes of protic positions to the isotope effect and would therefore constitute a proton inventory of the studied reaction.

Only sites for which $\phi \neq 1$ and which experience changes in ϕ on conversion of reactants to transition states contribute to the isotope effect (172). The Gross-Butler equation is given in equation 1,

$$k_n = {}^{\text{D}_2\text{O}}k \left[\frac{\prod_i^x (1 - n + n\phi_i^{\text{T}})}{\prod_i^x (1 - n + n\phi_i^{\text{R}})} \right] Z_k^{-n} \quad (1)$$

where k_n is the ratio of the rate constant in H_2O to D_2O , ${}^{\text{D}_2\text{O}}k$ is the rate constant in 100% D_2O , n is the atom fraction of deuterium, ϕ_i^{T} and ϕ_i^{R} are the isotope exchange equilibrium

constants (or fractionation factors) for the transition state and the reactants which measure the tendency of a solute site to fractionally contain deuterium vs. the deuterium fraction of the solvent, and Z is the medium effect that accompanies transfer from H₂O to mixed isotopic solvents. This equation describes the functional dependence of k on the isotopic composition of the solvent. The fractionation factors are measures of the stiffness or tightness of binding of a solute site vs. the O-H(D) sites of solvent. In general, deuterium accumulates where binding is tighter, $\phi > 1$. Since $\phi^R \cong 1$ for most enzyme amino acid side chains involved in nucleophilic and/or proton transfer catalysis, equation 1 reduces to equation 2.

$$k_n = {}^{D_2O}k \prod_i^x (1 - n + n\phi_i^T) \quad (2)$$

Therefore, if a single transition state proton bridge contributes to the solvent isotope effect, the rate ratio (${}^n k$) will be a linear function of atom fraction of deuterium (n).

Plots with multiple proton transfer are bowl shaped and bulge downward from the linear dependence of the single proton model.

Data Processing Reciprocal initial velocities were plotted as a function of reciprocal substrate concentrations and all plots were linear. Data were fitted using the appropriate rate equations and the program EnzFitter. Data for pH profiles that exhibit a decrease with a limiting slope of 1 at low pH were fitted using equation 3. Data for pH profiles that exhibit a decrease with a limiting slope of 2 at low pH were fitted using

equation 4. Data for V and V/K deuterium isotope effects were fitted using equation 5.

Data for proton inventory experiments utilized a simplified form of the Gross-Butler equation, eq. 2, to determine the number of protons in flight in the rate-determining transition state.

$$\log Y = \log \left(\frac{C}{1 + \frac{H}{K_1}} \right) \quad (3)$$

$$\log Y = \log \left(\frac{C}{1 + \frac{H}{K_1} + \frac{H^2}{K_1 K_2}} \right) \quad (4)$$

$$v = \frac{VA}{(K_a(1 + F_1 E_{V/K}) + A(1 + F_1 E_V))} \quad (5)$$

In equations 3 and 4, Y is the value of V or V/K at any pH, C is the pH independent value of Y, H is the hydrogen ion concentration, and K_1 and K_2 represent acid dissociation constants for enzyme or substrate functional groups. In equation 5, v is the initial velocity, V is the maximum velocity, A is the concentration of substrate A, K_a is K_m for the variable substrate, F_1 is the fraction of D_2O in solvent, and $E_{V/K}$ and E_V are the isotope effects minus 1 on V/K and V, respectively. In eq. 2, k represents the rate at any % D_2O , n is the fraction of D_2O , ^{H_2O}k is the rate in H_2O , and ϕ^T is the fractionation factor for the proton transferred in the transition state.

Results

pH Dependence of Kinetic Parameters for HiSAT. The pH dependence of the kinetic parameters provides information on the protonation state of enzyme and/or reactant functional groups required for enzyme conformation, binding, and catalysis. To be certain the kinetic mechanism of the enzyme does not change with pH, select initial velocity patterns diagnostic for the proposed kinetic mechanism were obtained at the extremes of pH. Initial velocity patterns obtained for SAT in the direction of L-serine acetylation are consistent with an ordered mechanism at pH 6.5 and the ordered mechanism is maintained at pH 7.5, but changes to steady-state ordered (170). Initial velocity patterns obtained at pH extremes in the direction of CoA acetylation are consistent with a sequential kinetic mechanism in which CoA is the first substrate bound and OAS binds second.

In the direction of L-serine acetylation, V_1/E_t and $V_1/K_{\text{serine}}E_t$ decrease at low pH giving a limiting slope of 1 and a single pK of about 7, Fig. 7. L-Serine has no pK values over the pH range studied, and the pK exhibited in the pH-rate profiles likely reflects an enzyme side chain important in catalysis. On the other hand, $V_1/K_{\text{AcetylCoA}}E_t$ decreases at low pH with a limiting slope of 2 and giving an average pK of 6 for the two groups titrated.

Figure 7. pH(D) profiles for V , V/K_{serine} , and V/K_{AcCoA} in the forward reaction direction.

The V and V/K pH independent values can be estimated from fit C values. The SKIE is estimated from the antilog of the difference in the pH independent values. The curves are theoretical and based on a fit to eq. 3, while the points are experimental. The acetyl CoA data were fitted to eq. 4. The top profile of each is in H_2O and the bottom profile of each is in D_2O .

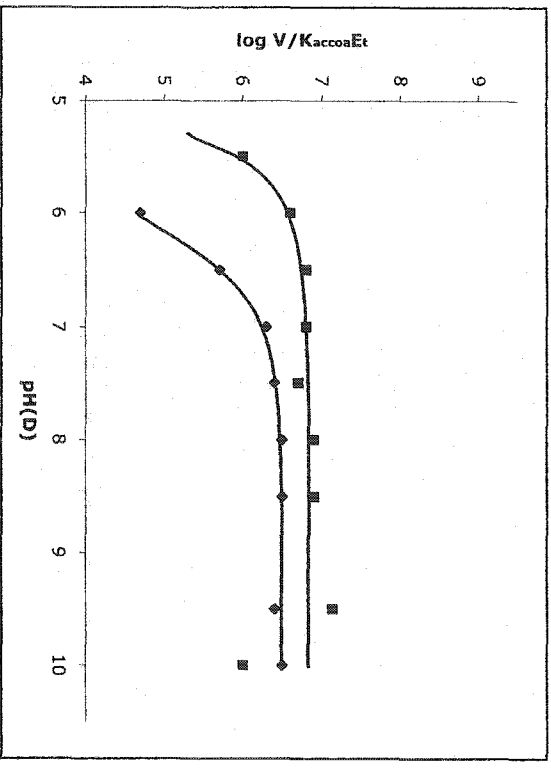
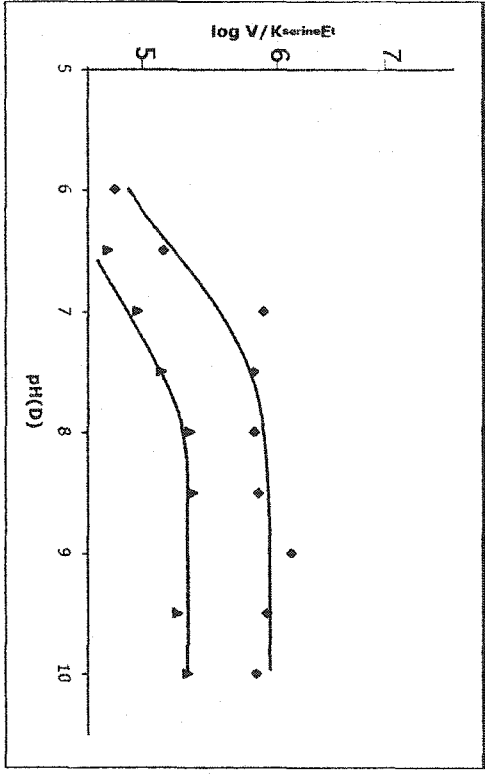
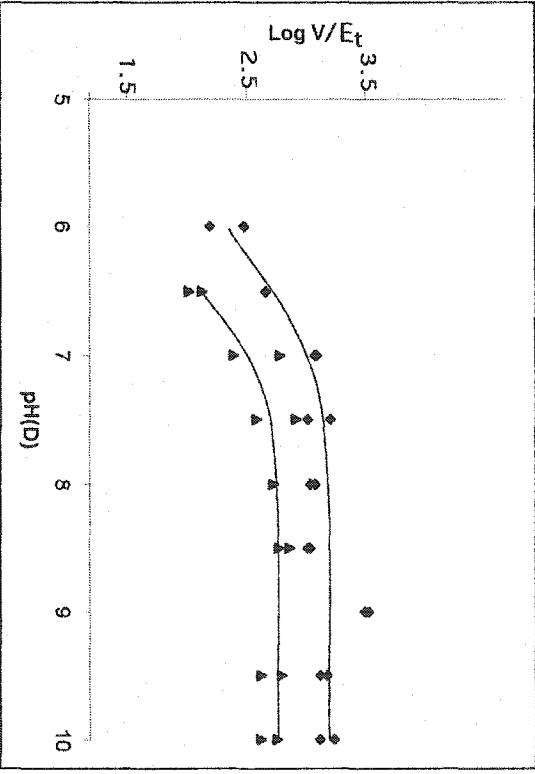
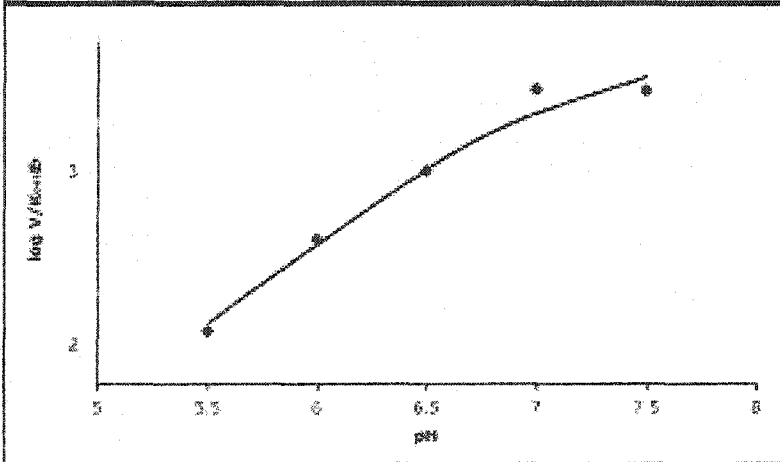
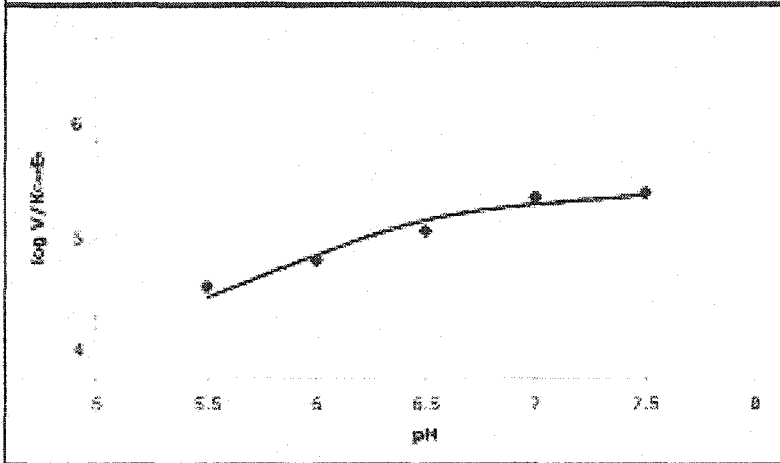
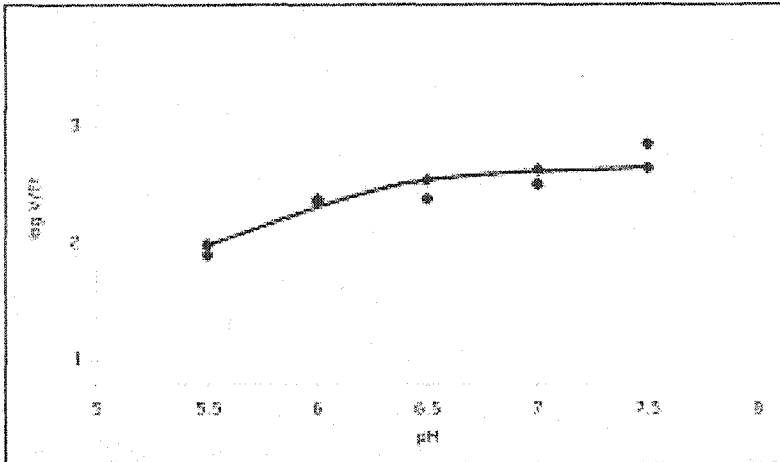


Figure 8. pH profiles for V , V/K_{OAS} , and V/K_{CoA} in the reverse reaction direction. The V and V/K pH independent can be estimated from fit C values. The curves are theoretical and based on a fit to eq. 3, while the points are experimental. The top profile of each is in H_2O and the bottom profile of each is in D_2O .



Acetyl CoA also has no pK values over the range studied. Since acetyl CoA is the first reactant bound, the pH dependence reflects groups required for binding of acetyl CoA.

Estimates of the pH independent values of the kinetic parameters are summarized in table 6.

In the reverse reaction direction, V_2/E_t and $V_2/K_{OAS}E_t$ decrease at low pH with limiting slopes of +1, giving pKs of 6.1 and 7., while the $V_2/K_{CoA}E_t$ pH profile decreases below a pK of 6.4 with a limiting slope of +1, Fig. 8. As observed in the forward reaction direction, the pK observed in the V and V/K_{OAS} profiles reflects a catalytic group, while that observed in the V/K_{CoA} likely reflects an enzyme group important for binding CoA.

Estimates of the pH independent values of the kinetic parameters are summarized in table 6.

pH Dependence of the K_i for Glycine. Glycine was utilized as a dead-end inhibitor. At pH 6 and pH 8, estimated K_i values for glycine are 36 mM and 55 mM, respectively, within error pH independent. Data are consistent with the pH independence of K_{serine} and thus the pH independence of amino acid binding over the pH range studied.

Solvent Deuterium Kinetic Isotope Effects and Proton Inventory Experiments. The pD profiles for V_1/E_t and $V_1/K_{serine}E_t$ (Fig 7), V_2/E_t and $V_2/K_{OAS}E_t$ (Fig. 9) were measured in order to obtain an estimate of the solvent deuterium kinetic isotope effect. The pD-rate profiles for V_1/E_t , $V_1/K_{serine}E_t$, V_2/E_t and $V_2/K_{OAS}E_t$ are qualitatively identical to the pH-rate profiles, (Figs. 7, 8, 9) but the pK values are increased as predicted (see Materials and Methods). Data are summarized in table 6. The pH(D) independent values of the

parameters give estimates of the solvent deuterium kinetic isotope effects (SKIE) as summarized in table 6. The pD dependence of $V/K_{\text{AcCoA}}E_t$ was also measured. As expected, the pK values in all cases are shifted to higher pD by 0.4 to 0.6.

To better define the estimated values of $^{D20}V_1$, and $^{D20}(V_1/K_{\text{serine}})$, $^{D20}V_2$, and $^{D20}(V_2/K_{\text{OAS}})$, the saturation curve for serine was measured as a function of the percentage of D_2O in solution, Fig. 10. Estimates of the solvent kinetic isotope effects are obtained as a ratio of the values of the parameters at 0 and 100% D_2O . Values of ^{D20}V and $^{D20}(V/K_{\text{serine}})$ are 1.9 ± 0.12 and 2.8 ± 0.17 , respectively. Replots of the slope (V_1/K_{serine}) and intercept (V_1) vs. % D_2O are linear, indicating a single proton in flight in the rate-determining transition state (172).

Discussion

Interpretation of pH Dependence of Kinetic Parameters. The V/K for a reactant is obtained at limiting concentration of one of the reactants. V is obtained at saturating concentrations of substrate and the enzyme form that builds up in the steady state predominates. The pH dependence of V/K thus reflects the protonation state of group(s)

Table 6. Summary of pH Data

^aC is the pH(D) independent value of the parameter

	H ₂ O	pK ± S.E.	C ^a ± S. E.	D ₂ O	C ± S. E.	pK ± S. E.	SKIE ± S.E.
V ₁ (s ⁻¹)		6.8 ± 0.2	3300±350	V ₁	1300± 180	7.0 ± 0.2	2.5 ± 0.4
V/K _{serine} (M ⁻¹ s ⁻¹)		7.2 ± 0.2	(9.6± 0.4) x10 ⁵	V/K _{serine}	(2± 0.2) x10 ⁵	7.2 ± 0.3	4.8 ± 1
V/K _{AcCoA} (M ⁻¹ s ⁻¹)		6	3.3x10 ⁶	V/K _{AcCoA}	2.0x10 ⁶	6.3	
V ₂ (s ⁻¹)		6.1 ± 0.1	420±50	V ₂	920± 130	6.4 ± 0.2	0.45 + 0.1
V/K _{OAS} (M ⁻¹ s ⁻¹)		7.0 ± 0.2	(2.1± 0.5) x10 ⁴	V/K _{OAS}	(1.9± 1) x10 ⁴	6.1 ± 0.5	1.08 + 0.08
V/K _{CoA} (M ⁻¹ s ⁻¹)		6.4 ± 0.2	(4.2 + 0.7) x10 ⁵	V/K _{CoA}	(3.5± 1.5) x10 ⁵	7.5 ± 0.3	

Figure 9. pD profiles for V , V/K_{OAS} , and V/K_{CoA} in the reverse reaction direction. The V and V/K pH independent values can be estimated from the fit C values. The SKIE is estimated from the antilog of the difference in the pH independent values. The curve is theoretical and based on a fit to eq. 3, while the points are experimental.

Figure 9.

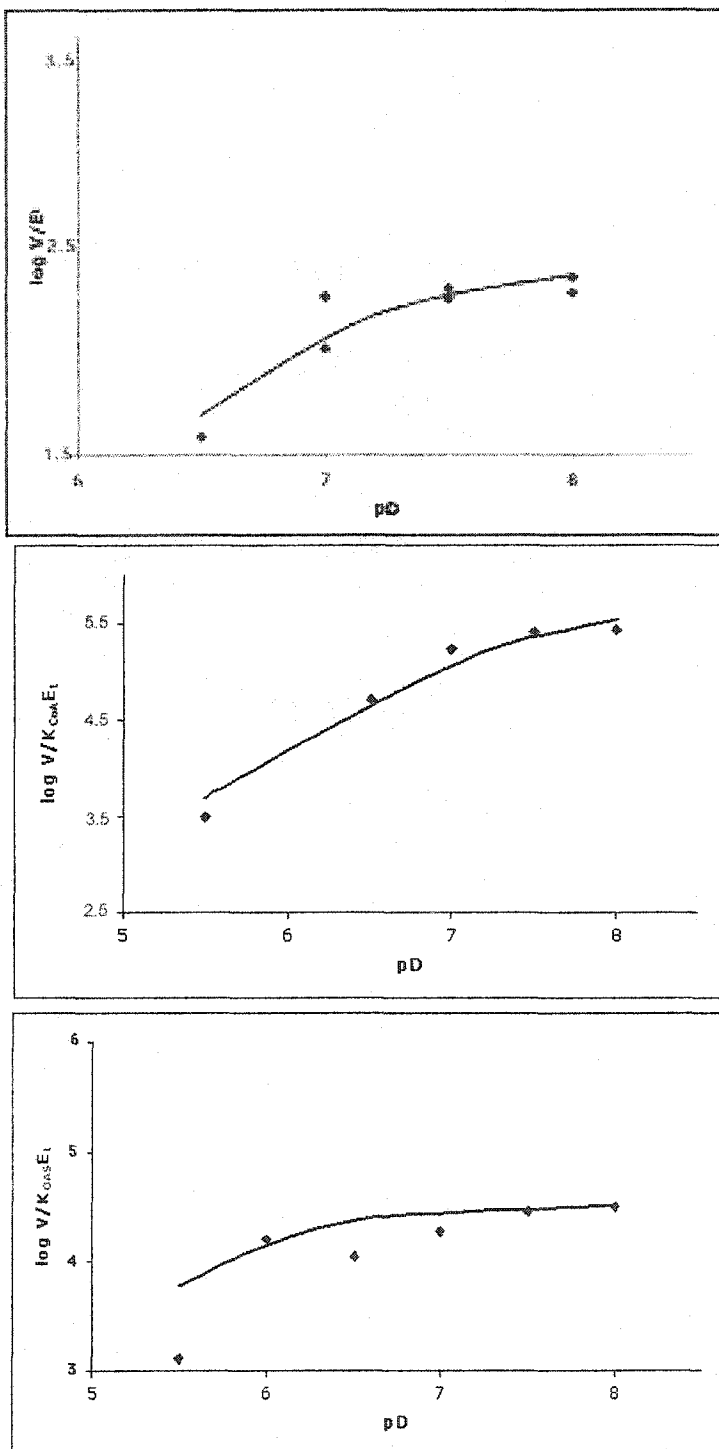
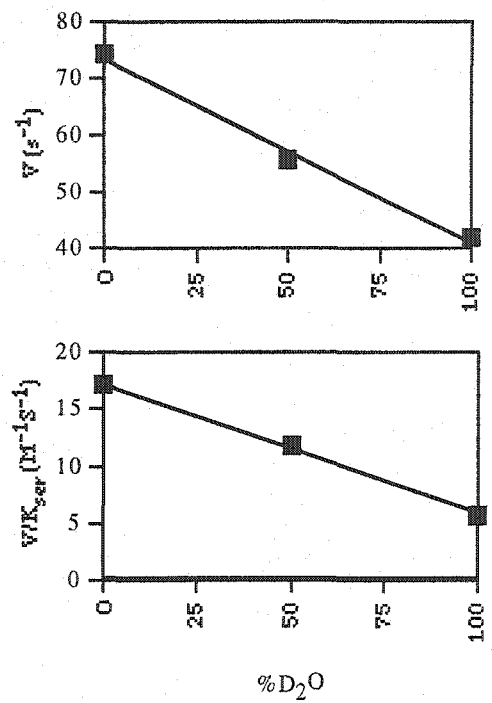
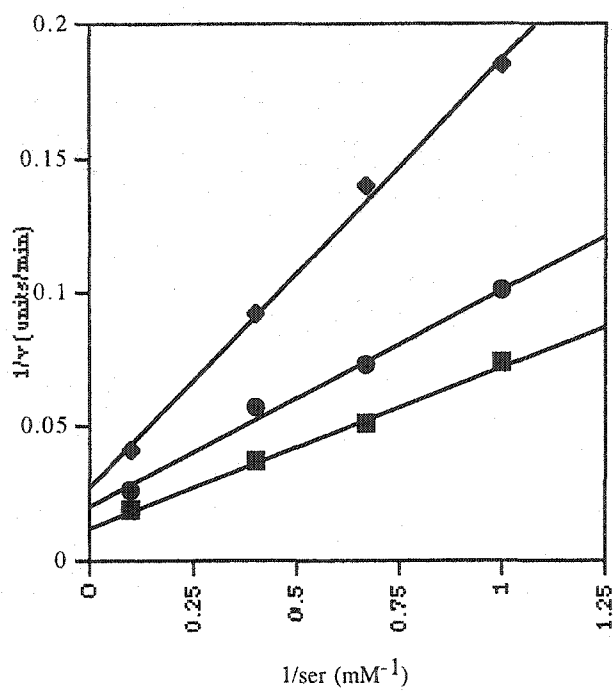


Figure 10. Proton inventory results. V_1 and V/K_{serine} were measured at the pH(D) independent value of 8.5 in 100% H₂O (diamond), 46% D₂O (circle), and 96% D₂O (square). Isotope effects of 1.9 ± 0.12 and 2.8 ± 0.17 are observed for ^{D_2O}V and $^{D_2O}(V/K_{\text{serine}})$, respectively. A single proton in flight is indicated by the linearity of the replots of V and V/K_{serine} vs. %D₂O.

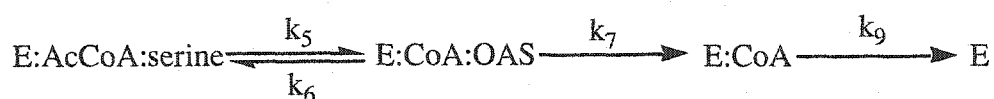


on free enzyme and/or reactant responsible in a given protonation state for binding and/or catalysis, while the pH dependence of V reflects groups on enzyme required for catalysis. The determination of an ordered mechanism for HiSAT (170) allows the pH profiles to be interpreted in terms of enzyme forms or species predominate under given conditions. Free enzyme and acetyl CoA predominate for the V/K_{AcCoA} profile, the E:acetyl CoA enzyme form and serine predominate for the V/K_{serine} profile, and central complexes (primarily E:acetyl CoA:serine) predominate for the V_1 profile. In the reverse reaction direction, E and CoA predominate for V/K_{CoA} , E:CoA and OAS predominate for V/K_{OAS} , and central complexes (primarily E:CoA:OAS) predominate for V_2 . The V/K_{AcCoA} decreases at low pH with a limiting slope of 2, indicating two enzyme residues are titrated with an average pK of 6 that are necessary for binding the acetyl donor. The V_1/K_{serine} , and V_2/K_{OAS} profiles decrease at low pH below a single pK value of about 7, while V_1 and V_2 also decrease at low pH below a single pK slightly lower than that observed for the V/K_s . On the basis of the acid-base chemistry required in the acetyl transfer reaction, the group with a pK of 7 is believed to represent a general base required to accept a proton from the serine hydroxyl in the acetyl transfer reaction. In the reverse reaction direction, the same group must be unprotonated to accept a proton from CoA. When comparing the pK values in V/K and V profiles, the same group is observed with little perturbation. Therefore, binding of serine is with equal affinity to the protonated and unprotonated enzyme (173). In agreement, no pH dependence was observed for the K_i value of glycine.

Proton Inventory Experiments. The pH(D) independent SKIEs on V and V/K_{serine}

are about 1.9 and 2.8, respectively. The proton inventories are linear indicating a single proton in flight in the rate-determining step of the reaction (172). The step in which the proton is transferred is likely the chemical step once the E:serine:acetyl CoA complex is formed as indicated by the large isotope effects on both parameters. Thus, the nucleophilic attack by the serine hydroxyl is likely limiting, with a general base accepting a proton in this reaction.

The difference in value of the V/K_{serine} and V isotope effects show that the steps accompanying proton transfer are not solely rate-limiting under V conditions. The isotope effect on V/K represents the reaction from the binding of the first substrate, acetyl CoA, until the release of the first product, OAS. The V profile represents the reaction from when both products are bound, to the release of both products and reformation of the free enzyme. The differing values of 2.8 and 1.9 for the V/K and V solvent deuterium kinetic isotope effects, respectively, show that some step represented only in the V profile also contributes to rate-limitation. If we assume that 2.9 is the intrinsic solvent kinetic isotope effect, then an estimate of the relative rate of CoA release compared to the chemical step can be obtained. The mechanism for SAT is shown schematically below at saturating reactant concentrations (Scheme 19). The equation for the solvent deuterium kinetic isotope effect on K_{eq} as represented by the scheme is shown in equation 6. The equations for V and the solvent deuterium kinetic isotope effects on V are shown in equations 7 and 8.



Scheme 19.

The value of K_{OAS} (24 mM) and K_{iOAS} (80 mM) as a product inhibitor (170) is very high suggesting rapid release of OAS. The relative values of V_1 and V_2 are within a factor of 4 suggesting $k_7 > k_5, k_6$ and equation 6 reduces to equation 7. Substituting values of 1.9 for ^{D_2O}V and 2.8 for $^{D_2O}k_5$ gives a value of 1 for k_5/k_9 . Thus the release of CoA is equal to the rate of the chemical step.

$$^{D_2O}K_{eq} = \frac{^{D_2O}k_5}{^{D_2O}k_6} \quad (6)$$

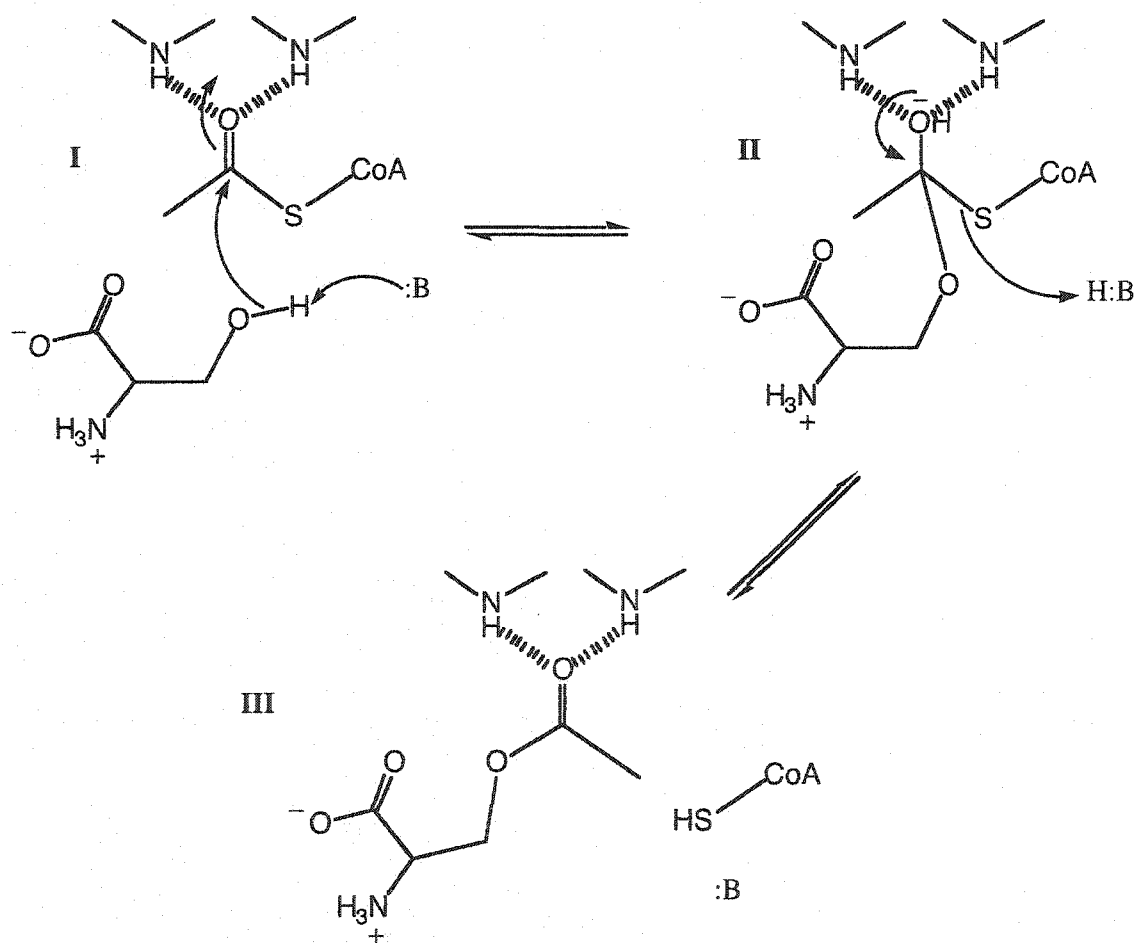
$$v = \frac{k_5}{\left(1 + k_5 \left(\frac{1}{k_7} + \frac{1}{k_9} \right) + \frac{k_6}{k_7} \right)} \quad (7)$$

$$^{D_2O}V = \frac{^{D_2O}k_5 + k_5 \left(\frac{1}{k_7} + \frac{1}{k_9} \right) + ^{D_2O}K \left(\frac{k_6}{k_7} \right)}{1 + k_5 \left(\frac{1}{k_7} + \frac{1}{k_9} \right) + \frac{k_6}{k_7}} \quad (8)$$

$$^{D_2O}V = \frac{^{D_2O}k_5 + \frac{k_5}{k_9}}{1 + \frac{k_5}{k_9}} \quad (9)$$

Chemical Mechanism. The pH(D) profiles and solvent isotope effects experiments

allow a chemical mechanism to be proposed as shown in Scheme 20. The single group observed in both reaction directions suggests general base catalysis by a single enzyme residue. Once both substrates are bound, the reaction sequence is proposed to begin by nucleophilic attack of the oxygen from the serine side chain hydroxyl on the carbonyl carbon of acetyl CoA (I in Scheme 20). The general base accepts the proton from the side chain hydroxyl in the transition state. The carbonyl oxygen is likely stabilized by positive dipoles from backbone nitrogens (9). The nucleophilic attack of the serine oxygen on the



Scheme 20.

acetyl CoA carbonyl results in a tetrahedral intermediate. The same general base residue then acts as a general acid and donates a proton to the sulfur atom of CoA (II in Scheme 20) as the tetrahedral intermediate collapses giving the products OAS and CoA (III in Scheme 20).

The solvent isotope effect studies support the proposed general base mechanism. The single proton in flight, as identified by the proton inventory experiments, is accepted by the general base from the serine side chain hydroxyl in the transition state. The identity of the general base catalytic residue has not been determined. As discussed in the previous chapter, cysteine binds to the active site and occupies what appears to be the serine binding site. Crystal structures show several potential general base residues in the active site in the E:cysteine complex (9) (Fig. 11.). Two residues of primary interest are H154A and histidine H189B, which are located on either side of and within hydrogen-bonding distance to the cysteine thiol. The identity of the general base is currently under investigation via site-directed mutagenesis studies of these two residues. Both histidine residues have been changed to asparagine via site-directed mutagenesis.

Figure 11 shows serine acetyltransferase with cysteine bound at the serine site. The three-dimensional structures were solved and provided by S.L. Roderick and coworkers (9). Upon binding, a loop labeled in Fig. 11 undergoes a conformational change to prohibit the binding of acetyl CoA. The H154N mutant shows a 2000 fold decrease in V_1/E_t when compared to wild type HiSAT, while the value of K_{serine} for the mutant is almost the same as wild type at 7 mM. On the other hand, the H189N mutant shows a 2-

fold decrease in V_1/E_t , while its value of K_{serine} is increased to ~ 230 mM. This indicates that the His 189 residue contributes to binding of serine but is not essential for catalysis.

Preliminary work has begun on the H154Q mutant. Again, the H154Q mutant has a K_{serine} of ~ 8 mM, which is identical to wild type, and therefore does not participate in substrate binding.

The side chains of aspartate 88 and aspartate 153 have been identified by the crystal structure as interacting with the amino group of cysteine (9). The carboxyl group interacts with a water molecule that also helps to stabilize binding.

An extended, 10 residue L β H loop projects into the space between two adjacent L β H domains. This same loop is largely disordered in the apoenzyme and therefore may be involved in conformational changes upon binding. The loop may form the tunnel upon binding of substrate that shields the bound enzyme:substrate complex and provides the conformational changes necessary for proper orientation of the substrate and catalysis. These loops have been found at the active site of other hexapeptide acyltransferases (12, 13, 38, 40, 41) and are thought to be important to how these enzymes have evolved structural and functional diversity at their active sites (9).

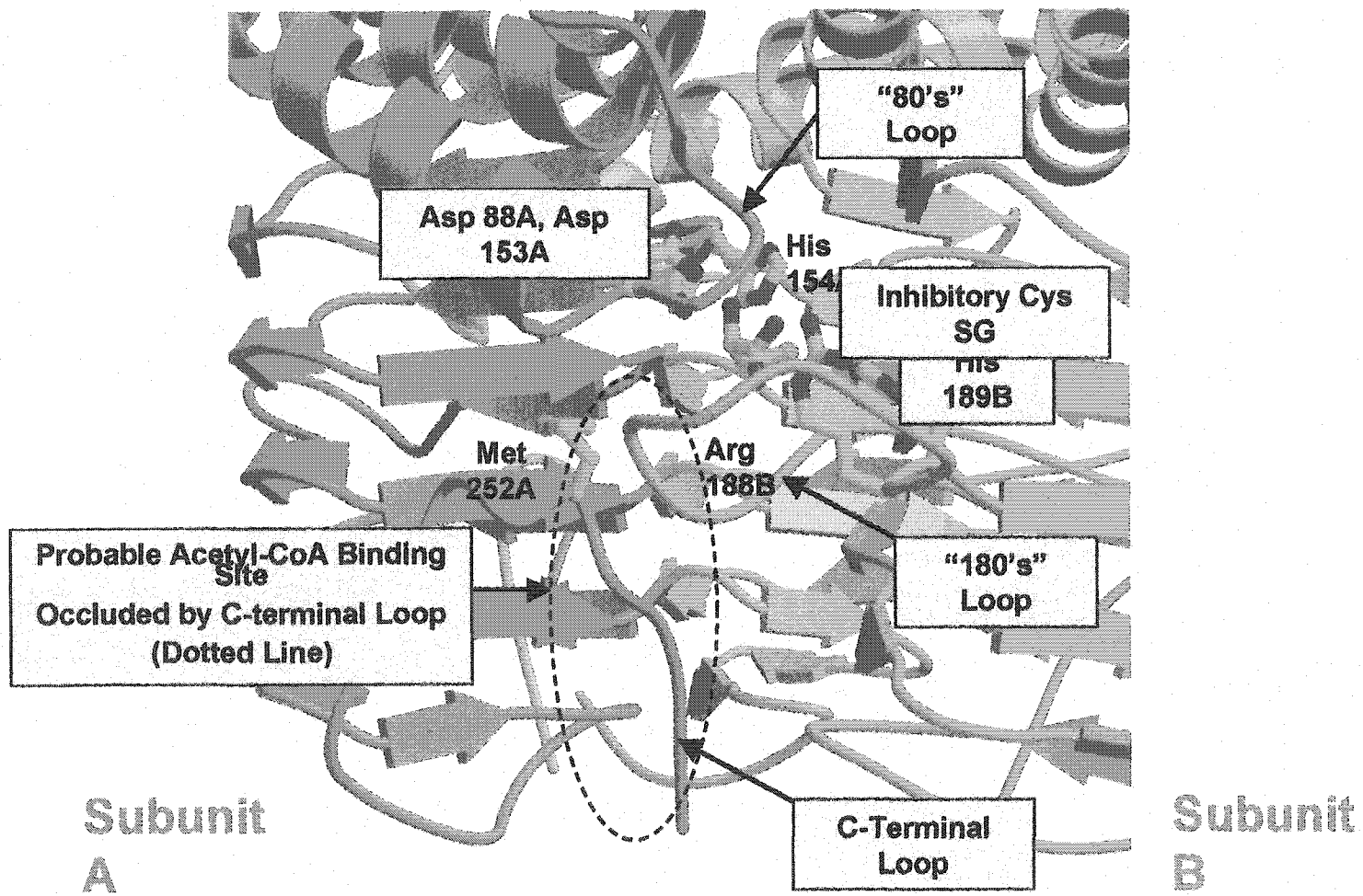
A C-terminal segment of HiSAT has also been identified as contacting the L β H loop. Desensitization to cysteine inhibition has been shown to be a direct result of structural perturbations that affect the conformation of this C-terminal segment or the L β H loop (137). Truncating the C-terminal 20 residues for SAT from *E. coli* reduces cysteine inhibition significantly (133, 165). These observations along with the crystallographic data

by Roderick (40) suggest that the L β H loop is ordered by the C-terminal segment of the enzyme and the binding of cysteine. Once cysteine binds to the active site, its solvent accessibility is reduced 93%. A conformational change that would allow the diffusion of the inhibitor would have to come from the L β H loop. This movement is inhibited by the loops interaction with the C-terminal segment (40).

Comparison with Other Enzymes. SAT is a member of the hexapeptide acyltransferase family of enzymes in which a six amino acid residue motif directs folding of a structural domain known as the left-handed β -helix (L β H) (1). All of the known hexapeptide acyltransferases have similar active site locations and patterns of interaction (13). All of the mechanistic work accomplished to date for this enzyme family shows similar sequential kinetic mechanisms (12, 13, 40, 174). Similar hexapeptide proteins such as uridyl diphosphate-N-acetylglucosamine 3-O-acyltransferase, the xenobiotic acetyltransferase from *Pseudomonas aeruginosa* (PaXAT), and Vat (D), a streptogramin acetyltransferase, all have identified histidines as important catalytic residues (6, 13, 21)

Even nonhexapeptide proteins that catalyze similar acetyl transfer reactions such as chloramphenicol acetyltransferase and carnitine acetyltransferase do so by general base catalysis by means of a catalytic histidine residue. In the case of carnitine acetyltransferase, the histidine is part of a catalytic Glu-His dyad (29, 52). In the case of SAT, one of the histidine residues, H154A is part of a Asp-His dyad (9). Additional work is necessary to identify common structural and mechanistic modalities within this diverse enzyme class.

Figure 11. Close up view of the active site of serine acetyltransferase from *Haemophilus influenzae* with cysteine bound to the serine binding site. Cysteine is tightly bound by all functional groups. Asp 88A and Asp 153A interact with the amine. Arg 188B forms two interactions with the carboxylate. The side chain thiol interacts with His 154A and His 189B. The C terminal loop undergoes a conformational change upon binding of serine and prohibits binding of acetyl CoA.



Chapter 5

Conclusions and Future Work

In the introduction to this dissertation, a review of acyl transfer to alcohols was discussed in order to pose questions concerning the kinetic and chemical mechanism of serine acetyltransferase from *Haemophilus influenzae*. The experiments carried out for this dissertation have answered these questions and provided new and more detailed information on serine acetyltransferase and acyltransferases in general. Many enzymes of this family are reported to exhibit sequential kinetic mechanisms (12, 13, 40, 166). Some have a proposed random mechanism, such as the NodL protein of *Rhizobium leguminosarum*. A random mechanism has also been proposed for the SAT from *Escherichia coli* at pH 7.5 (19). The work done in this dissertation indicates the *HiSAT* catalyzed reaction proceeds via an equilibrium ordered kinetic mechanism at pH 6.5. Although the two reports differ, they could be the same at the higher pH. Changes in the kinetic mechanism of creatine kinase, for example, as a function of pH have been reported. An equilibrium ordered mechanism is reported at low pH with MgATP adding prior to creatine (167), and this mechanism changes to steady state random at neutral pH (168) and to rapid equilibrium random at high pH (169).

The *HiSAT* reaction is general base catalyzed and follows a general chemical

mechanism similar to that of the other hexapeptide *O*-acyltransferases and even some nonhexapeptide acyltransferases. Some of the mechanistic similarities of the hexapeptide enzymes include a common active site location, separate binding sites for substrates, a conformational change to generate a tunnel that forms upon reactant binding that shields the substrates from bulk solvent and properly orients the substrates for catalysis, and a histidine residue important to catalysis which is possibly part of a catalytic dyad. The work accomplished with *HiSAT* helps to confirm these proposed mechanistic qualities for one enzyme and should aid in the study of all enzymes encompassed by *O*-acyltransfer.

Some speculation based on kinetic experiments has been made concerning what steps of the enzymatic *O*-acylation reaction contribute to rate limitation. For galactoside acetyltransferase, the primary rate-determining step is proposed to be either the loss of the acetylated acceptor from the binary complex or the interconversion of the substrate and the product ternary complexes (32). For the NodL protein, the off rate of the substrate analogue *O*-acetyl chitosan was proposed to be partially rate limiting (18). Isotope effects were used as a detailed and precise probe of the rate-determining transition state of *HiSAT*. The primary rate determining step in the reaction is the chemical step accompanying the proton transfer from the hydroxyl of serine to the general base catalyst. Only one proton is in flight during the rate-determining transition state and all data agree with the previously proposed general base mechanism. The isotope effects studies done for *HiSAT* are the first for a *O*-acetyltransferase hexapeptide enzyme and provide further insight into the chemical mechanism of *HiSAT*.

The availability of the solved crystal structure for HiSAT (9) has been invaluable to the interpretation of the results of the mechanistic work. The crystal structure with cysteine bound to the active site shows two histidine residues (His 154 and His 189) located on either side of the cysteine side chain thiol. The thiol is wedged between the NE2 of both imidazoles of the histidines. Residues His 154 and His 189 were therefore prime candidates for functioning as a general base for the reaction. Site-directed mutagenesis has been done to change each of the two histidine residues to asparagine. Preliminary results suggest that histidine 154 is the general base while histidine 189 contributes to serine binding.

The crystal structure also indicates the possibility of a catalytic dyad, which was mentioned earlier in the dissertation. Histidine 154A also interacts with aspartate 139B (A indicates the histidine is part of one subunit while B indicates that the aspartate residue is part of the neighboring subunit). This interaction causes the histidine to adopt a main chain torsion angle pair (φ , ψ) that place it in the disallowed region of the Ramachandran plot (175). This is the same catalytic dyad mentioned in chapter one for carnitine acetyltransferase, and thought to be a common feature of all the enzymes that catalyze their reaction by direct attack, both hexapeptide and nonhexapeptide, discussed in chapter one. The interaction of the L β H loop and the C-terminal segment as discussed in Chapter 4, are another feature thought to be common for the hexapeptide acetyltransferases.

Understanding the process of cysteine inhibition and the ability to produce large amounts of it is a point of interest to amino acid manufacturers. The design of cysteine

desensitized mutants that maintain catalytic activity is difficult due to the nature of the cysteine inhibition. As discussed in detail in chapter 3, cysteine binds to the serine binding site in the active site. Mutations disrupting this binding site would likely also disrupt binding of the isostructural natural substrate.

Cysteine is manufactured throughout the world and the need for cysteine has steadily increased in recent years. The food industry uses cysteine primarily in the production of reaction flavors for foods and pet foods to improve savory flavors, as an antioxidant, and as a natural dough conditioner, according to SRI Consulting, Menlo Park, California. In the United States, a key ingredient in dietary supplements is the amino acid product *N*-acetylcysteine. The overall world demand for cysteine is expected to grow 2 to 3 percent per year, reaching an estimated 4400 to 4600 metric tons in 2002 (176). The projected need for cysteine by Western Europe was even higher due to an increasing use in food and pet applications (176).

Some companies have already developed successful new cysteine manufacturing strategies. Before the newly developed strategies, cysteine was mainly obtained from human hair, and to a lesser extent, from feathers, pigs' bristles and hooves. These substances contain keratin, which is rich in cystine. Cystine is the oxidized form of cysteine comprised of two molecules of cysteine joined by a disulfide bond. Wacker-Kyowa developed a new fermentation technology for cysteine production utilizing an *Escherichia coli* strain and dextrose as a starting material. No foreign genes were introduced to the strain of *E. coli*. The strain releases large quantities of cysteine into the nutrient

medium, where it oxidizes in the presence of atmospheric oxygen to cystine, which in turn crystallizes (176). The company Ajinomota combines chemical and enzymatic processes to synthesize cysteine. Japan utilizes this cysteine in the manufacture of expectorants and in hair growth formulas. The process uses methyl acrylate as a substrate (177). The need for manufactured cysteine, the medical, pharmaceutical, and industrial interest in amino acid metabolism, and the wide range of *O*-acyltransfer reactions in nature ensure an interest in the work for serine acetyltransferase and other similar enzymes in the future.

REFERENCES

1. Vaara, M. (1992) *FEMS Microbiol. Lett.* 97, 249-254.
2. Bairoch, A. (1993) *Nucleic Acids Res.* 21, 3097-3103.
3. Anderson, M. S., and Raetz, C. R. H. (1987) *J. Biol. Chem* 262, 5159-5169.
4. Downie, J. A. (1989) *Mol. Microbiol.* 3, 1649-1651.
5. Gilvarg, C., and Weinberger, S. (1970) *J. Bacteriol.* 101, 323-324.
6. Murray, I. A., and Shaw, W. V. (1997) *Antimicrob. Agents Chemother.* 41, 1-6.
7. Kelly, T. M., Stachula, S. A., Raetz, C. R. H., and Anderson, M. S. (1993) *J. Biol. Chem* 268, 19866-19874.
8. Raetz, C. R. H., and Roderick, S. L. (1995) *Science* 270, 997-1000.
9. Olsen, L. R., Huang, B., Vetting, M. W., and Roderick, S. L. (2004) *Biochemistry* submitted.
10. Kisker, C., Schindelin, H., Alber, B. E., Ferry, J. G., and Rees, D. C. (1996) *EMBO J.* 15, 2323-2330.
11. Beaman, T. W., Binder, D. A., Blanchard, J. S., and Roderick, S. L. (1997) *Biochemistry* 36, 489-494.
12. Beaman, T. W., Sugantino, M., and Roderick, S. L. (1998) *Biochemistry* 37, 6689-6696.
13. Sugantino, M., and Roderick, S. L. (2002) *Biochemistry* 41, 2209-2216.
14. Kredich, N. M., and Tomkins, G. M. (1966) *J. Biol. Chem* 241, 4955-65.

15. Becker, M. A., Kredich, N. M., and Tomkins, G. M. (1969) *J. Biol. Chem* 244, 2418-2427.
16. Leu, L.-S., and Cook, P. F. (1994) *Biochemistry* 33, 2667-2671.
17. Mino, K., Yamanoue, T., Sakiyama, T., Eisaki, N., Matsuyama, A., and Nakanishi, K. (2000) *Biosci. Biotechnol. Biochem.* 64, 1628-1640.
18. Hindson, V. J., Moody, P. C., Rowe, A. J., and Shaw, W. V. (2000) *J. Biol. Chem* 275, 461-466.
19. Hindson, V. J. (2003) *Biochem. J.* 375, 745.
20. Raetz, C. R. H. (1990) *Annu. Rev. Biochem.* 59, 129-170.
21. Wyckoff, T. J. O., and Raetz, C. H. R. (1999) *J. Biol. Chem* 274, 27047-27055.
22. Spaink, H. P., Wijfjes, A. H. M., Geiger, O., Bloemberg, G. V., Ritsema, T., and Lugtenberg, B. J. J. (1993) *Nature* 354, 125-130.
23. Van Brussel, A. A. N., Bakhuizen, R., van Spronsen, R., Spaink, H. P., Tak, T., Lugtenberg, B. J. J., and Kijne, J. (1992) *Science* 257, 70-72.
24. Bloemberg, G. V., Lagas, R. M., Leeuwen, S., Van der Marel, G., Van Boom, J. H., Lugtenberg, B. J. J., and Spaink, H. P. (1995) *Biochemistry* 34, 12712-12720.
25. Bloemberg, G. V., Thomas-Oates, J. E., Lugtenberg, B. J. J., and Spaink, H. P. (1994) *Mol. Microbiol.* 11, 793-804.
26. Tennigkeit, J., and Matzura, H. (1996) *Gene* 98, 113-116.
27. Parent, R., and Roy, P. H. (1992) *J. Bacteriol.* 174, 2891-2897.
28. Tian, Y., Beaman, T. W., and Roderick, S. L. (1997) *Protiens: Struct., Funct.*

- Genet.* 28, 298-300.
29. Kleanthous, C., Cullis, P. M., and Shaw, W. V. (1985) *Biochemistry* 24, 5307-5313.
 30. Leslie, A. G. W., Moody, P. C. E., and Shaw, W. V. (1988) *Proc. Natl. Acad. Sci. U.S.A.* 85, 4133-4137.
 31. Leslie, A. G. W. (1990) *J. Mol. Biol.* 213, 167-186.
 32. Lewendon, A., Ellis, J., and Shaw, W. V. (1995) *J. Biol. Chem* 270, 26326-26331.
 33. Andrews, K. J., and Lin, E. C. C. (1976) *J. Bacteriol.* 128, 510-513.
 34. Zabin, I., Kepes, A., and Monod, J. (1962) *J. Biol. Chem* 237, 253-257.
 35. Wilson, T. H., and Kashket, E. R. (1969) *Biochim. Biophys. Acta* 173, 501-508.
 36. Musso, R. E., and Zabin, I. (1973) *Biochemistry* 12, 553-557.
 37. Alpers, D. H., Appel, S. H., and Tomkins, G. M. (1965) *J. Biol. Chem* 240, 10-13.
 38. Wang, X.-G., Olsen, L. R., and Roderick, S. L. (2002) *Structure* 10, 581-588.
 39. Kostrewa, D., D'Arcy, A., Takacs, B., and Kamber, M. (2001) *J. Mol. Biol.* 305, 279-289.
 40. Olsen, L. R., and Roderick, S. L. (2001) *Biochemistry* 40, 1913-1921.
 41. Sulzenbacher, G., Gal, L., Peneff, C., Fassy, F., and Bourne, Y. (2001) *J. Biol. Chem* 276.
 42. Lo Leggio, L., Dal Degan, F., Sorenson, S. O., Harlow, K., Harris, P., and Larsen,

- S. (2001) *Acta Crystallogr. D57*, 1915-1918.
43. Boos, W., Ferenci, T., and Shuman, H. A. (1981) *J. Bacteriol.* 146, 725-732.
 44. Mengin-Lecreulx, D., and van Hiejenoort, J. (1994) *J. Bacteriol.* 176, 5788-5795.
 45. Gehrig, A. M., Lees, W. J., Mindiola, D. J., Walsh, C. T., and Brown, E. D. (1996) *Biochemistry* 35, 579-585.
 46. Alber, B. E., and Ferry, J. G. (1994) *Proc. Natl. Acad. Sci. U.S.A.* 91, 6909-6913.
 47. Peterofsky, B., and Gilvarg, C. (1961) *J. Biol. Chem* 236, 1432-1438.
 48. Roy, A. M., and Coleman, J. (1994) *J. Bacteriol.* 176, 1639-1646.
 49. Shaw, W. V., and Unowsky, J. (1968) *J. Bacteriol.* 95, 1976.
 50. Ramsay, R. R., and Arduini, A. (1993) *Arch. Biochem. Biophys.* 302, 307-314.
 51. Miyajima, R., and Shiio, I. (1973) *J. Biochem.* 73, 1061-1068.
 52. Wu, D., Govindasamy, L., Lain, W., Gu, Y., Kukar, T., Agbandje-McKenna, M., and McKenna, R. (2003) *J. Biol. Chem* 278, 13159-13165.
 53. Shaw, W. V. (1983) *CRC Crit. Rev. Biochem.*, 1.
 54. Shaw, W. V., and Leslie, A. G. W. (1991) *Annu. Rev. Biophys. Biophys. Chem.* 20, 363.
 55. Lewendon, A., Murray, I. A., Shaw, W. V., Gibbs, M. R., and Leslie, G. W. (1994) *Biochemistry* 33.
 56. Kleanthous, C., and Shaw, W. V. (1984) *Biochem. J.*, 211.
 57. Ellis, J., Bagshaw, C. R., and Shaw, W. V. (1991) *Biochemistry* 30, 10806.
 58. Ellis, J., Bagshaw, C. R., and Shaw, W. V. (1995) *Biochemistry* 34, 16852-16859.

59. Beiber, L. L. (1988) *Annu. Rev. Biochem.* 57, 261-283.
60. Chase, J. F., and Tubbs, P. K. (1966) *Biochem. J.* 99, 32-40.
61. Falquet, L., Pagni, M., Bucher, P., Hulo, N., Sigrist, C. J., Hoffman, K., and Bairoch, A. (2002) *Nucleic Acids Res.* 30, 235-238.
62. Gobin, S., Bonnefont, J. P., Prip-Buus, C., Mugnier, C., Ferrec, M., Demaugre, F., Saudubray, J. M., Rostane, H., Djouadi, F., Wilcox, W., Cederbaum, S., Haas, R., Nyhan, W. L., Green, A., Gray, G., Girard, J., and Thuillier, L. (2002) *Hum. Genet.* 111, 178-189.
63. McGarry, J. D., and Brown, N. F. (1997) *Eur. J. Biochem.* 244, 1-14.
64. Ramsay, R. R., Gandour, R. D., and Van der Leij, F. R. (2001) *Biochim. Biophys. Acta* 1546, 21-43.
65. Prentki, M., and Corkey, B. E. (1996) *Diabetes* 45, 273-283.
66. Zammit, V. A. (1999) *Biochem. J.* 343.
67. Fraser, F., Corstophine, C. G., and Zammit, V. A. (1997) *Biochem. J.* 323, 711-718.
68. Oda, Y. (1999) *Pathol. Int.* 49, 921-937.
69. Hersh, L. B. (1982) *J. Biol. Chem* 257, 12820-12825.
70. Wu, D., and Hersh, L. B. (1995) *J. Biol. Chem* 270, 29111-29116.
71. Iyer, P. P., and Ferry, J. G. (2001) *J. Bacteriol.* 183, 4244-4250.
72. Henkin, J., and Abeles, R. H. (1976) *Biochemistry* 15, 3472-3479.
73. Latimer, M. T., and Ferry, J. G. (1993) *J. Bacteriol.* 175, 6822-6829.

74. Rasche, M. E., Smith, K. S., and Ferry, J. G. (1997) *J. Bacteriol.* 179, 7712-7717.
75. Jencks, W. P. (1975) *Adv. Enzymol. Relat. Areas Mol. Biol.* 43, 219-410.
76. Hibbert, F., Kyrtopoulos, S. A., and Satchell, D. P. N. (1971) *Biochim. Biophys. Acta* 242, 39-54.
77. Born, T. L., Franklin, M., and Blanchard, J. S. (2000) *Biochemistry* 39, 8556-8564.
78. Bourhy, P., Martel, A., Margarita, D., Saint Girons, I., and Belfaiza, J. (1997) *J. Bacteriol.* 179, 4396-4398.
79. Wyman, A., and Paulus, H. (1975) *J. Biol. Chem* 250, 3897-3903.
80. Born, T. L., and Blanchard, J. S. (1999) *Biochemistry* 38, 14416-14423.
81. Leu, L.-S., and Cook, P. F. (1994) *Protein and Peptide Letters* 1, 157-162.
82. Brumlick, M. J., and Buckley, J. T. (1996) *J. Bacteriol.* 178, 2060-2064.
83. Karlsson, M., Contreras, J. A., Hellman, U., Tornqvist, H., and Holm, C. (1997) *J. Biol. Chem* 272, 27218-27233.
84. Lands, W. E. M., and Crawford, C. G. (1976) (Martonosi, A., Ed.) pp 3-85, Plenum Press, New York.
85. Holub, B. J., and Kuskis, A. (1978) *Adv. Lipid Res* 16, 1-125.
86. Nakagawa, Y., and Waku, K. (1989) *Prog. Lipid Res.* 28, 205-243.
87. MacDonald, J. I., and Sprecher, H. (1991) *Biochim. Biophys. Acta* 1084, 105-121.

88. Snyder, F., Lee, T.-C., and Blank, M. L. (1992) *Prog. Lipid Res.* 31, 65-86.
89. Yamashita, A., Sugiura, T., and Waku, K. (1997) *J. Biochem. (Tokyo)* 122, 1-16.
90. Choy, P. C., and Arthur, G. (1989) in *Phosphatidylcholine Metabolism* (Vance, D. E., Ed.) pp 87-101, CRC Press, Boca Raton, FL.
91. Breslow, J. L. (1996) *Science* 272, 685-688.
92. Fielding, C. J., Shore, V. G., and Fielding, P. E. (1972) *Biochem. Biophys. Res. Commun.* 46, 1493-1498.
93. Wang, J., Sykes, B. D., and Ryan, R. O. (2002) *Proc. Natl. Acad. Sci. U.S.A.* 99, 1188-1193.
94. Jonas, A. (2000) *Biochim. Biophys. Acta* 1529, 245-256.
95. Borhani, D. W., Rogers, D. P., Engler, J. A., and Brouillette, C. G. (1997) *Proc. Natl. Acad. Sci. U.S.A.* 94, 12291-12296.
96. Vickaryous, N. K., Teh, E. M., Stewart, B., Dolphin, P. J., Too, C. K. L., and McLeod, R. S. (2003) *Biochim. Biophys. Acta* 1646, 164-172.
97. Yang, C., Manoogian, Q., Pao, F., Lee, F., Knapp, R., Gotto Jr., A., and Pownall, H. (1987) *J. Biol. Chem* 262, 3086-3091.
98. Cygler, M., and Schrag, J. (1997) *Methods Enzymol.* 284, 3-27.
99. Jennens, M., and Lowe, M. (1994) *J. Biol. Chem* 269, 25470-5-25474.
100. Dugi, K., Dichek, H., Talley, G., Brewer Jr., H., and Santamarina-Fojo, S. (1992) *J. Biol. Chem* 267, 25086-25091.
101. Adimoolam, S., and Jonas, A. (1997) *Biochem. Biophys. Res. Commun.* 232,

783-787.

102. Peelman, F., Vinaimont, N., Verhee, A., Vanloo, B., Verschelde, J.-L., Labeur, C., Seguret-Mace, S., Durverger, N., Hutchinson, G., Vandekerckhove, J., Tavernier, J., and Rosseneu, M. (1998) *Protein Sci.*
103. Knipping, G., Hermetter, A., and Hubmann, M. R. (1993) *Int. J. Biochem.* 25, 505-511.
104. Roosebeek, S., Vanloo, B., Durverger, N., Caster, H., Breyne, J., De Beun, I., Patel, H., Vanderckhove, J., Shoulders, C., Rosseneu, M., and Peelman, F. (2001) *J. Lipid Res.* 42, 31-40.
105. Giovanelli, J., Mudd, S. H., and Datko, A. H. (1980) *Sulfur Amino Acids in Plants*, Vol. 5, Academic Press, New York.
106. Kredich, N. M. (1996) in *Biosynthesis of cysteine* (Neidhardt, F. C., Ed.) pp 514-527, ASM Press, Washington D. C.
107. Bykowski, T., van der Ploeg, J. R., Iwanicka-Nowicka, R., and Hryniewicz, M. M. (2002) *Mol Microbiol* 43, 1347-58.
108. Sirko, A., Hryniewicz, M. M., Hulanicka, M. D., and Bock, A. (1990) *J. Bacteriol.* 172, 3351-3357.
109. Hellinga, H. W., and Evans, P. R. (1985) *Eur. J. Biochem.* 149, 363-373.
110. Hryniewicz, M. M., and M., K. N. (1991) *J. Bacteriol.* 173, 5876-5886.
111. Robbins, P. W., and Lipmann, F. (1958) *J. Biol. Chem* 233, 686-690.
112. Liu, C., Martin, E., and Leyh, T. S. (1994) *Biochemistry* 33, 2042-2047.

113. Leyh, T. S., Taylor, J., and Markham, G. D. (1988) *J. Biol. Chem* 263, 2409-2416.
114. Leyh, T. S., and Suo, Y. (1992) *J. Biol. Chem* 267, 542-545.
115. Leyh, T. S., Vogt, T. F., and Suo, Y. (1992) *J. Biol. Chem* 267, 10405-10410.
116. Leyh, T. S. (1993) *Crit Rev Biochem Mol Biol* 28, 515-542.
117. Sathishchandran, C., and Markham, G. D. (1989) *J. Biol. Chem* 264, 15012-15021.
118. Sathishchandran, C., Hickman, Y. N., and Markham, G. D. (1992) *Biochemistry* 31, 11684-11688.
119. Demerec, M., Gillespie, D. H., and Mizobuchi, L. (1963) *Genetics* 48, 997-1009.
120. Krone, F. A., Westphal, G., and Schwenn, J. D. (1991) *Mol. Gen. Genet.* 225, 314-319.
121. Tsang, M. L.-S., and Schiff, J. A. (1973) *J. Bacteriol.* 134, 131-138.
122. Tsang, M. L.-S. (1983) in *Thioredoxins-structure and function* (Gadal, P., Ed.) pp 103-110, Paris.
123. Siegel, L. M., and Davis, P. S. (1974) *J. Biol. Chem* 249, 1587-1598.
124. Siegel, L. M., Murphy, M. J., and Kamin, H. (1973) *J. Biol. Chem* 248, 251-261.
125. Siegel, L. M., Davis, P. S., and Kamin, H. (1974b) *J. Biol. Chem* 249, 1572-1586.
126. Warren, M. J., Roessner, C. A., Santander, P. J., and Scott, A. I. (1990) *Biochem. J.* 265, 725-729.
127. Nakamura, T., Iwahashi, H., and Eguchi, Y. (1984) *J. Bacteriol.* 158, 1122-1127.

128. Tai, C.-H., Nalabolu, S. N., Jacobson, T. M., Minter, D. E., and Cook, P. F. (1993) *Biochemistry* 32, 6433-6442.
129. Kredich, N. M., Becker, M. A., and Tomkins, G. M. (1969) *J. Biol. Chem* 244, 24280-2439.
130. Lebo, R. V., and Kredich, N. M. (1978) *J. Biol. Chem* 253, 2615-2623.
131. Cook, P. F., and Wedding, R. T. (1977) *J. Biol. Chem* 251, 2023-2029.
132. Srere, P. A., and Ovadi, J. (1990) *FEBS Lett.* 268, 360-364.
133. Denk, D., and Bock, A. (1987) *J. Gen. Microbiol.* 133, 515-525.
134. Mino, K., Yamanoue, T., Sakiyama, T., Eisaki, N., Matsuyama, A., and Nakanishi, K. (1999) *Biosci. Biotechnol. Biochem.* 63, 168-179.
135. Bogdanova, N., and Hell, R. (1997) *Plant, J.* 11, 251-262.
136. Mino, K., Hiraoka, K., Imamura, K., Sakiyama, T., Eisaki, N., Matsuyama, A., and Nakanishi, K. (2000) *Biosci. Biotechnol. Biochem.* 64, 1874-1880.
137. Takagi, H., Kobayashi, C., Kobayashi, S., and Nakamori, S. (1999) *FEBS Lett.* 452, 323-327.
138. Inoue, K., Noji, M., and Saito, K. (1999) *Eur. J. Biochem.* 25, 281-305.
139. Nakamura, T., and Tamura, G. (1990) *Allium tuberosum. Agric. Biol. Chem.* 54, 649-656.
140. Droux, M., Martin, J., Sajus, P., and Douce, R. (1992) *Arch. Biochem. Biophys.* 295, 379-390.
141. Ruffet, M.-L., Droux, M., and Douce, R. (1994) *Biochim. Biophys. Acta* 227,

288-295.

142. Mino, K., Imamura, K., Sakiyama, T., Eisaki, N., Matsuyama, A., and Nakanishi, K. (2001) *Biosci. Biotechnol. Biochem.* 65, 865-874.
143. Becker, M. A., and Tomkins, G. M. (1969) *J. Biol. Chem* 248, 6023-6030.
144. Hulanicka, M. D., Hallquist, S. G., M., K. N., and Majica-A, T. (1979) *J. Bacteriol.* 140, 141-146.
145. Kredich, N. M. (1971) *J. Biol. Chem* 246, 3474-3484.
146. Nakamura, T., Kon, Y., Iwahashi, H., and Eguchi, Y. (1983) *J. Bacteriol.* 156, 656-662.
147. Byrne, C. R., Monroe, R. S., Ward, K. A., and M., K. N. (1988) *J. Bacteriol.* 170, 3150-3157.
148. Burkhard, P., Rao, G. S. J., Hohenester, E., Cook, P. F., and Jansonius, J. N. (1998) *J. Mol. Biol.* 283, 111-120.
149. Hyde, C. C., Ahmed, S. A., Podlan, E. A., Miles, E. W., and Davies, D. R. (1988) *J. Biol. Chem* 263, 7857-7871.
150. Arnone, M. I., Birolo, L., Giamberini, M., Cubellis, M. V., Nitti, G., Sannia, G., and Marino, G. (1992) *Eur. J. Biochem.* 204, 1183-1189.
151. Rege, V., M., K. N., Tai, C.-H., Karsten, W. E., Schnackerz, K. D., and Cook, P. F. (1996) *Biochemistry* 35, 13485-13493.
152. Cook, P. F., Hara, S., Nalabolu, S. N., and Schnackerz, K. D. (1992) *Biochemistry* 31, 2298-2303.

153. Schnackerz, K. D., Tai, C.-H., Simmons, J. W., III, Jacobson, T. M., Rao, G. S. J., and Cook, P. F. (1995) *Biochemistry* 34, 12152-12160.
154. Schnackerz, K. D., and Cook, P. F. (1995) *Arch. Biochem. Biophys.* 324, 71-77.
155. Tai, C.-H., Nalabolu, S. N., Simmons, J. W., III, Jacobson, T. M., and Cook, P. F. (1995) *Biochemistry* 34, 12311-12322.
156. Woehl, E. U., Tai, C.-H., Dunn, M. F., and Cook, P. F. (1996) *Biochemistry* 35, 4776-4783.
157. Hwang, C.-C., Woehl, E. U., Dunn, M. F., and Cook, P. F. (1996) *Biochemistry* 35, 6358-6365.
158. Tai, C.-H., and Cook, P. F. (2000) *Adv. Enzymol. Relat. Areas Mol. Biol.* 74, 185-234.
159. McClure, G. D., and Cook, P. F. (1994) *Biochemistry* 33, 1674-1683.
160. Benci, S., Vaccari, S., Mozzaerlli, A., and Cook, P. F. (1997) *Biochemistry* 36, 15419-15427.
161. Benci, S., Vaccari, S., Mozzaerlli, A., and Cook, P. F. (1999) *Biochim. Biophys. Acta* 1429, 317-330.
162. Strambini, G., Cioni, P., and Cook, P. F. (1996) *Biochemistry* 35, 8392-8400.
163. Burkhard, P., Tai, C.-H., Ristroph, C. M., Cook, P. F., Jansonius, J. N., and Abeles, R. H. (1999) *J Mol Biol* 291, 941-953.
164. Burkhard, P., Tai, C.-H., Jansonius, J. N., and Cook, P. F. (2000) *J. Mol. Biol.* 303, 279-286.

165. Nakamori, S., Kobayashi, S. I., Kobayashi, C., and Takagi, H. (1998) *Appl. Environ. Microbiol.* 64, 1607-1611.
166. Hindson, V. J., Moody, P. C., Rowe, A. J., and Shaw, W. V. (1990) *J. Biol. Chem* 275, 461-466.
167. Schimerlik, M. I., and Cleland, W. W. (1973) *J. Biol. Chem* 248, 8418-8423.
168. Cook, P. F., Kenyon, G. L., and Cleland, W. W. (1981) *Biochemistry* 20, 1204-1210.
169. Morrison, J. F., and Cleland, W. W. (1966) *J. Biol. Chem* 241, 673-683.
170. Johnson, C. M., Huang, B., Roderick, S. L., and Cook, P. F. (2004) *Arch. Biochem. Biophys.* Submitted.
171. Schowen, R. L. (1977) pp 64, University Park Press, Baltimore, MD.
172. Quinn, D. M., and Sutton, L. D. (1991) in *Enzyme Mechanism from Isotope Effects* pp 73-126, CRC Press, Boca Raton, FL.
173. Cleland, W. W. (1979) *Methods Enzymol.* 63, 103-138.
174. Hirvas, L., Koski, P., and Vaara, M. (1990) *Biochem. Biophys. Res. Commun.* 173, 53-59.
175. Ramachandran, G. N., Ramakrishnan, C., and Sasisekharan, V. (1963) *J. Mol. Biol.* 7, 95-99.
176. Van Arnum, P. (2001) in *Chemical Market Reporter*.
177. Tremblay, J.-F. (2001) in *Chemical and Engineering News* pp 45-49.